2008

Instrumentation development for coupling ion/ion reactions and ion mobility in biological mass spectrometry

Matthew William Soyk
Iowa State University

Instrumentation development for coupling ion/ion reactions and ion mobility in biological mass spectrometry

by

Matthew W. Soyk

A dissertation submitted to the graduate faculty

in partial fulfillment of the requirements for the degree of

DOCTOR OF PHILOSOPHY

Major: Analytical Chemistry

Program of Study Committee:
R. S. Houk, Major Professor
Victor Shang-Yi Lin
Nicola Pohl
Emily Smith
Hans Stauffer

Iowa State University

Ames, Iowa

2008

TABLE OF CONTENTS

ABSTRACT

The development of mass spectrometry (MS) instrumentation for novel biological applications, specifically, the development of instrumentation that integrates ion/ion reaction capabilities in an ion trap (IT) with ion mobility-quadrupole-time-of-flight (IMS-q-TOF) analysis is presented. Chapter 1 provides a general introduction to protein analysis by MS, ion/ion reactions and ion/ion reaction instrumentation, and IMS techniques and IMS instrumentation. Chapter 2 describes the construction and performance of a linear ion trap (LIT) made with primarily commercially available components. The LIT has two ion sources for independent analyte ion and reagent ion formation. The LIT functions as a reaction vessel for gas-phase ion/ion reactions and as a mass spectrometer using mass-selective axial ejection. Initial experiments demonstrate the LIT's ability to perform both dual polarity storage mode and transmission mode proton transfer ion/ion reactions. Chapter 3 describes the construction and performance of an IT-IMS-q-TOF with three independent ion sources. This instrument is the first MS to combine ion/ion reaction capabilities with IMS-q-TOF analysis. Chapter 4 describes novel experiments performed on the IT-IMS-q-TOF instrument constructed in our lab. The gas phase conformation of cytochrome *c* ions in multiple different charge states is investigated using proton transfer ion/ion reactions and IMS-q-TOF analysis.

CHAPTER 1.

General Introduction

Biological Mass Spectrometry

Over the last 15 to 20 years, mass spectrometry (MS) has become more important in the area of biological molecule identification [1]. Specifically, advances in MS instrumentation and analytical methods have improved the speed, specificity, and sensitivity of MS, making it an appealing technique for protein identification and structural characterization.

Early experiments in protein analysis used fast atom bombardment (FAB) [2] and plasma desorption [3] to create gaseous peptide ions. These methods suffered from the limitation that they were able to ionize peptides, but not intact proteins. The development of two ionization techniques in the late 1980's, namely electrospray ionization (ESI) [4] and matrix assisted laser desorption/ionization (MALDI) [5] had major impacts on the analysis of biological molecules. Electrospray and MALDI have since become the popular ionization methods for most biological molecules including peptides, proteins, oligonucleotides, and carbohydrates. Both ESI and MALDI typically create protonated ions—i.e. protons are attached to the analyte molecule that carries the charge. Therefore, the mass-to-charge ratio (m/z) of the ion is the mass of the neutral molecule plus the mass of the proton(s) attached to the molecule divided by the total charge of the ion.

In a MALDI experiment, the analyte ions created are predominantly singly charged [6]. When using MALDI for protein analysis, the m/z range of the mass analyzer must be considered. For example, cytochrome *c* is a small protein with molecular weight of 12228. The +1 charge state of cytochrome *c* generated by MALDI will have an m/z of 12229 Th.

The mass analyzer must have an m/z range above the mass of this ion; time-of-flight (TOF) is commonly used.

Alternatively, ESI creates ions in a distribution of charge states that are usually highly multiply charged [4]. Using cytochrome *c* as an example again, an ESI spectrum of cytochrome *c* can have charge states ranging from ~+5 to ~+20 (m/z = 2447 to m/z = 612) depending on solution conditions. These higher charge states allow for the analysis of intact proteins using mass analyzers with lower m/z ranges such as quadrupoles.

A very significant analog of ESI, known as nano-electrospray ionization or nanospray [7], has become a popular technique. There are several advantages of nano-ESI over traditional ESI. Less sample is consumed with nano-ESI—the flow rate of nano-ESI is ~10 nL/min opposed to ~10 μL/min. Nano-ESI is more sensitive than traditional ESI. The sample does not have to be pumped in nano-ESI. A stable spray cannot be generated in ESI with a 100% water solution. An organic modifier, such as methanol, needs to be added to the ESI spray solution. Nano-ESI creates smaller initial droplets, therefore, it can create a spray with 100% water solution, so no organic modifier is needed [7].

There have been two general methods developed for protein identification and characterization known as “bottom-up” protein analysis and “top-down” protein analysis. Each of these techniques will be described below.

“Bottom-up” Protein Analysis

Bottom-up protein analysis is started by utilizing a one- or two-dimensional (2D) gel electrophoresis separation of a mixture of proteins. The individual spots are then extracted and subjected to proteolysis [1]. The peptides created from the digests are then measured

directly by MS. The masses of the peptides create a mass fingerprint that is characteristic of the original protein. The peptide masses are then used in a database search that identifies the protein [8, 9]. This technique is most useful for proteins from relatively pure samples.

In the context of the bottom-up approach it is sometimes more useful to subject the peptides to tandem MS (MS/MS) analysis [10]. Briefly, MS/MS involves the isolation of a single m/z ion followed by fragmentation of the ion. The fragmentation is usually achieved by collision induced dissociation (CID), using collisions between the ions and a neutral buffer gas. The fragment ions are then mass analyzed. The MS/MS spectra of the peptides carry information on the amino acid sequence of the peptide and, in turn, the parent protein [11].

In bottom-up experiments there may be many isobaric peptides (peptides with the same m/z, but different amino acid sequence). A common technique used to address this problem is to perform a liquid chromatography (LC) separation after the digestion and before MS and MS/MS analysis. The isobaric peptides, while they appear at the same place in the mass spectrum may have different retention times in the LC separation, and are therefore separated. The separated peptides are then subjected to MS/MS experiments in which their sequence is identified. These LC separations greatly increase the number of proteins that can be identified in a single experiment [12-14], and they can be done either online with the MS, or fractions of the LC effluent can be collected and analyzed individually by MS.

There are some very significant limitations to the bottom-up approach of protein analysis. Some proteins, such as hydrophobic membrane proteins, proteins at low abundance, and proteins with extremely high or low isoelectric points are poorly represented in gel electrophoresis separations [11, 15]. These effects are also overcome by utilizing LC

separation prior to MS. A second issue with the bottom-up approach is that when an unfractionated protein mixture is digested, it greatly increases the number of components to be analyzed by MS and complicates the isolation of individual diagnostic peptides or single parent peptides to be dissociated [11]. Third, even though only one unique peptide is needed to indentify a protein, a lot of time can be spent unnecessarily analyzing multiple peptides of the same protein, or the same peptide may be present in multiple LC peaks. Fourth, up to 25% of peptide MS/MS spectra are unassignable due to factors such as the spectrum being too complex, the peptide ions are too low in abundance, or there is no diagnostic ion for the protein [11, 16]. Therefore, there are proteins in the mixture that are not identified. Lastly, the proteins are digested before analysis, causing information about the proteins to be lost. For example, the molecular weight of the proteins is not measured, which can give information about possible post-translational modifications. Also, some peptides generated from protein digests are not represented in the mass spectrum, making complete protein structure analysis impossible. Due to these limitations of bottom-up protein analysis, new methods were developed to address the problems.

"Top-down" Protein Analysis

Top-down protein analysis was pioneered by McLafferty and co-workers [11, 17]. Protein primary structure (i.e. the amino acid sequence) can be identified from the direct measurement of the intact protein by MS and MS/MS experiments. In a typical top-down experiment, a mixture of intact proteins is transformed into gaseous ions by ESI and transferred into the MS. A mass spectrum of all the ions is taken, providing molecular weight information for all the proteins in the sample. Then, one by one, protein ions in a single

charge state are isolated and fragmented, and the fragment ions are mass analyzed. The combination of the protein molecular weight and partial sequence information from the MS/MS spectrum can provide enough information to identify the protein [18, 19]. The identification can be made by the 'sequence tag' method [20-22], database searching of the fragment ion spectrum [23], or through 'de novo' sequencing [24, 25].

There are several advantages of the top-down method. First, there is much less sample preparation in top-down analysis. There is no in-gel or solution phase digestion of the proteins prior to MS. Second, there is less of a need for multi-dimensional separation before the MS analysis [26]. A complex mixture of intact proteins can still have fewer total components than a mixture of peptides generated from a digest of a single protein. Third, intact protein masses from several proteins are spread over a wider m/z range than the peptide masses from a digest, making the spectra less complex. Fourth, redundant peptide identification is avoided. Fifth, by performing MS/MS on intact proteins, the entire sequence of the protein is available for analysis [11]. Therefore, the protein can be completely characterized more easily, including possible total primary structure and any post-translational modification identities and locations [23, 27-29].

Even though there are major advantages to top-down protein analysis, there are also some challenges. The first challenge was overcome when ionization techniques were developed, namely ESI and MALDI, that can transform intact protein ions into the gas phase. The second challenge is the development of mass analyzers with the performance characteristics to generate significant structural information from intact protein ions. The voltage required to fragment an ion is inversely proportional to the ion's charge. Therefore, +1 protein ions are very difficult to fragment. Ions created by MALDI are primarily +1.

Conversely, ESI creates protein ions that are highly multiply charged, so the protein ions generated from ESI fragment more readily than those made with MALDI.

An added difficulty with the interpretation of an MS/MS spectrum of a multiply charged intact protein ion formed via ESI is that the fragment ions will have charges ranging from +1 up to the charge of the precursor protein ion. It is possible for two fragment ions with different masses and different charges to appear at the same nominal mass in the MS/MS spectrum. Therefore, in order to interpret the fragment ion mass spectrum, the charge on each ion must be determined because the charge is not known beforehand. The best way to determine the charge state of an ion is to measure the isotopic distribution (mainly ^{13}C) of the protein fragment ions. The separation of the isotopic peaks is equal to 1/ion charge, so as the ion charge state increases the separation of the isotopic peaks decreases. Early MS/MS experiments with intact proteins were done on triple quadrupole instruments with limited mass resolution that could not resolve the isotopic peaks of the multiply charged fragment ions [30-35]. These experiments resulted in spectra in which the ion's charge states could not be identified completely, limiting the usefulness of the spectra to protein fingerprinting analysis [11, 32]—a method that compares uninterpreted fragment ion spectra for protein identification. Two methods have been developed to overcome the product ion charge state ambiguity problem—high resolution fragment ion analysis and fragment ion charge state manipulation. Each method will be discussed further below.

High Resolution MS. High mass resolution instrumentation can be used to resolve the ^{13}C isotopic distribution of the multiply charged fragment ions. The first instruments used for these analyses were Fourier transform-ion cyclotron resonance (FT-ICR) [17, 20, 22-25,

27, 28, 36-40] mass spectrometers that have mass resolving power greater than 100000 and mass accuracies better than 10 ppm. FT-ICR instruments have suitable performance that allows for fragment ion charge state interpretation, so protein sequence information can readily be obtained from the MS/MS spectra of intact, multiply charged protein ions. Multiple ion activation techniques have been employed in FT-ICR instruments to fragment intact proteins: CID, also known as collisionally activated dissociation (CAD) [27, 36-41], infrared multi-photon dissociation (IRMPD) [42, 43], and blackbody infrared radiative dissociation [44]. Electron capture dissociation (ECD) [45-48] is a technique that gives complementary fragmentation to the methods stated above was developed by McLafferty and co-workers. An example of ECD of the intact protein cytochrome *c* followed by high resolution MS is shown in Figure 1 [48]. The multiply charged protein ion captures a low energy electron, creating an odd electron species that quickly dissociates via cleavage of the N—αC bond of the protein or peptide backbone. The resulting fragment ions are referred to as “c” and “z” ions. These fragment ions are different than the “b” and “y” ions usually formed by the cleavage of the C—N amide bond in CID. Labile post-translational modifications, such as phosphorylation and glycosylation, are usually dissociated from the protein in CID but not ECD, allowing for their identity and position along the protein backbone to be determined [28, 49].

More recently, the Orbitrap mass spectrometer [50] was developed for high resolution mass measurements. These instruments are capable of 150,000 mass resolution and 2-5 ppm mass accuracy.[50] An added advantage of the Orbitrap is that there is no superconducting magnet like in FT-ICR. The Orbitrap operates using only static DC voltages, so compared to the FT-ICR, it is simpler and less expensive to maintain.

Ion/Ion Reactions. Ion/ion reactions are gas phase reactions inside the mass spectrometer. Positive and negative ions are trapped simultaneously in the same volume, usually in an ion trap [11], and the electrostatic attraction of the ions creates an overlap of the ion clouds. The reaction occurs either via the creation of a long lived reaction complex, via a hopping mechanism, or via a coulombically bound orbit [51]. In either case, the multiple charging associated with ESI is advantageous because as the positive and negative ions react, there will still be a net charge associated with the reaction pair, allowing traditional ion optics to be used to control the reactants.

The use of ion/ion reactions is the second method used to overcome the charge state ambiguity of multiply charged protein fragment ions. Specifically, proton transfer ion/ion reactions are used to reduce the fragment ion charge to primarily +1 [11, 21, 52-62]. The reagent ion is chosen to enable the stripping of protons from the protein fragment ions, thereby reducing the charge. Reducing the charge on the fragment ions to primarily +1 expands the ion population out on the m/z scale, creating more space between peaks and separating fragment ions that initially had different mass and different charge but the same m/z. It also lessens the requirements of the mass spectrometer resolving power and mass accuracy. With the use of proton transfer ion/ion reactions, structural information of multiply charged protein fragment ions can be obtained using mass analyzers with resolving powers of $m/\Delta m$ ~500 to 1000 [21, 59-62]. An example of proton transfer ion/ion reactions being used to identify fragment ions generated from CID of the intact protein ubiquitin is shown in Figure 2 [63].

Another type of ion/ion reaction that has recently been developed and studied is electron transfer dissociation (ETD) [64]. When using ion traps for protein analysis, ECD is not possible without adding a magnet to the instrument [65]. Ion traps have a low mass cut-off (LMCO), or a minimum m/z that can be trapped. Free electrons have an m/z that is much lower than that of even the lightest ion, therefore, they cannot be trapped by an ion trap. ETD is the ion/ion reaction equivalent to ECD. Positive protein or peptide ions are reacted with a reagent ion that acts as an electron donor. The electron is transferred from the reagent ion to the protein or peptide ion, which then dissociates to create the same c and z ions as ECD [64].

McLuckey and coworkers have discovered reagent ions that enable other types of ion/ion reactions. Cation switching reactions [66, 67] use protonated protein or peptide ions with a metal containing anion. For example, consider the reaction between a doubly protonated peptide $[M+2H]^{2+}$ and $Na(NO_3)_2^-$. The products of this reaction are $[M+Na]^+$ and $2HNO_3$. The cation has replaced the protons on the peptide as the charge carrier. The last type of ion/ion reaction that has been developed is a charge inversion reaction. Reagent ions have been found that can transfer multiple protons in a single step, so charge inversion reactions are possible without going through a neutral intermediate [68]. These reactions can transform a depronated, negatively charged ion into a prontated, positively charged ion and vice versa.

Each of these reactions, proton transfer, ETD, cation switching, and charge inversion have useful properties for structural characterization of protein ions, but not every MS is capable of ion/ion reactions. The next section will discuss instrument capabilities needed for ion/ion reactions and a brief history of ion/ion reaction instrumentation development.

Instrumentation for Ion/Ion Reactions. Instruments capable of ion/ion reactions must have several key components. First, there needs to be a gas phase ion/ion reaction vessel that provides for physical overlap between the analyte and reagent ions. Second, there must be at least two distinct ion sources to create both polarities of ions in a single experiment. Third, the instrument should have MS/MS capabilities for protein structural analysis. Finally, there must be a mass analyzer.

The gas phase reaction vessel has either been external to the MS vacuum system at near atmospheric pressure or inside the MS at pressures in the millitorr range [69]. The external reaction vessels used have been a y-tube reactor prior to quadrupole MS, using two ESI emitters[70] or one ESI and one atmospheric pressure chemical ionization (APCI) source [70, 71], and a charge reduction chamber prior to TOF MS, using one ESI source and either an α-particle source [72], or a corona discharge source [73]. The advantages of these techniques are ease of integration to various MS instruments, flexibility with the type of MS used for mass analysis, and no restriction of the reactions caused by trapping parameters [69]. Conversely, these reaction chambers are limited to reducing the charge of all ions created by the analyte ESI source with little control over any of the reactant or product ions, and there is no possibility of MS/MS experiments prior to the ion/ion reaction event [69]. More flexibility in the ion/ion reaction parameters has been achieved when using reaction vessels inside the MS.

To date all ion/ion reaction experiments inside the MS have been done in electrodynamic ion traps [69], including 3d quadrupole traps based on the Paul trap [54] and linear ion traps based on linear quadrupoles [64, 74-76]. Ion traps have several characteristics

that make them attractive as gas phase reaction vessels. They provide simple methods for simultaneous storage of both positive and negative ions. They are capable of multi-stage MS measurements (MS^n) via "tandem in time" experiments [77], including ion/ion reaction steps in between stages of MS [69], satisfying the requirement for MS/MS for protein structure analysis. Finally, ion traps allow for separation of the ionization and ion/ion reaction events because ions can be created outside the ion trap and injected into the trap for reaction and mass analysis.

The 3d ion trap (Figure 3 [78]) consists of a ring electrode between two endcap electrodes. It is able to trap both positive and negative ions simultaneously in all 3 dimensions using only the RF voltage applied to the ring electrode [79, 80]. A bath gas inside the ion trap, typically He at a pressure of ~1 mTorr, is used to cool the ions to the center of the trap. The cooling promotes spatial overlap of the ion clouds and minimizes the relative translational energy of the reactant pair [69], which affects the ion/ion reaction rate [81]. This bath gas is also beneficial for mass analysis in ion traps regardless of whether ion/ion reactions are performed or not [69]. Therefore, no modifications need to be made to 3d ion traps to enable ion/ion reactions.

The multiple ion sources for ion/ion reactions using 3d ion traps have been configured in many different orientations. Early ion/ion reaction experiments in 3d ion traps utilized inter-ion trap ionization by electron impact ionization (EI) or chemical ionization (CI) with the electron beam coming through a hole machined in the ring electrode [80]. The second source was an ESI source used to create multiply negatively charged ions that were admitted to the ion trap through a hole one of the endcap electrodes. Both proton transfer [80, 82] and electron transfer reactions [83] of multiply charged anions were studied.

The first instrument used to study the reactions between multiply charged cations and singly charged anions was a 3d ion trap with an ESI source that admitted ions through an endcap electrode of the ion trap and an atmospheric sampling glow discharge ionization (ASGDI) source that admitted ion into the trap through a hole machined through the ring electrode of the ion trap [54]. This instrument was used primarily for the study of proton transfer ion/ion reactions of multiply charged proteins.REF Another instrument with a similar configuration was developed by the Glish group [84]. In these studies the ASGDI source was replaced with a laser desorption source for the study of reactions between multiply charged peptide or protein ions with either Fe^+ or $FeCO_2^-$.

Some significant disadvantages limit the usefulness of admitting ions through the ring electrode of 3d ion traps. Namely, the trapping efficiency of ions admitted through the ring electrode is lower than that for ions admitted through the endcap [69]. Also, the ions admitted through the ring electrode experience stronger fields than ions admitted through the endcap, causing more fragmentation [85]. Therefore, it was beneficial to develop instrumentation to admit both analyte and reagent ions through the endcap electrode.

The “dueling” ESI ion trap mass spectrometer [86] was developed that integrates two ESI sources arranged 180^o from each other and 90^o from the main optical axis of the instrument. The ions are steered down the main optical axis of the instrument by a turning quadrupole. In order to sequentially fill the ion trap with positive and negative ions, the DC voltages on the turning quadrupole and the lenses between it and the ion trap are switched using computer controlled switches. This instrument was the first to allow ion/ion reaction experiments between opposite polarity, multiply charged ions created by ESI in an ion trap reaction vessel [87, 88].

The integration of multiple ion sources through a turning quadrupole led to more complex instrumentation that incorporated multiple different ion sources. Badman and co-workers developed an ion trap instrument with four independent ion sources; two ESI sources and one source for either ESI or ASGDI are integrated through the turning quadrupole and one ASGDI source is orthogonal to the ion trap that admits ions through the ring electrode of the ion trap [63]. This instrument is capable of creating multiple different reagent ions from distinct ion sources to enable different types of ion/ion reactions in a single experiment. For example, positive cytochrome *c* ions from one ESI source were reacted with negative cytochrome *c* ions from the second ESI source to create positive cytochrome *c* dimer ions. These first generation product ions were then charge reduced using PDCH ions generated at the orthogonal ASGDI source [63]. Several novel combinations of analyte/reagent ions have been reacted in sequential ion/ion reactions using this instrument [68, 89, 90]. The design of having three independent ion sources integrated to an ion trap through a turning quadrupole is the technique used in the instrumentation developed in our lab, the results of which are presented in chapters 2, 3, and 4 of this dissertation.

Six years ago two new linear ion traps (LIT) [91, 92] were introduced. Both of these devices are based on linear quadrupoles that provide the trapping in the radial direction (x and y-directions) using the RF voltages applied to the quadrupole rods, and the trapping in the axial direction (z-direction, i.e. the central axis of the quadrupole array) is provided by DC voltages on the entrance and exit lenses. However, there are significant differences between the two types of LITs.

The Thermo Finnigan LTQ is made from a quadrupole rod array that is divided into three sections—a short section 12 mm long at the front, the main rod section that is 37 mm

long, and a second short section 12 mm long at the back—also known as a tri-filter configuration. A diagram of the LTQ is shown in Figure 4 [92]. Each rod section has the same RF voltage applied to it, but they all have independent DC bias voltages applied to them, allowing the ions to be moved from one section to another. The LTQ uses a radial ejection technique. Narrow slots are cut in the center section of one opposing set of rods. The ions are ejected from the LIT through these slots cut in the rods and are collected by an ion detector. The tri-filter configuration also helps the radial ion ejection event avoid the fringe fields near the ends of the rods [92].

The other type of LIT, the QTRAP developed by ABI /MDS Sciex (Figure 5)[91], is based on the ion path of a triple qudrupole MS. These instruments can use either quadrupole 2 (q2) or qudrupole 3 (Q3) as LITs. The LITs in this design are single section quadrupole rods without the tri-filter capabilities of the LTQ. They also employ a different ejection technique called mass selective axial ejection (MSAE) [93] that utilizes the fringe field coupling of the RF voltage applied to the LIT rods with the DC voltage applied to the exit lens of the LIT to eject the ions axially out of the LIT.

Dual polarity trapping in LITs is not achieved when using DC trapping voltages on the entrance and exit lenses. Two methods have been developed to simultaneously trap both polarity ions in all three directions on these LITs. The first method is the addition of an auxiliary RF voltage to the containment lenses of the LIT to store both polarity of ions in all three dimensions as demonstrated by the Hunt group on a modified Finnigan LTQ linear ion trap [64]. These experiments take advantage of the tri-filter configuration of this LIT, as shown in Figure 6 [64]. During an ion/ion reaction experiment the analyte ions are injected and moved into the front (left) section of the LIT. The reagent ions are then injected into the

back (right) and/or center section of the LIT (the reagent ion source is at the back of the LIT, while the analyte ion source is at the front, see Figure 6). The reagent and analyte ions are mixed by simultaneously removing the DC bias between the rod sections, removing the DC bias between the rods and the containment lenses, and adding the auxiliary RF voltage to the containment lenses. Finally, the reaction is ended by simultaneously removing the auxiliary RF and adding the repulsive DC bias to the containment lenses. Segregating the ions prior to ion/ion reaction allows for isolation of a single reagent ion prior to the ion/ion reaction, giving an added level of control over the type of reaction that is enabled, especially if multiple reagent ions are generated by a single ion source [94].

A second method for dual polarity trapping in an LIT was developed by the McLuckey lab. This method employs an unbalanced RF field in the quadrupole rod array [74]. When the DC bias on the containment lenses and the rod array are equal, subtracting a portion of the RF amplitude from one pair of quadrupole rods and adding an equivalent portion of RF amplitude to the other quadrupole rod pair causes the ions to feel an axial RF field near the entrance and exit lens that is similar to applying the auxiliary RF voltage directly to the lenses as described above. Ion/ion reactions using this method were carried out in a prototype QTRAP mass spectrometer with Q3 (see Figure 5) as the ion/ion reaction vessel. However, the presence of an axial RF field detracts from the performance of the LIT, such as lowering the injection efficiency of the LIT and degrading the MSAE performance. Therefore, further experiments on these QTRAP instruments, using either q2 [95] or Q3[96] as the ion/ion reaction vessel, have used the addition of an auxiliary RF voltage on the containment lenses because the axial RF field can be turned off during analyte ion injection and MSAE steps.

A new method for ion/ion reactions in an LIT has been developed to avoid the need for dual polarity trapping. Transmission mode reactions [97, 98] are ion/ion reactions in which at least one polarity of ions participating in the reaction are not trapped during the reaction. There are essentially three methods for enabling transmission mode ion/ion reactions in an LIT. First, both polarity of ions can be passed through the LIT in opposite directions. This method has not been demonstrated yet. Second, the analyte ions can be trapped in the LIT, and the reagent ions are transmitted through the trapped analyte ions [97, 98]. Third, the reagent ions are trapped, and the analyte ions are passed through the trapped reagent ions [76, 97, 98]. An advantage of transmission mode reactions is that no additional electronics are required to superimpose the auxiliary RF on the containment lenses or to unbalance the RF on the quadrupole rod array.

The ion source configurations for ion/ion reactions in LITs have also gone through several generations of instrumentation, depending greatly on the method of ejection from the ion trap. Radial ejection LITs, such as the Finnigan LTQ [92], have both ends of the LIT available for ion injection. Therefore, these LITs have two ion sources positioned at opposite ends of the LIT as seen in Figure 6 [64]. Recently, the LTQ-Orbitrap hybrid instrument [99] was shown to enable ETD reactions using two ion sources still positioned at opposite ends of the instrument. The difference is that the reagent ions must pass through multiple collision cells and the c-trap [100] before reaching the LIT.

The other LIT ion ejection method, MSAE, differs from radial ejection in that the ions are ejected out of the end of the quadrupole array instead of radially through slots cut in the rods. The implication of MSAE on ion/ion reactions is that only one end of the LIT is available for ion injection. The first ion/ion reaction experiments on an LIT that employed

MSAE used two ion source interfaces with the LIT. The analyte ions were admitted to the LIT using an ESI source on the optical axis of the instrument, and the reagent ions were injected radially into the LIT by an ASGDI source mounted orthogonal to the LIT [76]. Radial injection of the reagent ions requires instrument hardware modification to add the atmosphere to vacuum interface and ion optics orthogonal to the LIT reaction vessel. In order to avoid these modifications, it was beneficial to develop methods to axially inject either positive or negative ions into the LIT.

Two methods have been developed to axially inject either positive or negative ions into an axial ejection LIT—sonic spray ionization and multiple pulsed ion sources. Sonic spray ionization (SSI) [101, 102] has been shown to create both positive and negative ions in a single spray. Using electronics that switch the voltages on the ion optics, ion/ion reaction experiments using a single SSI source as the ion source for both analyte and reagent ions has been investigated [103]. An advantage of SSI is that both polarity of ions are focused into the LIT using the same set of ion optics with different voltages applied to them and the same atmosphere to vacuum interface, simplifying the instrument hardware. Conversely, a drawback of SSI as the dual polarity source is that the analyte and reagent molecules must be sprayed from the same solution, presenting an increase in the probability of matrix suppression of the analyte or reagent ions [69].

A second method to axially inject either polarity of ions into the LIT, a pulsed dual ESI source, was developed by Mcluckey and co-workers [95]. Like SSI, the pulsed dual ESI source uses a single atmosphere to vacuum interface and one set of ion optics to inject both positive and negative ions into the LIT. The source consists of a nano-ESI emitter for analyte ion formation and an ESI emitter for reagent ion formation. The nano-ESI and ESI emitters

are pulsed on and off to sequentially inject positive and negative ions into the LIT. This arrangement overcomes the matrix suppression effects of SSI because the ionization of each reactant species can be independently optimized with distinct ESI emitters. This source was shown to enable proton transfer, charge inversion, and protein-protein complex formation [95]. A similar ion source was developed that incorporated one nano-ESI and one APCI emitter that also operates in a pulsed fashion [104]. This source has been shown to enable proton transfer and ETD ion/ion reactions [104]. Using pulsed ion sources for ion/ion reactions is not limited to only two sources. A pulsed triple ionization source [96] was developed that utilizes a nano-ESI emitter for analyte ion formation with an ESI emitter and either APCI or nano-ESI for reagent ion formation. This pulsed triple ionization source can be used for sequential ion/ion reactions, such as sequential charge inversions to increase analyte ion charge state, sequential proton-transfer charge inversion and ETD of phophopeptides, and sequential ETD and proton transfer ion/ion reactions for ubiquitin identification [96].

The mass analysis of ion/ion reaction products created in ion traps has primarily been accomplished by scanning the product ions out of the ion trap. The advantages of using the ion trap for both the ion/ion reaction vessel and mass analyzer are that the instrument hardware is kept simple by not adding additional mass analyzers and that the m/z range for ion traps can be extended by resonance ejection at low q-values [54, 105]. Despite these advantages, other mass analyzers capable of higher resolution and mass accuracy are attractive for analysis of ion/ion reaction product ions. Recently, a quadrupole-TOF instrument (QSTAR XL, Applied Biosystems/MDS Sciex) was modified to make the q2 collision cell into an LIT for ion/ion reactions [75]. Proton transfer reactions, ETD, and

parallel ion parking have been demonstrated using the LIT-TOF. Other novel experiments using this LIT-TOF include combining ion/ion reactions with beam-type CID for MS^n [106]. Another mass analyzer that has been used to analyze ETD product ions is the Orbitrap [99, 107]. The ETD reactions are done in the LTQ portion of the hybrid LTQ-Orbitrap, and then the product ions are transferred to the Orbitrap for m/z analysis.

Ion Mobility Spectrometry

Ion Mobility Spectrometry (IMS) is the study of how rapidly an ion moves through a buffer gas in the presence of a uniform electric field [108]. Ion mobility measurements are performed in a drift tube consisting of alternating electrodes and insulating spacers and containing a neutral buffer gas. The electrodes are connected with a resistor chain used to create a uniform electric field down the length of the drift tube by applying DC voltages to the front and back plates of the drift tube. The electric field accelerates the ions down the drift tube, while collisions with the buffer gas slow the ions, resulting in a constant drift velocity down the length of the drift tube. The mobility of the ions, *K*, is the ratio of the drift velocity, υ_D, to the electric field, *E* [108].

$$K = \frac{\upsilon_D}{E} \qquad (1)$$

The injected ion drift tube technique, developed by Hasted and co-workers [109], is the injection of a packet of m/z selected ions that are created external to the drift tube. As the ion packet travels down the drift tube, ions with different mobilities will be separated. For polyatomic ions, the mobility is determined by the ion's average collision cross section. Ions with smaller collision cross sections encounter fewer collisions with the buffer gas and travel faster through the drift cell, while ions with larger collision cross sections encounter more

collisions and travel more slowly through the drift cell. Thus, ion mobility is a method to separate ions based on differences in collision cross section [108].

Ion Mobility Calculations. Calculating the mobilities of ions traveling through the drift tube depends on several variables. Equation 1 does not take into account the experimental parameters of normal drift tube operation. The reduced mobility, K_0, calculated using experimental parameters and adjusting the number density of the buffer gas to standard temperature and pressure, is given by

$$K_0 = \frac{L^2}{t_D V} \text{ x } \frac{273.3}{T} \text{ x } \frac{p}{760} \qquad (2)$$

where L is the length of the drift tube, t_D is the drift time (i.e. the time it takes for the ions to travel the length of the drift tube), V is the voltage drop across the drift tube, p is the pressure of the buffer gas in Torr, and T is the temperature [108].

Another important parameter that defines the energy of the ions inside the drift tube is the ratio of the electric field to the buffer gas number density (E/N). At low E/N, the drift velocity is small compared to thermal velocity, and the ions are said to be within the low-field limit. Conversely, when the mobility is dependent on E/N and the drift velocity is high compared to thermal velocity, the ions are in the high-field limit. When IMS measurements are done within the low field limit, the calculated mobility is independent of the electric field strength [108]. In the low-field limit, the mobility is calculated by

$$K = \frac{(18\pi)^{1/2}}{16} \left[\frac{1}{m} + \frac{1}{m_b}\right]^{1/2} \frac{ze}{(k_b T)^{1/2}\, \Omega_{avg}^{(1,1)}} \frac{1}{N} \qquad (3)$$

where m is the mass of the ion, m_b is the mass of the buffer gas, z is the charge on the ion, T is the temperature, N is the buffer gas number density, and $\Omega_{avg}^{(1,1)}$ is the average collision cross section. Combining equations 2 and 3, and solving for $\Omega_{avg}^{(1,1)}$ gives the equation

$$\Omega_{avg}^{(1,1)} = \frac{(18\pi)^{1/2}}{16}\left[\frac{1}{m}+\frac{1}{m_b}\right]^{1/2}\frac{ze}{(k_bT)^{1/2}}\frac{1}{N}\frac{t_DV}{L^2}\frac{760}{p}\frac{T}{273.3} \qquad (4)$$

used to calculate an ion's average collision cross section from the measured drift time and other experimental parameters [108].

Protein IMS. There are a couple of characteristics of IMS that are useful for protein analysis. Ion mobility separates ions based on cross section instead of m/z, providing an additional means of separation for ions with similar m/z but different collision cross sections. For example, it has been shown that IMS of multiply charged protein fragment ions disperses the ions in time prior to MS analysis [110]. This technique reduces the spectral congestion of the multiply charged fragment ions, helping charge state determination and ion identification. It was also shown that protein fragment ions that have a different number of residues and the same charge (i.e. a charge state family) will fall on a diagonal line in the mobility spectrum [110], giving another method to help identify the charge state of multiply charged protein fragment ions.

The other characteristic of IMS useful for protein analysis is the ability to determine an ion's average collision cross section from the IMS experimental parameters. The gas-phase conformations of protein ions can be studied by measuring the collision cross section [108, 111, 112]. Unfolded protein ions will have a larger collision cross section than folded protein ions. Studies on cytochrome *c* ions in charge states from $[M+20H]^{20+}$ to $[M+3H]^{3+}$

were conducted to calculate the collision cross sections. The higher charge states have larger collision cross sections, meaning the ions have more unfolded conformations. The low charge states have smaller collision cross sections, meaning the ions have more folded conformations. The $[M+9H]^{9+}$ to $[M+5H]^{5+}$ charge state have multiple resolvable peaks, corresponding to multiple different resolvable conformations [108]. These studies have also shown that the charge states with multiple conformations can be heated by increasing the drift tube injection energy. Heating the ions causes the more folded conformations to open up to the more unfolded conformations [108, 110]. The lowest three charge states in these studies, $[M+5H]^{5+}$ to $[M+3H]^{3+}$, were created by adding a neutral base to the desolvation region. Chapter 4 of this dissertation will discuss similar experiments investigating the gas-phase conformations of cytochrome *c* at various charge states where ion/ion reactions are used to create the lower charge state ions. All of these studies are

Ion Mobility Instrumentation. Injected ion drift tube instruments initially consisted of an ion source to generate ions, an MS to m/z select an ion, the drift tube, and a second MS with an ion detector. These instruments used several different ion sources including pulsed laser desorption [113], pulsed laser vaporization [114], MALDI [115], and ESI [112]. Clemmer and Valentine created an injection ion drift tube instrument that did not incorporate an MS prior to the drift tube [116]. This instrument had an ESI source, a desolvation region with the ability to add neutral base molecules for proton transfer ion/molecule reactions, a drift tube, and a quadrupole MS with ion detector. Chemical reactivity measurements, including H-D exchange of cytochrome *c*, collisional annealing and dissociation, and thermal annealing experiments were performed using this instrument [108, 116].

Following those studies, Clemmer and co-workers have made several advances in IMS instrumentation, several of which have been duplicated by other research groups. An important improvement was the replacement of the quadrupole MS after the drift tube with a TOF [117]. The disbursement of ions by IMS occurs on the 1 to 10 ms time scale, while TOF m/z analysis occurs on the microsecond time scale. Therefore, several m/z spectra are taken across each mobility peak. This technique is referred to as nested drift (flight) time measurements [117]. An example of a nested drift (flight) time spectrum is shown in Figure 7 [118]. Further advancements in IMS instrumentation have all been based on this initial ESI-IMS-TOF instrument. The addition of an ion trap before the drift tube as an ion accumulation/storage device improved the duty cycle of the IMS-TOF experiments [119-121]. In previous instrument designs an ion gate was used to allow a short packet of ions from the continuous ESI source into the drift tube. With the addition of an ion trap, the mobility separation is started by pulsing the ions out of the ion trap into the drift tube. Another important advancement was the addition of a collision cell between the drift tube and TOF for mobility labeling experiments [118, 122]. In these experiments, ions are separated by IMS and are sequentially fragmented in the collision cell followed by TOF MS of the fragment ions. Each of the fragment ions appears at the same drift time as the parent ion in the nested drift (flight) time spectrum. Therefore, mobility labeling allows for parallel CID experiments [118].

A different type of IMS instrument was recently made commercially available. This instrument, the SYNAPT HDMS made by Waters Corp., uses a traveling wave technology instead of the weak uniform electric field in traditional IMS [123, 124]. Experiments have been done to compare the traveling wave technology to traditional IMS. The mobility

characteristics of protein ions in the traveling wave instrument are similar to traditional IMS, but the relationship between drift time and mobility is different. Some calibrations of the traveling wave instrument are needed with ions of known cross section to be able to use the traveling wave technology for cross section measurements [124].

More recent instrumentation advancements include the construction of IMS-IMS-TOF [125, 126] and IMS-IMS-IMS-TOF [126] instruments that are the IMS analogs of MS/MS and MS/MS/MS experiments. In between the stages of IMS, the ions are mobility selected (instead of being m/z selected in an MS/MS experiment) and activated to either unfold protein ions or fragment the ions prior to the next stage of IMS [125, 126]. These instruments also incorporate ion funnels [127-129], developed by Smith and co-workers, at the end of each drift tube segment that re-focus the dispersed ion cloud near the end of the drift tube, increasing the sensitivity of IMS measurements[129]. An ion funnel placed before the drift tube is also used as an ion accumulation device in place of an ion trap [125, 126].

Dissertation Objectives and Organization

This dissertation focuses on the continued development of MS instrumentation for novel biological applications, specifically, the development of instrumentation that integrates ion/ion reaction capabilities with IMS-q-TOF analysis. Chapter 2 is a manuscript that was accepted with revisions for publication in the *Journal of the American Society for Mass Spectrometry*. This manuscript describes the construction and performance of an LIT made with primarily commercially available components. The LIT has two ion source and ion/ion reaction capabilities in either dual polarity storage mode or transmission mode. Chapter 3 is a manuscript that is ready for submission to the *Journal of the American Society for Mass*

Spectrometry. This paper describes the construction and performance of an IT-IMS-q-TOF with three independent ion sources. This instrument is the first MS to combine ion/ion reaction capabilities with IMS-q-TOF analysis. Chapter 4 is also a manuscript ready for submission to the *Journal of the American Society for Mass Spectrometry*. This manuscript describes experiments performed on the IT-IMS-q-TOF instrument constructed in our lab. The gas phase conformation of cytochrome *c* ions in multiple different charge states is investigated using proton transfer ion/ion reactions and IMS. Chapter 5 summarizes the work presented in chapters 2, 3, and 4 and discusses future research directions.

References

1. Aebersold, R.; Goodlett, D. R. Mass spectrometry in proteomics *Chem. Rev.* **2001**, *101*, 269-295
2. Barber, M.; Bordoli, R. S.; Sedgwick, R. D.; Tyler, A. N. Fast Atom Bombardment of Solids (Fab) - a New Ion-Source for Mass-Spectrometry *J. Chem. Soc.-Chem. Commun.* **1981**, 325-327
3. Sundqvist, B.; Macfarlane, R. D. Cf-252 Plasma Desorption Mass-Spectrometry *Mass Spectrom. Rev.* **1985**, *4*, 421-460
4. Fenn, J. B.; Mann, M.; Meng, C. K.; Wong, S. F.; Whitehouse, C. M. Electrospray Ionization for Mass-Spectrometry of Large Biomolecules *Science* **1989**, *246*, 64-71
5. Karas, M.; Hillenkamp, F. Laser Desorption Ionization of Proteins with Molecular Masses Exceeding 10000 Daltons *Anal. Chem.* **1988**, *60*, 2299-2301
6. Karas, M.; Gluckmann, M.; Schafer, J. Ionization in matrix-assisted laser desorption/ionization: singly charged molecular ions are the lucky survivors *J. Mass Spectrom.* **2000**, *35*, 1-12
7. Wilm, M.; Mann, M. Analytical properties of the nanoelectrospray ion source *Anal. Chem.* **1996**, *68*, 1-8
8. Yates, J. R.; Speicher, S.; Griffin, P. R.; Hunkapiller, T. Peptide Mass Maps - a Highly Informative Approach to Protein Identification *Anal. Biochem.* **1993**, *214*, 397-408
9. Mann, M.; Hojrup, P.; Roepstorff, P. Use of Mass-Spectrometric Molecular-Weight Information to Identify Proteins in Sequence Databases *Biol. Mass Spectrom.* **1993**, *22*, 338-345
10. Hunt, D. F.; Yates, J. R.; Shabanowitz, J.; Winston, S.; Hauer, C. R. Protein Sequencing by Tandem Mass-Spectrometry *Proc. Natl. Acad. Sci. U. S. A.* **1986**, *83*, 6233-6237

11. Reid, G. E.; McLuckey, S. A. 'Top down' protein characterization via tandem mass spectrometry *J. Mass Spectrom.* **2002**, *37*, 663-675
12. Washburn, M. P.; Wolters, D.; Yates, J. R. Large-scale analysis of the yeast proteome by multidimensional protein identification technology *Nat. Biotechnol.* **2001**, *19*, 242-247
13. Davis, M. T.; Beierle, J.; Bures, E. T.; McGinley, M. D.; Mort, J.; Robinson, J. H.; Spahr, C. S.; Yu, W.; Luethy, R.; Patterson, S. D. Automated LC-LC-MS-MS platform using binary ion-exchange and gradient reversed-phase chromatography for improved proteomic analyses *Journal of Chromatography B* **2001**, *752*, 281-291
14. Wolters, D. A.; Washburn, M. P.; Yates, J. R. An automated multidimensional protein identification technology for shotgun proteomics *Anal. Chem.* **2001**, *73*, 5683-5690
15. Gygi, S. P.; Corthals, G. L.; Zhang, Y.; Rochon, Y.; Aebersold, R. Evaluation of two-dimensional gel electrophoresis-based proteome analysis technology *Proc. Natl. Acad. Sci. U. S. A.* **2000**, *97*, 9390-9395
16. Simpson, R. J.; Connolly, L. M.; Eddes, J. S.; Pereira, J. J.; Moritz, R. L.; Reid, G. E. Proteomic analysis of the human colon carcinoma cell line (LIM 1215): Development of a membrane protein database *Electrophoresis* **2000**, *21*, 1707-1732
17. Kelleher, N. L.; Lin, H. Y.; Valaskovic, G. A.; Aaserud, D. J.; Fridriksson, E. K.; McLafferty, F. W. Top down versus bottom up protein characterization by tandem high-resolution mass spectrometry *J. Am. Chem. Soc.* **1999**, *121*, 806-812
18. VerBerkmoes, N. C.; Strader, M. B.; Smiley, R. D.; Howell, E. E.; Hurst, G. B.; Hettich, R. L.; Stephenson, J. L. Intact protein analysis for site-directed mutagenesis overexpression products: Plasmid-encoded R67 dihydrofolate reductase *Anal. Biochem.* **2002**, *305*, 68-81
19. VerBerkmoes, N. C.; Bundy, J. L.; Hauser, L.; Asano, K. G.; Razumovskaya, J.; Larimer, F.; Hettich, R. L.; Stephenson, J. L. Integrating "top-down" and "bottom-up" mass spectrometric approaches for proteomic analysis of Shewanella oneidensis *J. Proteome Res.* **2002**, *1*, 239-252
20. Mortz, E.; Oconnor, P. B.; Roepstorff, P.; Kelleher, N. L.; Wood, T. D.; McLafferty, F. W.; Mann, M. Sequence tag identification of intact proteins by matching tandem mass spectral data against sequence data bases *Proc. Natl. Acad. Sci. U. S. A.* **1996**, *93*, 8264-8267
21. Cargile, B. J.; McLuckey, S. A.; Stephenson, J. L. Identification of bacteriophage MS2 coat protein from E-coli lysates via ion trap collisional activation of intact protein ions *Anal. Chem.* **2001**, *73*, 1277-1285
22. Demirev, P. A.; Lin, J. S.; Pineda, F. J.; Fenselau, C. Bioinformatics and mass spectrometry for microorganism identification: Proteome-wide post-translational modifications and database search algorithms for characterization of intact H-pylori *Anal. Chem.* **2001**, *73*, 4566-4573
23. Meng, F. Y.; Cargile, B. J.; Miller, L. M.; Forbes, A. J.; Johnson, J. R.; Kelleher, N. L. Informatics and multiplexing of intact protein identification in bacteria and the archaea *Nat. Biotechnol.* **2001**, *19*, 952-957

24. Horn, D. M.; Zubarev, R. A.; McLafferty, F. W. Automated de novo sequencing of proteins by tandem high-resolution mass spectrometry *Proc. Natl. Acad. Sci. U. S. A.* **2000**, *97*, 10313-10317
25. Horn, D. M.; Zubarev, R. A.; McLafferty, F. W. Automated reduction and interpretation of high resolution electrospray mass spectra of large molecules *J. Am. Soc. Mass Spectrom.* **2000**, *11*, 320-332
26. Stephenson, J. L.; McLuckey, S. A.; Reid, G. E.; Wells, J. M.; Bundy, J. L. Ion/ion chemistry as a top-down approach for protein analysis *Curr. Opin. Biotechnol.* **2002**, *13*, 57-64
27. Fridriksson, E. K.; Beavil, A.; Holowka, D.; Gould, H. J.; Baird, B.; McLafferty, F. W. Heterogeneous glycosylation of immunoglobulin E constructs characterized by top-down high-resolution 2-D mass spectrometry *Biochemistry* **2000**, *39*, 3369-3376
28. Shi, S. D. H.; Hemling, M. E.; Carr, S. A.; Horn, D. M.; Lindh, I.; McLafferty, F. W. Phosphopeptide/phosphoprotein mapping by electron capture dissociation mass spectrometry *Analytical Chemistry* **2001**, *73*, 19-22
29. Reid, G. E.; Stephenson, J. L.; McLuckey, S. A. Tandem mass spectrometry of ribonuclease A and B: N-linked glycosylation site analysis of whole protein ions *Analytical Chemistry* **2002**, *74*, 577-583
30. Loo, J. A.; Edmonds, C. G.; Udseth, H. R.; Smith, R. D. Collisional Activation and Dissociation of Large Multiply Charged Proteins Produced by Electrospray Ionization *Anal. Chim. Acta* **1990**, *241*, 167-173
31. Loo, J. A.; Edmonds, C. G.; Smith, R. D. Primary Sequence Information from Intact Proteins by Electrospray Ionization Tandem Mass-Spectrometry *Science* **1990**, *248*, 201-204
32. Smith, R. D.; Loo, J. A.; Barinaga, C. J.; Edmonds, C. G.; Udseth, H. R. Collisional Activation and Collision-Activated Dissociation of Large Multiply Charged Polypeptides and Proteins Produced by Electrospray Ionization *J. Am. Soc. Mass Spectrom.* **1990**, *1*, 53-65
33. Loo, J. A.; Edmonds, C. G.; Smith, R. D. Tandem Mass-Spectrometry of Very Large Molecules - Serum-Albumin Sequence Information from Multiply Charged Ions Formed by Electrospray Ionization *Anal. Chem.* **1991**, *63*, 2488-2499
34. Loo, J. A.; Edmonds, C. G.; Smith, R. D. Tandem Mass-Spectrometry of Very Large Molecules .2. Dissociation of Multiply Charged Proline-Containing Proteins from Electrospray Ionization *Anal. Chem.* **1993**, *65*, 425-438
35. Lightwahl, K. J.; Loo, J. A.; Edmonds, C. G.; Smith, R. D.; Witkowska, H. E.; Shackleton, C. H. L.; Wu, C. S. C. Collisionally Activated Dissociation and Tandem Mass-Spectrometry of Intact Hemoglobin Beta-Chain Variant Proteins with Electrospray Ionization *Biol. Mass Spectrom.* **1993**, *22*, 112-120
36. Speir, J. P.; Senko, M. W.; Little, D. P.; Loo, J. A.; McLafferty, F. W. High-Resolution Tandem Mass-Spectra of 37-67-Kda Proteins *J. Mass Spectrom.* **1995**, *30*, 39-42
37. Oconnor, P. B.; Speir, J. P.; Senko, M. W.; Little, D. P.; McLafferty, F. W. Tandem Mass-Spectrometry of Carbonic-Anhydrase (29-Kda) *J. Mass Spectrom.* **1995**, *30*, 88-93

38. Wood, T. D.; Chen, L. H.; Kelleher, N. L.; Little, D. P.; Kenyon, G. L.; McLafferty, F. W. Direct sequence data from heterogeneous creatine kinase (43 kDa) by high-resolution tandem mass spectrometry *Biochemistry* **1995**, *34*, 16251-16254
39. Wood, T. D.; Chen, L. H.; White, C. B.; Babbitt, P. C.; Kenyon, G. L.; McLafferty, F. W. Sequence Verification of Human Creatine-Kinase (43 Kda) Isozymes by High-Resolution Tandem Mass-Spectrometry *Proc. Natl. Acad. Sci. U. S. A.* **1995**, *92*, 11451-11455
40. Maier, C. S.; Yan, X. G.; Harder, M. E.; Schimerlik, M. I.; Deinzer, M. L.; Pasa-Tolic, L.; Smith, R. D. Electrospray ionization Fourier transform ion cyclotron resonance mass spectrometric analysis of the recombinant human macrophage colony stimulating factor beta and derivatives *J. Am. Soc. Mass Spectrom.* **2000**, *11*, 237-243
41. Loo, J. A.; Quinn, J. P.; Ryu, S. I.; Henry, K. D.; Senko, M. W.; McLafferty, F. W. High-Resolution Tandem Mass-Spectrometry of Large Biomolecules *Proc. Natl. Acad. Sci. U. S. A.* **1992**, *89*, 286-289
42. Little, D. P.; Speir, J. P.; Senko, M. W.; Oconnor, P. B.; McLafferty, F. W. Infrared Multiphoton Dissociation of Large Multiply-Charged Ions for Biomolecule Sequencing *Anal. Chem.* **1994**, *66*, 2809-2815
43. Freitas, M. A.; Hendrickson, C. L.; Marshall, A. G. Determination of relative ordering of activation energies for gas-phase ion unimolecular dissociation by infrared radiation for gaseous multiphoton energy transfer *J. Am. Chem. Soc.* **2000**, *122*, 7768-7775
44. Ge, Y.; Horn, D. M.; McLafferty, F. W. Blackbody infrared radiative dissociation of larger (42 kDa) multiply charged proteins *Int. J. Mass Spectrom.* **2001**, *210*, 203-214
45. Zubarev, R. A.; Kelleher, N. L.; McLafferty, F. W. Electron capture dissociation of multiply charged protein cations. A nonergodic process *J. Am. Chem. Soc.* **1998**, *120*, 3265-3266
46. Zubarev, R. A.; Kruger, N. A.; Fridriksson, E. K.; Lewis, M. A.; Horn, D. M.; Carpenter, B. K.; McLafferty, F. W. Electron capture dissociation of gaseous multiply-charged proteins is favored at disulfide bonds and other sites of high hydrogen atom affinity *J. Am. Chem. Soc.* **1999**, *121*, 2857-2862
47. Kruger, N. A.; Zubarev, R. A.; Carpenter, B. K.; Kelleher, N. L.; Horn, D. M.; McLafferty, F. W. Electron capture versus energetic dissociation of protein ions *Int. J. Mass Spectrom.* **1999**, *183*, 1-5
48. Zubarev, R. A.; Horn, D. M.; Fridriksson, E. K.; Kelleher, N. L.; Kruger, N. A.; Lewis, M. A.; Carpenter, B. K.; McLafferty, F. W. Electron capture dissociation for structural characterization of multiply charged protein cations *Anal. Chem.* **2000**, *72*, 563-573
49. Mirgorodskaya, E.; Roepstorff, P.; Zubarev, R. A. Localization of O-glycosylation sites in peptides by electron capture dissociation in a fourier transform mass spectrometer *Anal. Chem.* **1999**, *71*, 4431-4436
50. Hu, Q. Z.; Noll, R. J.; Li, H. Y.; Makarov, A.; Hardman, M.; Cooks, R. G. The Orbitrap: a new mass spectrometer *J. Mass Spectrom.* **2005**, *40*, 430-443
51. McLuckey, S. A. Gas-Phase Bio-Ion/Ion Reactions: The Hows and Whys of Reagent Selection,*56th ASMS Conference on Mass Spectrometry and Applied Topics* Denver, CO, June 1-5, 2008.

52. Stephenson, J. L.; McLuckey, S. A. Ion/ion proton transfer reactions for protein mixture analysis *Anal. Chem.* **1996**, *68*, 4026-4032
53. Stephenson, J. L.; McLuckey, S. A. Ion/ion reactions in the gas phase: Proton transfer reactions involving multiply-charged proteins *J. Am. Chem. Soc.* **1996**, *118*, 7390-7397
54. Stephenson, J. L.; McLuckey, S. A. Adaptation of the Paul Trap for study of the reaction of multiply charged cations with singly charged anions *Int. J. Mass Spectrom. Ion Process.* **1997**, *162*, 89-106
55. Stephenson, J. L.; McLuckey, S. A. Simplification of product ion spectra derived from multiply charged parent ions via ion/ion chemistry *Anal. Chem.* **1998**, *70*, 3533-3544
56. Stephenson, J. L.; McLuckey, S. A. Charge manipulation for improved mass determination of high- mass species and mixture components by electrospray mass spectrometry *J. Mass Spectrom.* **1998**, *33*, 664-672
57. McLuckey, S. A.; Stephenson, J. L.; Asano, K. G. Ion/ion proton-transfer kinetics: Implications for analysis of ions derived from electrospray of protein mixtures *Anal. Chem.* **1998**, *70*, 1198-1202
58. McLuckey, S. A.; Stephenson, J. L. Ion ion chemistry of high-mass multiply charged ions *Mass Spectrom. Rev.* **1998**, *17*, 369-407
59. Wells, J. M.; Stephenson, J. L.; McLuckey, S. A. Charge dependence of protonated insulin decompositions *Int. J. Mass Spectrom.* **2000**, *203*, A1-A9
60. Reid, G. E.; Wu, J.; Chrisman, P. A.; Wells, J. M.; McLuckey, S. A. Charge-state-dependent sequence analysis of protonated ubiquitin ions via ion trap tandem mass spectrometry *Anal. Chem.* **2001**, *73*, 3274-3281
61. Newton, K. A.; Chrisman, P. A.; Reid, G. E.; Wells, J. M.; McLuckey, S. A. Gaseous apomyoglobin ion dissociation in a quadrupole ion trap: [M+2H](2+)-[M+21H](21+) *Int. J. Mass Spectrom.* **2001**, *212*, 359-376
62. Chrisman, P. A.; Newton, K. A.; Reid, G. E.; Wells, J. M.; McLuckey, S. A. Loss of charged versus neutral heme from gaseous holomyoglobin ions *Rapid Commun. Mass Spectrom.* **2001**, *15*, 2334-2340
63. Badman, E. R.; Chrisman, P. A.; McLuckey, S. A. A quadrupole ion trap mass spectrometer with three independent ion sources for the study of gas-phase ion/ion reactions *Anal. Chem.* **2002**, *74*, 6237-6243
64. Syka, J. E. P.; Coon, J. J.; Schroeder, M. J.; Shabanowitz, J.; Hunt, D. F. Peptide and protein sequence analysis by electron transfer dissociation mass spectrometry *Proc. Natl. Acad. Sci. U. S. A.* **2004**, *101*, 9528-9533
65. Silivra, O. A.; Kjeldsen, F.; Ivonin, I. A.; Zubarev, R. A. Electron capture dissociation of polypeptides in a three-dimensional quadrupole ion trap: Implementation and first results *J. Am. Soc. Mass Spectrom.* **2005**, *16*, 22-27
66. Newton, K. A.; McLuckey, S. A. Generation and manipulation of sodium cationized peptides in the gas phase *J. Am. Soc. Mass Spectrom.* **2004**, *15*, 607-615
67. Newton, K. A.; Amunugama, R.; McLuckey, S. A. Gas-phase ion/ion reactions of multiply protonated polypeptides with metal containing anions *J. Phys. Chem. A* **2005**, *109*, 3608-3616

68. He, M.; McLuckey, S. A. Two ion/ion charge inversion steps to form a doubly protonated peptide from a singly protonated peptide in the gas phase *J. Am. Chem. Soc.* **2003**, *125*, 7756-7757
69. Xia, Y.; McLuckey, S. A. Evolution of instrumentation for the study of gas-phase ion/ion chemistry via mass spectrometry *J. Am. Soc. Mass Spectrom.* **2008**, *19*, 173-189
70. Loo, R. R. O.; Udseth, H. R.; Smith, R. D. Evidence of Charge Inversion in the Reaction of Singly Charged Anions with Multiply Charged Macroions *J. Phys. Chem.* **1991**, *95*, 6412-6415
71. Loo, R. R. O.; Udseth, H. R.; Smith, R. D. A New Approach for the Study of Gas-Phase Ion-Ion Reactions Using Electrospray Ionization *J. Am. Soc. Mass Spectrom.* **1992**, *3*, 695-705
72. Scalf, M.; Westphall, M. S.; Smith, L. M. Charge reduction electrospray mass spectrometry *Anal. Chem.* **2000**, *72*, 52-60
73. Frey, B. L.; Lin, Y.; Westphall, M. S.; Smith, L. M. Controlling gas-phase reactions for efficient charge reduction electrospray mass spectrometry of intact proteins *J. Am. Soc. Mass Spectrom.* **2005**, *16*, 1876-1887
74. Yu, X.; Jin, W.; McLuckey, S. A.; Londry, F. A.; Hager, J. W. Mutual storage mode ion/ion reactions in a hybrid linear ion trap *J. Am. Soc. Mass Spectrom.* **2005**, *16*, 71-81
75. Xia, Y.; Chrisman, P. A.; Erickson, D. E.; Liu, J.; Liang, X. R.; Londry, F. A.; Yang, M. J.; McLuckey, S. A. Implementation of ion/ion reactions in a quadrupole/time-of-flight tandem mass spectrometer *Anal. Chem.* **2006**, *78*, 4146-4154
76. Wu, J.; Hager, J. W.; Xia, Y.; Londry, F. A.; McLuckey, S. A. Positive ion transmission mode ion/ion reactions in a hybrid linear ion trap *Anal. Chem.* **2004**, *76*, 5006-5015
77. Louris, J. N.; Brodbeltlustig, J. S.; Cooks, R. G.; Glish, G. L.; Vanberkel, G. J.; McLuckey, S. A. Ion Isolation and Sequential Stages of Mass-Spectrometry in a Quadrupole Ion Trap Mass-Spectrometer *Int. J. Mass Spectrom. Ion Process.* **1990**, *96*, 117-137
78. March, R. E. An introduction to quadrupole ion trap mass spectrometry *J. Mass Spectrom.* **1997**, *32*, 351-369
79. Mather, R. E.; Todd, J. F. J. The Quadrupole Ion Store (Quistor) .7. Simultaneous Positive-Negative Ion Mass-Spectrometry *Int. J. Mass Spectrom. Ion Process.* **1980**, *33*, 159-165
80. Herron, W. J.; Goeringer, D. E.; McLuckey, S. A. Ion-Ion Reactions in the Gas-Phase - Proton-Transfer Reactions of Protonated Pyridine with Multiply-Charged Oligonucleotide Anions *J. Am. Soc. Mass Spectrom.* **1995**, *6*, 529-532
81. McLuckey, S. A.; Reid, G. E.; Wells, J. M. Ion parking during ion/ion reactions in electrodynamic ion traps *Anal. Chem.* **2002**, *74*, 336-346
82. Herron, W. J.; Goeringer, D. E.; McLuckey, S. A. Product ion charge state determination via ion/ion proton transfer reactions *Anal. Chem.* **1996**, *68*, 257-262
83. Herron, W. J.; Goeringer, D. E.; McLuckey, S. A. Gas-Phase Electron-Transfer Reactions from Multiply-Charged Anions to Rare-Gas Cations *J. Am. Chem. Soc.* **1995**, *117*, 11555-11562

84. Payne, A. H.; Glish, G. L. Gas-phase ion/ion interactions between peptides or proteins and iron ions in a quadrupole ion trap *Int. J. Mass Spectrom.* **2001**, *204*, 47-54
85. Reid, G. E.; Wells, J. M.; Badman, E. R.; McLuckey, S. A. Performance of a quadrupole ion trap mass spectrometer adapted for ion/ion reaction studies *Int. J. Mass Spectrom.* **2003**, *222*, 243-258
86. Wells, J. M.; Chrisman, P. A.; McLuckey, S. A. "Dueling" ESI: Instrumentation to study ion/ion reactions of electrospray-generated cations and anions *J. Am. Soc. Mass Spectrom.* **2002**, *13*, 614-622
87. Wells, J. M.; Chrisman, P. A.; McLuckey, S. A. Formation of protein-protein complexes in vacuo *J. Am. Chem. Soc.* **2001**, *123*, 12428-12429
88. Wells, J. M.; Chrisman, P. A.; McLuckey, S. A. Formation and characterization of protein-protein complexes in vacuo *J. Am. Chem. Soc.* **2003**, *125*, 7238-7249
89. He, M.; McLuckey, S. A. Increasing the negative charge of a macroanion in the gas phase via sequential charge inversion reactions *Anal. Chem.* **2004**, *76*, 4189-4192
90. Gunawardena, H. P.; McLuckey, S. A. Synthesis of multi-unit protein hetero-complexes in the gas phase via ion-ion chemistry *J. Mass Spectrom.* **2004**, *39*, 630-638
91. Hager, J. W. A new linear ion trap mass spectrometer *Rapid Commun. Mass Spectrom.* **2002**, *16*, 512-526
92. Schwartz, J. C.; Senko, M. W.; Syka, J. E. P. A two-dimensional quadrupole ion trap mass spectrometer *J. Am. Soc. Mass Spectrom.* **2002**, *13*, 659-669
93. Londry, F. A.; Hager, J. W. Mass selective axial ion ejection from a linear quadrupole ion trap *J. Am. Soc. Mass Spectrom.* **2003**, *14*, 1130-1147
94. Coon, J. J.; Ueberheide, B.; Syka, J. E. P.; Dryhurst, D. D.; Ausio, J.; Shabanowitz, J.; Hunt, D. F. Protein identification using sequential ion/ion reactions and tandem mass spectrometry *Proc. Natl. Acad. Sci. U. S. A.* **2005**, *102*, 9463-9468
95. Xia, Y.; Liang, X. R.; McLuckey, S. A. Pulsed dual electrospray ionization for ion/ion reactions *J. Am. Soc. Mass Spectrom.* **2005**, *16*, 1750-1756
96. Liang, X. R.; Han, H. L.; Xia, Y.; McLuckey, S. A. A pulsed triple ionization source for sequential ion/ion reactions in an electrodynamic ion trap *J. Am. Soc. Mass Spectrom.* **2007**, *18*, 369-376
97. Liang, X. R.; McLuckey, S. A. Transmission mode ion/ion proton transfer reactions in a linear ion trap *J. Am. Soc. Mass Spectrom.* **2007**, *18*, 882-890
98. Liang, X. R.; Hager, J. W.; McLuckey, S. A. Transmission mode Ion/Ion electron-transfer dissociation in a linear ion trap *Anal. Chem.* **2007**, *79*, 3363-3370
99. McAlister, G.; Coon, J. J. A Dual Reaction Cell, ETD-Enabled Orbitrap Mass Spectrometer for Top-Down Proteomics,*56th ASMS Conference on Mass Spectrometry and Applied Topics* Denver, CO, June 1-5, 2008.
100. Kholomeev, A.; Makarov, A.; Denisov, E.; Lange, O.; Balshun, W.; Horning, S. Squeezing a Camel through the Eye of a Needle: a Curved Linear Trap for Pulsed Ion Injection into Orbitrap Analyzer,*54th ASMS Conference on Mass Spectrometry and Applied Topics* Seattle, WA, May 28 - June 1, 2006.
101. Hirabayashi, A.; Sakairi, M.; Koizumi, H. Sonic Spray Mass-Spectrometry *Anal. Chem.* **1995**, *67*, 2878-2882

102. Hirabayashi, A.; Sakairi, M.; Koizumi, H. Sonic Spray Ionization Method for Atmospheric-Pressure Ionization Mass-Spectrometry *Anal. Chem.* **1994**, *66*, 4557-4559
103. Xia, Y.; Liang, X. R.; McLuckey, S. A. Sonic spray as a dual polarity ion source for ion/ion reactions *Anal. Chem.* **2005**, *77*, 3683-3689
104. Liang, X. R.; Xia, Y.; McLuckey, S. A. Alternately pulsed nanoelectrospray ionization/atmospheric pressure chemical ionization for ion/ion reactions in an electrodynamic ion trap *Anal. Chem.* **2006**, *78*, 3208-3212
105. Kaiser, R. E.; Cooks, R. G.; Stafford, G. C.; Syka, J. E. P.; Hemberger, P. H. Operation of a Quadrupole Ion Trap Mass-Spectrometer to Achieve High Mass Charge Ratios *Int. J. Mass Spectrom. Ion Process.* **1991**, *106*, 79-115
106. Xia, Y.; Thomson, B. A.; McLuckey, S. A. Bidirectional ion transfer between quadrupole arrays: MSn ion/ion reaction experiments on a quadrupole/time-of-flight tandem mass spectrometer *Anal. Chem.* **2007**, *79*, 8199-8206
107. McAlister, G. C.; Phanstiel, D.; Good, D. M.; Berggren, W. T.; Coon, J. J. Implementation of electron-transfer dissociation on a hybrid linear ion trap-orbitrap mass spectrometer *Anal. Chem.* **2007**, *79*, 3525-3534
108. Clemmer, D. E.; Jarrold, M. F. Ion mobility measurements and their applications to clusters and biomolecules *J. Mass Spectrom.* **1997**, *32*, 577-592
109. Kaneko, Y.; Megill, L. R.; Hasted, J. B. Study of Inelastic Collisions by Drifting Ions *J. Chem. Phys.* **1966**, *45*, 3741-&
110. Badman, E. R.; Myung, S.; Clemmer, D. E. Gas-phase separations of protein and peptide ion fragments generated by collision-induced dissociation in an ion trap *Anal. Chem.* **2002**, *74*, 4889-4894
111. Badman, E. R.; Myung, S.; Clemmer, D. E. Evidence for Unfolding and Refolding of Gas-Phase Cytochrome c Ions in a Paul Trap *J. Am. Soc. Mass Spectrom.* **2005**, *16*, 1493-1497
112. Clemmer, D. E.; Hudgins, R. R.; Jarrold, M. F. Naked Protein Conformations - Cytochrome-C in the Gas-Phase *J. Am. Chem. Soc.* **1995**, *117*, 10141-10142
113. Hunter, J. M.; Fye, J. L.; Boivin, N. M.; Jarrold, M. F. C-120(+) Isomers from Laser-Ablation of Fullerene Films *J. Phys. Chem.* **1994**, *98*, 7440-7443
114. Jarrold, M. F.; Bower, J. E.; Creegan, K. Chemistry of Semiconductor Clusters - a Study of the Reactions of Size Selected Si+N3-24 with C2h4 Using Selected Ion Drift Tube Techniques *J. Chem. Phys.* **1989**, *90*, 3615-3628
115. Vonhelden, G.; Wyttenbach, T.; Bowers, M. T. Conformation of Macromolecules in the Gas-Phase - Use of Matrix-Assisted Laser-Desorption Methods in Ion Chromatography *Science* **1995**, *267*, 1483-1485
116. Valentine, S. J.; Clemmer, D. E. H/D exchange levels of shape-resolved cytochrome c conformers in the gas phase *J. Am. Chem. Soc.* **1997**, *119*, 3558-3566
117. Hoaglund, C. S.; Valentine, S. J.; Sporleder, C. R.; Reilly, J. P.; Clemmer, D. E. Three-dimensional ion mobility TOFMS analysis of electrosprayed biomolecules *Anal. Chem.* **1998**, *70*, 2236-2242
118. Hoaglund-Hyzer, C. S.; Li, J. W.; Clemmer, D. E. Mobility labeling for parallel CID of ion mixtures *Anal. Chem.* **2000**, *72*, 2737-2740

119. Hoaglund, C. S.; Valentine, S. J.; Clemmer, D. E. An ion trap interface for ESI-ion mobility experiments *Anal. Chem.* **1997**, *69*, 4156-4161
120. Henderson, S. C.; Valentine, S. J.; Counterman, A. E.; Clemmer, D. E. ESI/ion trap/ion mobility/time-of-flight mass spectrometry for rapid and sensitive analysis of biomolecular mixtures *Anal. Chem.* **1999**, *71*, 291-301
121. Myung, S.; Lee, Y. J.; Moon, M. H.; Taraszka, J.; Sowell, R.; Koeniger, S.; Hilderbrand, A. E.; Valentine, S. J.; Cherbas, L.; Cherbas, P.; Kaufmann, T. C.; Miller, D. F.; Mechref, Y.; Novotny, M. V.; Ewing, M. A.; Sporleder, C. R.; Clemmer, D. E. Development of high-sensitivity ion trap ion mobility spectrometry time-of-flight techniques: A high-throughput nano-LC-IMS-TOF separation of peptides arising from a Drosophila protein extract *Anal. Chem.* **2003**, *75*, 5137-5145
122. Hoaglund-Hyzer, C. S.; Clemmer, D. E. Ion trap/ion mobility/quadrupole/time of flight mass spectrometry for peptide mixture analysis *Anal. Chem.* **2001**, *73*, 177-184
123. Kanu, A. B.; Dwivedi, P.; Tam, M.; Matz, L.; Hill, H. H. Ion mobility-mass spectrometry *J. Mass Spectrom.* **2008**, *43*, 1-22
124. Pringle, S. D.; Giles, K.; Wildgoose, J. L.; Williams, J. P.; Slade, S. E.; Thalassinos, K.; Bateman, R. H.; Bowers, M. T.; Scrivens, J. H. An investigation of the mobility separation of some peptide and protein ions using a new hybrid quadrupole/travelling wave IMS/oa-ToF instrument *Int. J. Mass Spectrom.* **2007**, *261*, 1-12
125. Koeniger, S. L.; Merenbloom, S. I.; Valentine, S. J.; Jarrold, M. F.; Udseth, H. R.; Smith, R. D.; Clemmer, D. E. An IMS-IMS analogue of MS-MS *Anal. Chem.* **2006**, *78*, 4161-4174
126. Merenbloom, S. I.; Koeniger, S. L.; Valentine, S. J.; Plasencia, M. D.; Clemmer, D. E. IMS-IMS and IMS-IMS-IMS/MS for separating peptide and protein fragment ions *Anal. Chem.* **2006**, *78*, 2802-2809
127. Shaffer, S. A.; Tang, K. Q.; Anderson, G. A.; Prior, D. C.; Udseth, H. R.; Smith, R. D. A novel ion funnel for focusing ions at elevated pressure using electrospray ionization mass spectrometry *Rapid Commun. Mass Spectrom.* **1997**, *11*, 1813-1817
128. Him, T.; Tolmachev, A. V.; Harkewicz, R.; Prior, D. C.; Anderson, G.; Udseth, H. R.; Smith, R. D.; Bailey, T. H.; Rakov, S.; Futrell, J. H. Design and implementation of a new electrodynamic ion funnel *Anal. Chem.* **2000**, *72*, 2247-2255
129. Tang, K.; Shvartsburg, A. A.; Lee, H. N.; Prior, D. C.; Buschbach, M. A.; Li, F. M.; Tolmachev, A. V.; Anderson, G. A.; Smith, R. D. High-sensitivity ion mobility spectrometry/mass spectrometry using electrodynamic ion funnel interfaces *Anal. Chem.* **2005**, *77*, 3330-3339

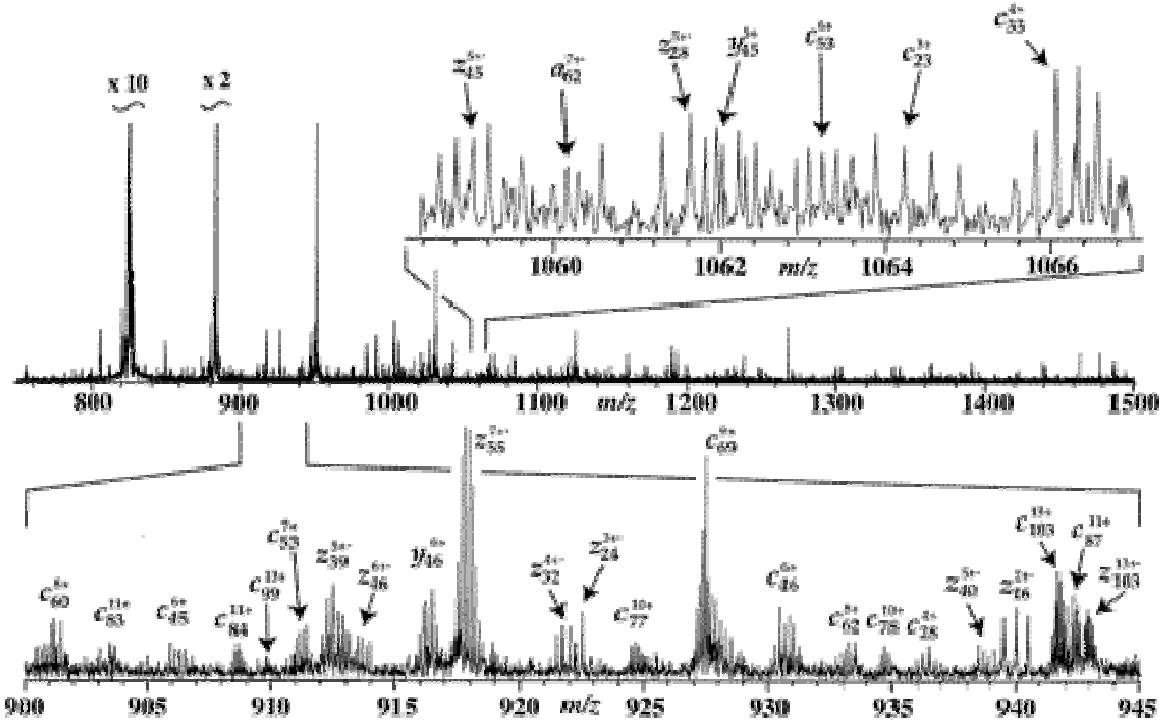

Figure 1. “ECD spectrum of 15+ ions from cytochrome *c*.” [48]

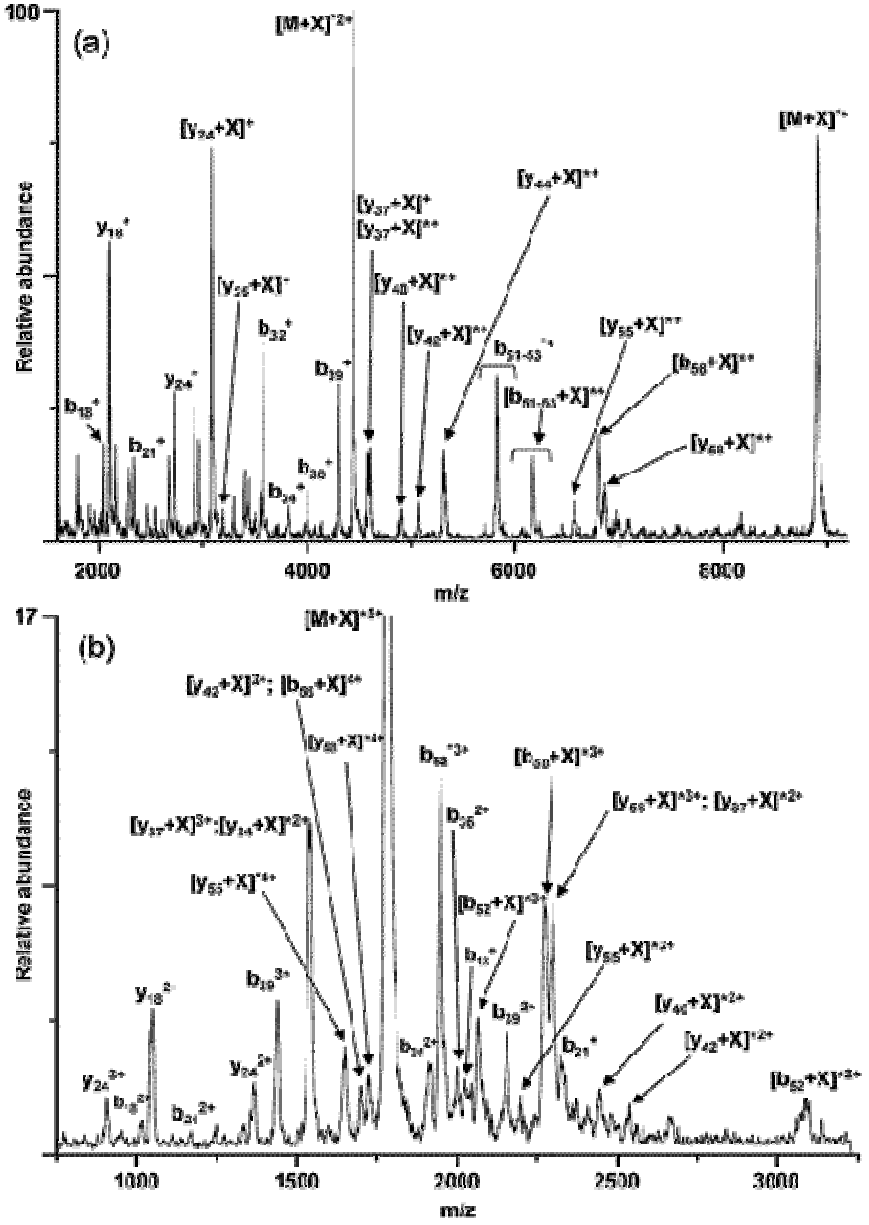

Figure 2. "(a) Charge-reduced, tandem mass spectrum of [ubiquitin + $Pt(CN)_6$ + 7H]$^{5+}$. Ubiquitin cation injection time = 300 ms; $Pt(CN)_6^{2-}$ injection time = 200 ms; ubiquitin/$Pt(CN)_6$ reaction time = 200 ms; activation for 300 ms at 89.0 kHz, 570 mV; PDCH anion injection time = 4 ms; PDCH/complex reaction time = 120 ms. Note: X = $Pt(CN)_6$, and the asterisk (*) denotes a small neutral molecule loss (NH_3 or H_2O) from the ion. (b) Pre-ion/ion MS/MS spectrum of the complex with the fragment ions labeled to shown the charge state of the fragments prior to charge reduction." [63]

Figure 3. “The three electrodes of the quadrupole ion trap shown in open array.” [78]

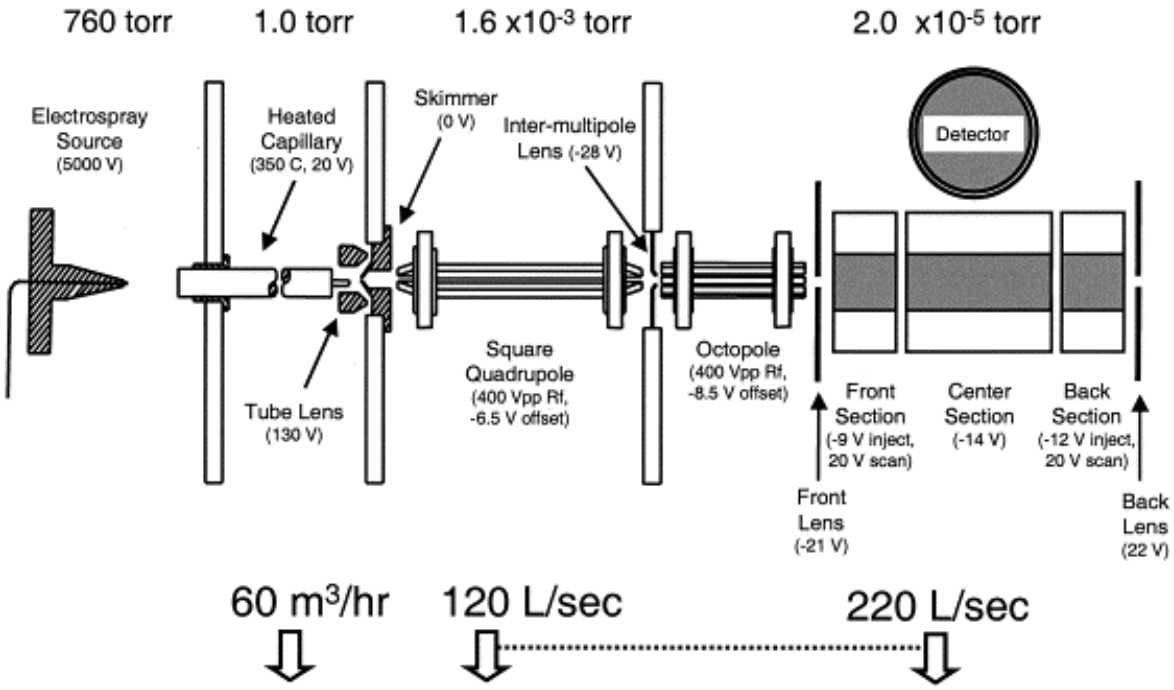

Figure 4. **"**The overall instrument configuration along with typical operating voltages and pressures." [92]

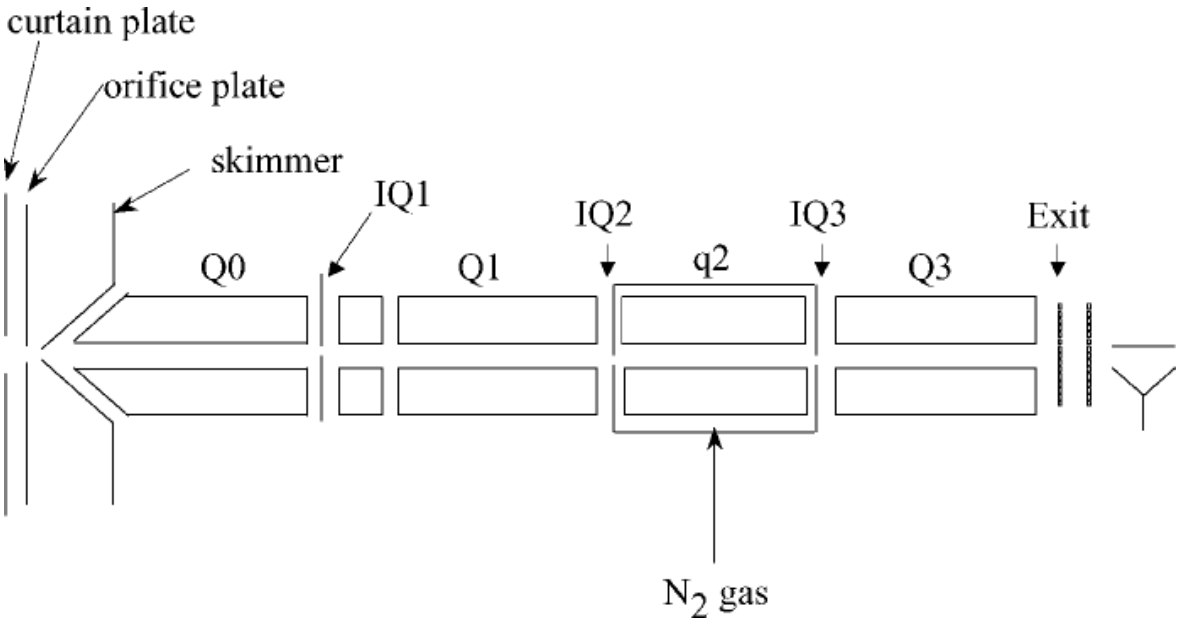

Figure 5. **“**Schematic portrayal of the experimental apparatus based on the ion path of a triple quadrupole mass spectrometer. The linear ion trap mass spectrometer was created using either q2 or Q3.” [91]

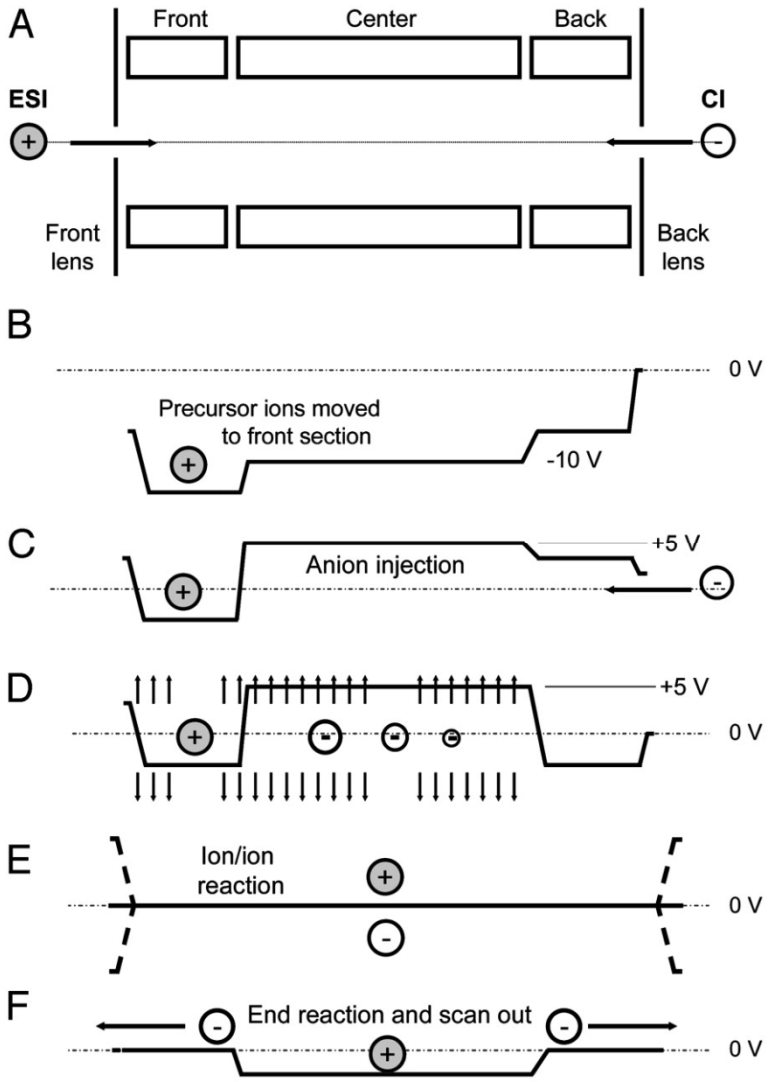

Figure 6. “Schematic of steps involved in the operation of the LTQ mass spectrometer for peptide sequence analysis by ETD. (*A*) Injection of multiply protonated peptide molecules (precursor ions) generated by ESI. (*B*) Application of a dc offset to move the precursor ions to the front section of the linear trap. (*C*) Injection of negatively charged reagent ions from the CI source into the center section of the linear trap. (*D*) Application of a supplementary dipolar broadband ac field to eject all ions except those within 3 mass-unit windows centered around the positively charged precursor ions and the negatively charged electron-donor reagent ions. (*E*) Removal of the dc potential well and application of a secondary RF voltage (100 V zero to peak, 600 kHz) to the end lens plates of the linear trap to allow positive and negative ion populations to mix and react. (F) Termination of ion/ion reactions by axial ejection of negatively charged reagent ions while retaining positive ions in the center section of the trap. This is followed by mass-selective, radial ejection of positively charged fragment ions to record the resulting MS/MS spectrum.” [64]

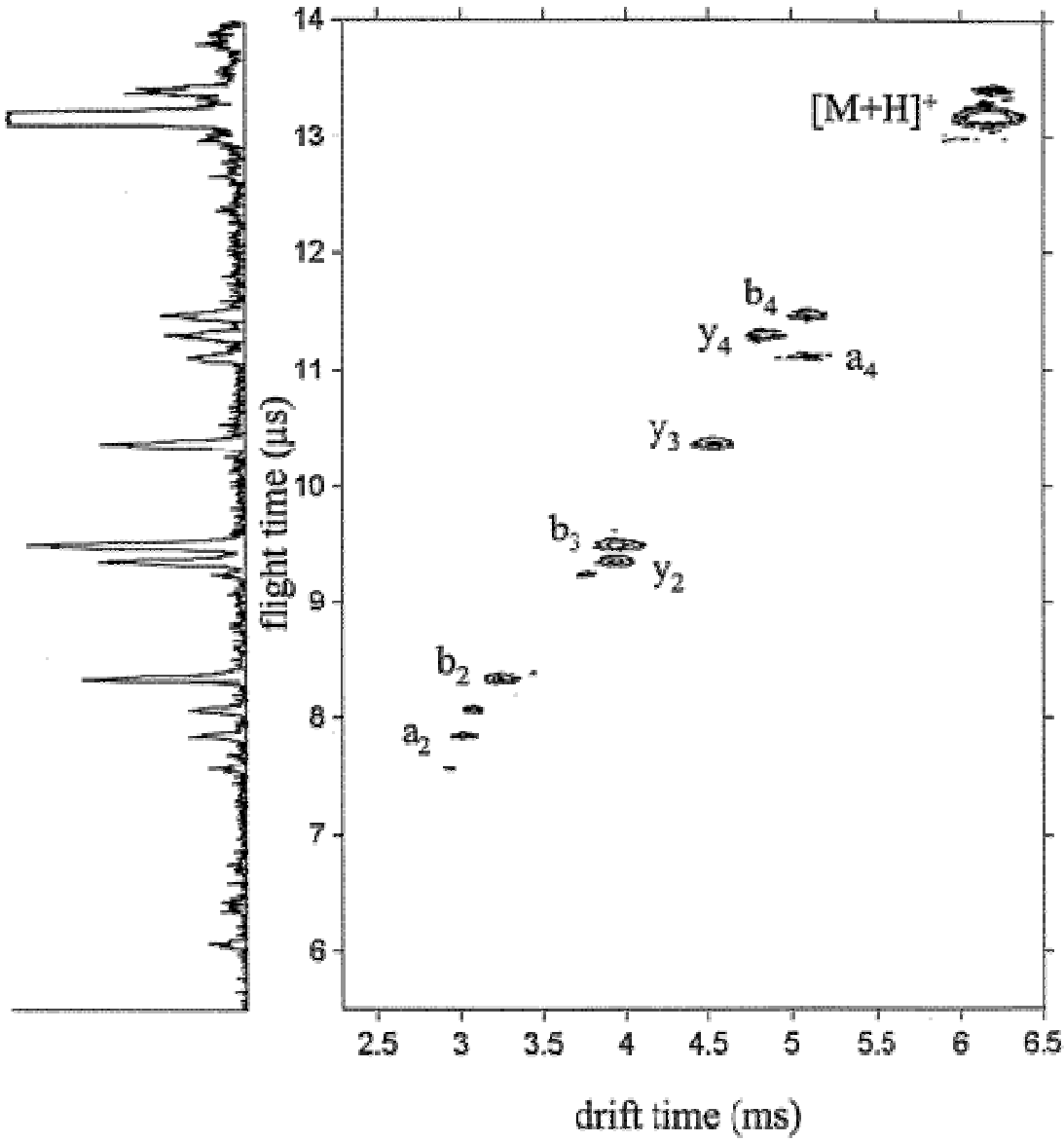

Figure 7. **"**Two-dimensional contour plot of nested drift (flight) time data for a mixture of ions formed from electrosprayed [D-Ala^{2,3}]methionine enkephalin. These data were recorded with no gas in the octopole collision cell. The contours are shown on a 10-point scale; this removes all features that contain fewer than 10 ion counts. The distribution includes a series of a-, b-, and y-type fragment ions that are formed upon high-energy injection into the drift tube (see text). The drift time axis has been normalized to a helium pressure of 2.70 Torr. Also shown (left) is the time-of-flight mass spectrum obtained by integrating the flight time data over the drift time range. (Data are plotted on a normalized intensity scale so that peak heights can be compared directly with the data in Figure 3.) The resolving power along the flight time axis is typically 200 ($m/\Delta m$ of a peak for a singly charged ion, where Δm is determined at half-maximum). Along the drift time axis, the resolving power ($t/\Delta t$, where Δt is determined at half-maximum) is between 20 and 30, for all peaks." [118]

CHAPTER 2.

A Linear Ion Trap Mass Spectrometer with Versatile Control and Data Acquisition for Ion/Ion Reactions

Matthew W. Soyk*†, Qin Zhao*, R.S. Houk*†, and Ethan R. Badman‡

*Iowa State University, Department of Chemistry, Ames, IA 50011 USA

†Ames Laboratory, U. S. Department of Energy, Ames, IA 50011 USA

‡Hoffman-La Roche Inc., Non-Clinical Safety, 340 Kingsland St., Nutley, NJ, 07100 USA

A manuscript accepted for publication in the *Journal of the American Society for Mass Spectrometry*, 2008, *published online* DOI: 10.1016/j.jasms.2008.08.020.

Abstract

A linear ion trap (LIT) with electrospray ionization (ESI) for top-down protein analysis has been constructed. An independent atmospheric sampling glow discharge ionization (ASGDI) source produces reagent ions for ion/ion reactions. The device is also meant to enable a wide variety of ion/ion reaction studies. To reduce the instrument's complexity and make it available for wide dissemination, only a few simple electronics components were custom built. The instrument functions as both a reaction vessel for gas-phase ion/ion reactions, and a mass spectrometer using mass-selective axial ejection. Initial results demonstrate trapping efficiency of 70 to 90% and the ability to perform proton transfer reactions on intact protein ions, including dual polarity storage reactions, transmission mode reactions, and ion parking.

Introduction

Linear quadrupole ion traps (LITs)[1] have been a subject of recent interest, primarily because of their higher performance compared to 3d ion traps. Until recently, LITs were mainly used as ion storage devices or as collision cells for tandem mass spectrometry (MS/MS) preceding another type of mass analyzer (e.g. TOF[2, 3] or FT-ICR[4, 5]). Compared to 3d traps, LITs offer higher injection efficiency (<10% vs. almost 100%, respectively) and, because of their larger volume, higher ion storage capacity, while still maintaining the ability to perform MS^N in a single device. More recently, two major innovations have led to widespread use of LITs as mass analyzers: radial[6] or axial[7] ejection methods. These LIT's still have high trapping efficiency and storage capacity, with the added benefits of mass analysis in a single device [8].

For top-down protein analysis, linear and 3d ion traps cannot achieve the ultrahigh mass resolution and accuracy of FT-ICR[9] or Orbitrap instruments[10] necessary to resolve and unambiguously identify the isotopic distributions of highly multiply-charged ions. However, traps are well-suited to ion/ion reactions [11-13] like proton transfer to simplify the resulting complex, overlapping product ion spectra. Electron transfer dissociation (ETD)[11] ion/ion reactions also provide an alternative tool for protein ion dissociation. Ion/ion reaction experiments have been carried out in both types of LITs, and although ETD capabilities are becoming more readily available on commercial ion traps, proton transfer reaction capabilities are not yet commercially available.

In addition, many researchers would like greater control and flexibility over instrumental parameters than is typically available in commercial devices, especially for

fundamental experiments and development of new methods. Here we discuss the development of an electrospray ionization (ESI)-linear ion trap mass spectrometer that has been constructed to enable complete control over all functions of the device. Mass scanning by radial ejection requires machining an exit slit and channel in at least one of the quadrupole rods. To simplify measurement of mass spectra and allow the future addition of subsequent components, e.g., ion mobility and time of flight analysis, this device is operated using mass-selective axial ejection (MSAE) [14]. Commercially available components were used primarily to reduce the complexity of the development and allow wide dissemination of this device to other researchers. Initial performance characteristics for MS and gas phase ion/ion reactions are described, as well as future uses for this device in bioanalytical MS and as a source for ion mobility-TOF instruments.

McLuckey and co-workers have demonstrated the great value of commercial LITs with multiple pulsed ion sources, e.g. positive ESI for analyte ion formation plus negative ESI,[15-18] negative atmospheric pressure chemical ionization,[16, 18-21] or negative atmospheric sampling glow discharge ionization (ASGDI)[12, 22] for reagent ion formation. The present paper demonstrates the first work using an LIT with multiple continuous ion sources interfaced through a turning quadrupole that has proven valuable with 3d ion traps [23, 24].

Experimental

Cytochrome *c*, ubiquitin and trypsin were purchased from Sigma-Aldrich (St. Louis, MO) and were used without further purification. Solutions of proteins were prepared at 20 to 30 μM in 1% aqueous acetic acid solutions for positive nano-ESI. Nano-ESI ionization

emitters were pulled from glass capillaries (1.5 mm o.d., 0.86 mm i.d.) with a micropipette puller (Model P-97, Sutter Instruments, Novato, CA). The nano-ESI voltage was +1 kV to +1.2 kV applied to a stainless steel wire through the back of the capillary. Perfluoro-1, 3-dimethylcyclohexane (PDCH) was purchased from Sigma-Aldrich (St. Louis, MO) and was used as the reagent ion for proton transfer ion/ion reactions. The PDCH was ionized using an ASGDI source identical to that described by Zhao and co-workers [25].

Instrumentation

Figure 1 shows a schematic diagram of the LIT with two ion sources: one ESI and one pulsed ASGDI source that are interfaced to the LIT through a quadrupole deflector. It should be noted that a third ion source could be added to the blank flange of the ion source cube shown in Figure 1. The LIT is a standard quadrupole mass filter modified to enable LIT functionality. Ions are detected with a conversion dynode/electron multiplier. Instrument control is via a commercially available ion trap controller and software. Figure 2 shows a schematic diagram of how the ion trap controller and software communicate with and control all components of the LIT. Details about each part of the instrument are given below.

Vacuum System. The two ion sources and ion optics are housed in an 8" conflat cube, and the LIT is housed in an 8" conflat 5-way cross. One turbo pump (Turbo-V550 MacroTorr, 550 l/s N_2, Varian Inc., Palo Alto, CA) is attached to the top of the cube that houses the ion sources, and a second, identical turbo pump is attached to the 5-way cross that houses the LIT. The turbo pump on the source cube is backed by a SD-301 mechanical pump (Varian Inc., Palo Alto, CA), and the turbo pump on the LIT 5-way cross is backed by an

E2M40 mechanical pump (BOC Edwards, Wilmington, MA). The chamber pressure is measured by a Micro-Ion Gauge (Helix Technology, Longmont, CO). The baseline pressure of the system is ~5 x 10^{-7} mbar.

Ion Sources and Ion Optics. Both ion sources have been described [24, 25]. Typical pressures in the ion source interface regions (i.e. behind the first 254 μm aperture to atmosphere and before the second 381 μm aperture to the high vacuum region) are 0.90 mbar and 0.80 mbar for the nano-ESI and ASGDI source, respectively. Each is pumped by a separate E2M40 mechanical pump. The pulsed ASGDI was initiated via a -400 V high voltage pulse supplied via a power supply (Model 556, Ortec, Oak Ridge, TN) through a fast pulser (Model PVX4150, Directed Energy Inc., Fort Collins, CO). Voltages for the interfaces and the first three lenses are supplied via 9 output power supplies (Model TD9500, Spectrum Solutions, Russelton, PA). The voltages on the quadrupole deflector (Model 81989, Extrel CMS, Pittsburgh, PA) and on the three lenses between the quadrupole deflector and the LIT are supplied via additional 9 output power supplies, but are switched using a computer-controlled fast relay switch to enable ions from each source to be focused separately to the LIT as required. The ASGDI source is the default ion source. A single TTL trigger is used to switch the optics to allow ESI ions to enter the trap, and a second TTL trigger is used to pulse on the ASGDI discharge.

Linear Ion Trap. The LIT is a commercially available tri-filter quadrupole in a collision cell housing (r_0 = 9.5 mm, Extrel CMS, Pittsburgh, PA). The rf trapping voltage is supplied by a standard Extrel 300 W rf only power supply providing 3600 $V_{0\text{-}p}$ (pole to

ground) at 880 kHz. In order to operate the quadrupole as an LIT, and perform MSAE [14] and MS/MS experiments, modifications were made to the quadrupole and rf electronics.

As described by Paul,[26] additional waveforms can be added to quadrupole rods to resonantly excite ions. Douglas and coworkers [2, 3] add dipolar excitation across a pair of opposite quadrupole rods to excite trapped ions for collision-induced dissociation and MS/MS. We implemented dipolar excitation by cutting the connections between one set of rods and add an extra rf post and hole through the collision cell housing. To add the dipolar excitation voltage to the rf trapping voltage on one set of rods, a toroidal transformer was used. The toroid (Model 5977003801, Fair-Rite, Wallkill, NY) was housed in a metal casing outside the vacuum chamber. The turn ratio between the primary and secondary was 1:1 using 16 turns of 22 gauge magnet wire (Belden Corporation, Chicago, IL). One of the outputs of the rf power supply was connected to the center tap of the secondary. The outputs of the secondary are then fed to the quadrupole rods through rf feedthroughs (Model 810998, Extrel CMS, Pittsburgh, PA). One side of the primary was grounded, and the other was connected to the waveform generator.

The MSAE and MS/MS waveforms were generated from the ion trap controller. The original 5 $V_{0\text{-}p}$ was amplified to 35.5 $V_{0\text{-}p}$ using a custom amplifier (PA09 op-amp, Apex Microtechnology, Tucson, AZ) and applied to the primary of the transformer through a 50 Ω, 51 W resistor.

Two additional modifications to the quadrupole were required for effective trapping and m/z analysis. The post-filter was removed, and the pre-filter was shorted to the center quad section. The center rod section is the only section that is aligned with high precision. Therefore, removing the post-filter ensures that the fringe fields necessary for MSAE occur

between the optimally-aligned center rod section and the exit aperture IQ2. Shorting the front and center sections together applies the full rf voltage to the entire trapping length and minimizes ion loss (from unequal potential well depths) as ions are trapped. This modification is especially important during charge reduction ion/ion reactions. As ions with a lower z –and correspondingly higher m/z—are formed, they will reside in increasingly shallower potential wells. Without the full rf voltage on both the center and the pre-filter section, ions at high m/z are no longer trapped and are lost.

DC voltages (0-4 V) from an Argos ion trap controller (described in detail below) are amplified to ± 200 V (PA97 op-amp, Apex Microtechnology, Tucson, AZ), and controlled in the scan function with the ion trap controller. These dc voltages are applied to the entrance and exit lenses (IQ1, IQ2) and LIT rods (Q). The IQ1 and IQ2 lenses are 8 mm diameter and both are covered with nickel mesh (90% transparency, 70 lines per inch, InterNet Inc., Anoka, MN) on the interior side of the lenses. The distance from the IQ1 lens to the end of the quadrupole rods is ~5 mm. The IQ2 lens was modified to make the distance from the lens to the end of the quadrupole rods ~2 mm.

In order to fully resonate the rf power supply after adding the toroidal transformer and changing the arrangement of the quad sections, the overall capacitance of the load was reduced by the following measures. 1) The original rf cable between the power supply and the transformer was shortened by 53 cm, from 166.3 cm to 113.3 cm. 2) the magnet wire used in the toroidal transformer was covered with Teflon tubing (1.7 mm O.D., 1.1 mm I.D.). 3) A 3 pF capacitor in the rf power supply near the output on both the toroid and non-toroid sides was removed. 4) The tap of the rf coil was moved to remove 2.25 turns on the toroid

side and 1 turn on the non-toroid side. By performing these steps, the power supply could generate nearly the maximum original rf voltage, as read by the internal feedback circuit.

To make sure similar rf voltages were applied to each of the quadrupole rods, two duplicate rf detector circuits identical to those used by the Extrel power supply were built. These devices convert the rf voltage to a current that can be read with a digital multimeter. Using this method, the two sides of the rf output could be tuned to be within 1.99 ± 0.25% of each other, limited by the accuracy of the digital multimeter.

The nitrogen buffer gas pressure in the LIT is adjusted using a variable leak valve (Model 203, Helix Technology, Longmont, CO) and measured by the pressure in the main chamber using the Micro-Ion Gauge. During a typical experiment, the chamber pressure is maintained at ~1.3×10^{-4} mbar with both sources open and nitrogen gas added to the LIT. Of course, the pressure inside the LIT is higher than that measured by the ion gauge. From the sizes of the IQ1 and IQ2 lenses (8 mm diameter), the 90% mesh covering the lenses, the measured pressure in the vacuum chamber (1.3×10^{-4} mbar), and the pumping speed (550 l/s), the pressure inside the LIT is estimated to be 5×10^{-3} mbar, assuming effusive flow out of IQ1 and IQ2.

Mass spectra are acquired using MSAE by ramping the rf voltage while applying a dipolar resonance excitation frequency and a small, constant, repulsive voltage to IQ2 (typically +1 to +3 V for positive ions), while the dc voltage on the LIT rods is kept at ground. Ejected ions are detected with an electron multiplier with conversion dynode (402A-H, Detector Technology Inc., Palmer, MA). Scans were measured only in the forward direction, from low m/z to high m/z.

Modifications for Ion/Ion Reactions with Dual Polarity Trapping. In order to perform dual polarity storage mode ion/ion reactions, and store both positive and negative ions simultaneously, AC voltages are applied to IQ1 and IQ2 during PDCH injection and subsequent reaction time [11]. This axial trapping voltage is generated via a multifunction PC card (Model 6251, National Instruments, Austin TX) with custom software written in Labview 8.0. The frequency and amplitude are set in the software—and are, therefore, fixed during an experiment—and the waveform is switched on and off via a TTL trigger (1 μs delay). The initial 0-5 $V_{0\text{-}p}$ sine wave is amplified via a custom amplifier (PA90, Apex Microtechnology, Tucson, AZ) up to 175 $V_{0\text{-}p}$ and split into two 180° out-of-phase signals. The ac voltages are added to the dc voltage for IQ1 and IQ2 using a simple mixer circuit. Typically, the waveform is applied at 100 kHz, with an amplitude of ~50 $V_{0\text{-}p}$, empirically determined to minimize ion loss during the reaction period. The amplitude and frequency of this waveform are lower than those used by McLuckey and coworkers [17].

In the first scan function segment of a dual polarity trapping ion/ion reaction, three processes are done simultaneously—the dc potentials on the IQ1 and IQ2 lenses are set to 0V (the same potential as the quadrupole rods), the axial trapping waveform is turned on, and the ASGDI source is pulsed on. In the second segment, the ASGDI source is turned off, and the analyte and reagent ions are allowed to react. To end the reaction, the axial trapping waveform is turned off and the dc potentials on the IQ1 and IQ2 lenses are, simultaneously, set to repel (i.e., trap) the positive analyte ions, while excess negative reagent ions are ejected out both ends of the LIT.

Ion/Ion Reactions in Transmission Mode and Ion Parking. Another method for enabling ion/ion reactions, transmission mode reactions, has been described previously [15, 19]. Transmission mode reactions are enabled by trapping the analyte ions using small repulsive dc voltages (typically 2 to 5 V) on the IQ1 and IQ2 lenses and passing the reagent ions, continuously generated by the ASGDI source during the reaction time, through the population of trapped analyte ions. Any unreacted reagent ions pass completely through the LIT and are lost. Ending the transmission mode reactions simply requires turning off the ASGDI source, thus turning off the reagent ion beam. The reaction product ions remain trapped in the LIT because they are the same polarity as the unreacted analyte ions.

Ion/ion reactions carried out using this method do not require the use of the axial trapping waveform, and there is only one scan segment for the reaction period. Therefore, the scan function for transmission mode ion-ion reactions is simpler than that for dual polarity trapping ion-ion reactions. Additionally, the electronics required to add the dual polarity trapping waveform to the containment lenses are not required, making the LIT hardware for transmission mode reactions much simpler than that for dual polarity storage mode reactions.

Ion parking [27] is a technique that was developed by McLuckey and co-workers in which the rate of reaction for ions at a single m/z value [27] or multiple m/z values [28, 29] are selectively reduced. Increasing the relative velocity of reactant ions, which reduces the ion/ion reaction capture cross section, during an exothermic ion/ion reaction decreases the rate of reaction between those ions [27]. To enable ion parking, a low amplitude auxiliary sine wave (~$1V_{0\text{-}p}$, ~ 40 kHz for the ions chosen here) is added to the x-rods of the LIT during the ion/ion reaction period. The auxiliary sine wave resonantly excites a particular product ion formed during the ion/ion reaction. The frequency and amplitude of the sine

wave are chosen so that the ion being parked is excited enough to inhibit the reaction rate but not so much that it is ejected from the LIT. These values are fine-tuned empirically to produce the desired results. As the reaction proceeds and the ion chosen to be parked is formed, it is resonantly excited by the applied auxiliary sine wave. The velocity of the excited ion relative to the reagent anion increases, thereby reducing its ion/ion reaction rate and minimizing further reaction. For the proton transfer ion/ion reactions on intact protein ions studied here, the result of an ion parking experiment is the concentration of most of the ions into a single charge state below that of the original ions.

Electronics. An Argos ion trap controller (Griffin Analytical Technology, West Lafayette, IN) controls the entire instrument and acquires data. The scan function is generated by the Argos software. TTL pulses ("relays") trigger the ASGDI source, switch the fast relay switch to enable injection of oppositely-charged ions, and toggle on the ion/ion trapping voltage. The two waveform outputs control the rf level (0-10 V control 0-3600 $V_{0\text{-}p}$ of rf) and generate MS/MS waveforms, respectively. Different from previous versions of the Argos software, this version provides time dependent dc voltages (0-4 V "registers") that control the voltages applied to IQ1, IQ2, and the LIT rods.

Data are acquired using the Argos data input (at a 250 kHz sampling rate), but as a result, the data acquisition time is limited to 250 ms or less. Primarily, this limits the ability to perform slow mass scans over a wide mass range.

Results and Discussion

LIT Performance. Initial characterization of the LIT includes determination of trapping efficiency, ion capacity, mass analysis efficiency, and measurement of mass accuracy. To determine the trapping efficiency, ions are gated into the trap for a specified time, cooled, and then dumped to the detector (in a non-mass selective manner) by dropping the IQ2 voltage. The response from the trapped ions is then compared to the response acquired during operation of the quadrupole as an rf-only ion guide for the same time as the trap fill time at the same rf level.

Table 2 shows trapping efficiencies at 4 different fill times for positive ions of cytochrome *c* and trypsin generated by ESI. Efficiencies average 83% with a range from 68 to 92%. These values agree with those determined previously from other LIT instruments [6, 7].

Figure 3 shows a plot of total ion current (TIC) vs. LIT fill time for cytochrome *c* that is used to measure the ion capacity of the LIT. The response is nearly linear from 5 to 40 ms, after which the signal levels off. The ion current on IQ1 was then measured—with all LIT and ion detector voltages turned off—using a picoammeter (Model 6485, Keithley Instruments, Cleveland, OH) to determine the real number of ions delivered to the trap. It was assumed that the rate of ions that strike the wires of the Ni mesh covering IQ1, after accounting for the 90% transmission, approximates the rate at which ions are delivered to the LIT during the fill step of a trapping experiment. Using the average measured ion current from the IQ1 Ni mesh (7.97 pA), the correction for the 90% transmission, the fill time at which the response levels off (40 ms), the measured trapping efficiency (83%), and the average charge state of the cytochrome *c* ions used for the measurement (+8.5), it was

determined that approximately $1.9x10^6$ ions can be trapped in the LIT. The maximum total charge in the LIT is thus ~ $1.6x10^7$ charges. In order to avoid space charge effects, the LIT is not filled to this capacity during normal operation.

Mass Spectra. A typical protein mass spectrum taken using MSAE is shown in Figure 4. The inset of Figure 4 shows the peak shape for the +9 charge state of cytochrome *c*. This peak has a full-width at half maximum (fwhm) of 1.11 Th, corresponding to a resolution of 1230. The measured fwhm from the LIT is about 1.4x larger than the calculated width of the isotopic envelope (0.77 Th, fwhm). Of course, resolving the isotopic distribution of this peak requires resolution in excess of ~18000 (50% valley).

Table 1 shows the trapping voltages and ejection conditions used to take the spectrum shown in Figure 4. These operating conditions are typical for mass spectra taken with the LIT. The spectrum in Figure 4 shows adduct or impurity peaks at 54 Da, 90 Da, and 130 Da above each protein peak. The scan function used to generate this spectrum includes a heating ramp in which a 1.9 $V_{0\text{-}p}$, 150 kHz sine wave is applied to the x-rods while the rf amplitude is ramped to bring the protein ions into resonance with the applied sine wave. Thus the ions are heated, and the adducts/impurities are dissociated. Without this heating ramp, the overall protein peak is very wide, encompassing the protein and all the adduct/impurity ions into a single wide peak. The adduct/impurity peaks could not be totally eliminated without severely reducing the intensity of the protein peak. It should also be noted that these same adduct peaks are seen from the same protein samples on another home-built MS in our lab [25].

The mass analysis efficiency is measured using a similar procedure as the trapping efficiency measurement. Protein ions are gated into the LIT for a specified time, cooled, and non-mass selectively emptied to the detector by dropping the potential on IQ2. In a second experiment, protein ions are gated into the LIT for the same specified time—ensuring that the number of ions inside the trap is approximately the same for both experiments—cooled, and mass analyzed using MSAE. The ratio of the TIC of the ions ejected under MSAE conditions to the TIC of all the ions trapped (measured by non-mass selectively ejecting ions) yields an average measured MSAE efficiency of 7.4±2.2%. Using the average measured MSAE efficiency and the overall length of the LIT (18.7 cm), it was calculated that the extraction region is 18.7 x 0.074 = 1.4 cm long. The measured efficiency and extraction region length are less than the results obtained by Hager [7] at similar LIT pressure. Conversely, the measured MSAE efficiency is slightly higher than recent results obtained by Douglas and co-workers [30]. Our measured efficiency may be higher due to higher pressure in the LIT and the lower spectral resolution than in the results recorded by Douglas.

Table 2 shows MSAE efficiency measurements for different fill times of cytochrome *c* and trypsin. The data shows that as fill time increases the MSAE efficiency decreases. Space charge effects may degrade the MSAE efficiency at longer fill times.

Mass accuracy was determined by spraying a 50:50 mixture of cytochrome *c* and ubiquitin. The peak maxima for $[M+9H]^{9+}$ and $[M+8H]^{8+}$ of the cytochrome *c* ions (m/z ~ 1360 and 1530) were used to calibrate the m/z axis and the m/z at the peak maxima of $[M+7H]^{7+}$ and $[M+6H]^{6+}$ ions of ubiquitin (m/z ~ 1224 and 1429) were measured. Measured mass accuracies range from 900 to 2200 ppm. The accuracy limitations are likely due to voltage stability for the rf trapping voltage, resonance excitation voltage, and/or IQ2 dc

voltage. The use of calibrant ions in a m/z window that span that of the analyte may also improve mass measurement accuracy.

To illustrate the performance of the LIT as a mass analyzer at moderate m/z values, a spectrum of the PDCH reagent anions from the glow discharge source is shown in Figure 5a. These ions are a mixture of $[M-F]^-$ and $M^{-\cdot}$ [31]. The inset shows the peak shape and resolution for the $[M-F]^-$ ion. The ^{13}C isotope peak is cleanly resolved from the main peak at m/z 381. The nominal resolution value $m/\Delta m$ = ~1080 at fwhm.

It should be noted that nonlinear resonance ejection peaks can be seen under certain conditions. These "ghost peaks" [32] occur at a q_z value of 0.64 (β=0.5 or 220 kHz in this system) consistent with octopolar field ejection [33]. Use of resonance ejection frequencies near this nonlinear resonance can produce asymmetric or split peaks. Therefore, the resonance ejection frequency is selected to avoid this nonlinear resonance value.

Dual Polarity Trapping Mode Ion/Ion Reactions. The application of the dual polarity storage mode waveform used for ion/ion reactions is similar to that described previously [11]. The dual polarity storage mode proton transfer ion/ion reaction scan function consists of the following steps: filling the trap with protein cations, a cooling segment, a heating ramp to eliminate adduct peaks from the protein, another cooling segment, a PDCH fill segment, an additional reaction segment, a final cooling segment, and mass analysis.

The results of such a dual polarity storage mode reaction between trypsin positive ions and negative PDCH ions are shown in Figure 5. The mass spectrum of the trypsin ions formed directly from ESI is shown in Figure 5b. The main ions observed under these sample and source conditions are the $[M+11H]^{11+}$ and $[M+10H]^{10+}$ charge states, with small amounts

of the $[M+9H]^{9+}$ and $[M+12H]^{12+}$ charge states. In the subsequent parts of Figure 5, the LIT is also filled with negative ions from PDCH (Figure 5a) for either 15 or 20 ms. The PDCH fill step is followed by a period of dual polarity storage where the positive trypsin ions and negative PDCH ions are allowed to react further. The amplitude of the LIT rf voltage during the ion/ion reaction periods is set at 360 V_{0-p}, leaving the most abundant PDCH ion ($[M-F]^-$) at q=0.74. This amplitude rf was empirically chosen to maximize the amount of high mass product ions that are trapped while still trapping the PDCH reagent ion. The dual polarity trapping waveform added to IQ1 and IQ2 during the ion/ion reaction periods is a 100 kHz sine wave with an amplitude of 50 V_{0-p}.

A PDCH fill time of 15 ms and additional reaction time of 100 ms converts the trypsin ions shown in Figure 5a to the $[M+3H]^{3+}$, $[M+2H]^{2+}$, and $[M+H]^+$ charge states (Figure 5c). Continuing the reaction for times in excess of 100 ms does not result in further conversion of trypsin ions to lower charge states (data not shown). Thus, all the PDCH anions that were trapped in a 15 ms fill time have been reacted after a 100 ms reaction.

Figure 5d results when this dual polarity storage mode reaction experiment is repeated with a PDCH fill time of 20 ms and an additional reaction time of 100 ms. The multiply charged trypsin ions from Figure 5b are converted to primarily $[M+H]^+$, m/z = ~24,000. The fwhm of the peak for this ion is 673 Th, and the resolution is 34. At this time, the $[M+H]^+$ ion of trypsin is the highest m/z ion created and ejected from this LIT. To achieve the mass range extension required to eject the $[M+H]^+$ ion of trypsin, a 35 kHz sine wave was added to the LIT rods during the mass scan. The amplitude of this resonant excitation sine wave was ramped from 8.9 V_{0-p} to 24.8 V_{0-p}. The dc voltage on the IQ2 lens was set to be 2.5 V relative to the LIT rod bias (0 V dc).

Transmission Mode Ion/Ion Reactions. Results of proton transfer ion/ion reactions of multiply charged ubiquitin cations with PDCH anions are shown in Figure 6. During the transmission mode reaction period, the amplitude of the LIT rf voltage is set at 360 $V_{0\text{-}p}$, leaving the most abundant PDCH ion ($[M\text{-}F]^-$) at q=0.74, an equivalent value to dual polarity trapping mode experiments. Also, injecting reagent anions at high q-values results in the greatest spatial overlap between the analyte and reagent ions, maximizing the ion/ion reaction rate [15, 19]. The dc voltages on IQ1 and IQ2 were set at 3 V repulsive relative to the rod dc bias (0 V).

Figure 6a shows the mass spectrum of ubiquitin obtained directly from ESI. The solution and ESI source conditions yield ubiquitin ions primarily in the $[M+6H]^{6+}$ to $[M+8H]^{8+}$ charge states. As shown in Figure 6b, transmission mode reaction with PDCH anions for 40 ms converts approximately half these ions to the $[M+3H]^{3+}$ to $[M+5H]^{5+}$ charge states, while the other half of the ions are lost. Extending the reaction period to 70 ms converts the ions to roughly equal amounts of $[M+H]^+$ and $[M+2H]^{2+}$ (Figure 6c). In the latter experiment, continuing the reaction long enough to reduce the ions to $[M+H]^+$ and $[M+2H]^{2+}$ results in peaks that are only ~10% as high as those for the original spectrum. Most of this is due to ion losses from the ion/ion reaction, but some is attributed to loss in detector response for ions with lower charge. The same effect is seen in Figure 5 for trypsin in dual polarity storage mode. Others also report ion losses of similar magnitude as a consequence of ion/ion reactions, in either 3d ion traps or LITs [15, 27].

Ion Parking. Ion parking should alleviate some of the ion losses during proton transfer reactions. Results from such an experiment involving cytochrome *c* ions are shown

in Figure 7. Here the vertical scales have been kept constant so the signals can be compared more easily. The pre-ion/ion reaction spectrum of cytochrome *c* (Figure 7a) shows mostly the $[M+9H]^{9+}$ and $[M+8H]^{8+}$ charge states. A transmission mode reaction enabled by passing PDCH anions through the population of trapped cytochrome *c* ions for 20 ms yields a variety of peaks from $[M+7H]^{7+}$ to $[M+4H]^{4+}$, all with low abundances (Figure 7b). In Figure 7c, a waveform selected to excite the $[M+7H]^{7+}$ ion (1.8 $V_{0\text{-}p}$ and 42 kHz) is applied to the x-rods during the transmission mode reaction period. With ion parking enabled, most of the resulting product ions remain in the $[M+7H]^{7+}$ charge state; about 20% react further to form $[M+6H]^{6+}$ and a small amount of $[M+5H]^{5+}$. The signal in the $[M+7H]^{7+}$ charge state after the reaction with ion parking (Figure 7c) is about half of the total ion signal present in the $[M+9H]^{9+}$ and $[M+8H]^{8+}$ charge states created directly from the ESI source (Figure 7a), which is a much less severe compromise of signal than that shown for ion/ion reactions without ion parking in Figures 5 and 6.

Conclusion

A research-grade LIT with multiple ion sources was designed and constructed using primarily commercially available components. Preliminary experiments show that its trapping efficiency is similar to that of commercial LITs and its performance as a mass spectrometer is good compared to the theoretical peak width of the cytochrome *c* charge states. Ion/ion reaction capabilities in both dual polarity storage mode and transmission mode were also demonstrated. The device operates under versatile computer control that should facilitate application to various schemes for ion/ion reactions and other ways to manipulate ions.

Future plans for this instrument include: enabling top-down protein analysis, including both collision induced dissociation followed by proton transfer ion/ion reactions as well as electron transfer dissociation (ETD) [11]. A second plan for this instrument is writing a data acquisition program in Labview 8.0 to enable data acquisition with the National Instruments multifunction PC card mentioned earlier. This modification should allow measurement times longer than the 250 ms limit of the Argos data acquisition system. Another future use for this instrument is to replace the 3d ion trap as the source for an ion mobility-time-of-flight (IMS-TOF) device that was built in our lab [25].

Acknowledgments

The authors acknowledge the following individuals: Chris Doerge and Don Douglas for helpful discussions and advice on construction of the toroidal transformer; Gregg Schieffer for help with testing of the custom electronics; Dick Egger, the late Steve Lee, and Terry Soseman (ISU Chemistry Machine Shop) for precision machining; Charlie Burg (Ames Lab ESG) for vacuum welding; Lee Harker (Ames Lab ESG) and Chuck Reese (ISU Chemistry) for custom electronics design, construction, and maintenance; Brian Regel and Brian Lippert at Extrel CMS for helpful discussion about the rf electronics; Brent Knecht, Brent Rardin and Mitch Wells (Griffin Analytical Technologies) for development and testing of the LIT software; Scott McLuckey for the plans for the computer-controlled fast relay switch; and James Hager, MDS Sciex, for discussions about improving the performance of the LIT. This work was funded by a grant from the Iowa State University Vice Provost for Research. MS acknowledges Extrel CMS for the Richard A. Schaeffer Memorial Travel Award to present this work at the 2006 ASMS Conference. MS also acknowledges the

Velmer A. and Mary K. Fassel Fellowship (Iowa State University, 2006-2007), the Conoco-Phillips Fellowship (Iowa State University, 2006-2007), and the GAANN Fellowship (Iowa State University, 2008) for financial support.

References

1. Douglas, D. J.; Frank, A. J.; Mao, D. M. Linear ion traps in mass spectrometry *Mass Spectrom. Rev.* **2005**, *24*, 1-29
2. Campbell, J. M.; Collings, B. A.; Douglas, D. J. A new linear ion trap time-of-flight system with tandem mass spectrometry capabilities *Rapid Commun. Mass Spectrom.* **1998**, *12*, 1463-1474
3. Collings, B. A.; Campbell, J. M.; Mao, D. M.; Douglas, D. J. A combined linear ion trap time-of-flight system with improved performance and MSn capabilities *Rapid Communications in Mass Spectrometry* **2001**, *15*, 1777-1795
4. Harkewicz, R.; Belov, M. E.; Anderson, G. A.; Pasa-Tolic, L.; Masselon, C. D.; Prior, D. C.; Udseth, H. R.; Smith, R. D. ESI-FTICR mass spectrometry employing data-dependent external ion selection and accumulation *J. Am. Soc. Mass Spectrom.* **2002**, *13*, 144-154
5. Syka, J. E. P.; Marto, J. A.; Bai, D. L.; Horning, S.; Senko, M. W.; Schwartz, J. C.; Ueberheide, B.; Garcia, B.; Busby, S.; Muratore, T.; Shabanowitz, J.; Hunt, D. F. Novel linear quadrupole ion trap/FT mass spectrometer: Performance characterization and use in the comparative analysis of histone H3 post-translational modifications *J. Proteome Res.* **2004**, *3*, 621-626
6. Schwartz, J. C.; Senko, M. W.; Syka, J. E. P. A two-dimensional quadrupole ion trap mass spectrometer *J. Am. Soc. Mass Spectrom.* **2002**, *13*, 659-669
7. Hager, J. W. A new linear ion trap mass spectrometer *Rapid Commun. Mass Spectrom.* **2002**, *16*, 512-526
8. Jonscher, K. R.; Yates, J. R. The quadrupole ion trap mass spectrometer - A small solution to a big challenge *Anal. Biochem.* **1997**, *244*, 1-15
9. Reid, G. E.; McLuckey, S. A. 'Top down' protein characterization via tandem mass spectrometry *J. Mass Spectrom.* **2002**, *37*, 663-675
10. Hu, Q. Z.; Noll, R. J.; Li, H. Y.; Makarov, A.; Hardman, M.; Cooks, R. G. The Orbitrap: a new mass spectrometer *J. Mass Spectrom.* **2005**, *40*, 430-443
11. Syka, J. E. P.; Coon, J. J.; Schroeder, M. J.; Shabanowitz, J.; Hunt, D. F. Peptide and protein sequence analysis by electron transfer dissociation mass spectrometry *Proc. Natl. Acad. Sci. U. S. A.* **2004**, *101*, 9528-9533

12. Yu, X.; Jin, W.; McLuckey, S. A.; Londry, F. A.; Hager, J. W. Mutual storage mode ion/ion reactions in a hybrid linear ion trap *J. Am. Soc. Mass Spectrom.* **2005**, *16*, 71-81
13. Stephenson, J. L.; McLuckey, S. A. Simplification of product ion spectra derived from multiply charged parent ions via ion/ion chemistry *Anal. Chem.* **1998**, *70*, 3533-3544
14. Londry, F. A.; Hager, J. W. Mass selective axial ion ejection from a linear quadrupole ion trap *J. Am. Soc. Mass Spectrom.* **2003**, *14*, 1130-1147
15. Liang, X. R.; McLuckey, S. A. Transmission mode ion/ion proton transfer reactions in a linear ion trap *J. Am. Soc. Mass Spectrom.* **2007**, *18*, 882-890
16. Liang, X. R.; Han, H. L.; Xia, Y.; McLuckey, S. A. A pulsed triple ionization source for sequential ion/ion reactions in an electrodynamic ion trap *J. Am. Soc. Mass Spectrom.* **2007**, *18*, 369-376
17. Xia, Y.; Liang, X. R.; McLuckey, S. A. Pulsed dual electrospray ionization for ion/ion reactions *J. Am. Soc. Mass Spectrom.* **2005**, *16*, 1750-1756
18. Xia, Y.; Chrisman, P. A.; Erickson, D. E.; Liu, J.; Liang, X. R.; Londry, F. A.; Yang, M. J.; McLuckey, S. A. Implementation of ion/ion reactions in a quadrupole/time-of-flight tandem mass spectrometer *Anal. Chem.* **2006**, *78*, 4146-4154
19. Liang, X. R.; Hager, J. W.; McLuckey, S. A. Transmission mode Ion/Ion electron-transfer dissociation in a linear ion trap *Anal. Chem.* **2007**, *79*, 3363-3370
20. Liang, X. R.; Xia, Y.; McLuckey, S. A. Alternately pulsed nanoelectrospray ionization/atmospheric pressure chemical ionization for ion/ion reactions in an electrodynamic ion trap *Anal. Chem.* **2006**, *78*, 3208-3212
21. Han, H. L.; Xia, Y.; McLuckey, S. A. Ion trap collisional activation of c and z(center dot) ions formed via gas-phase ion/ion electron-transfer dissociation *J. Proteome Res.* **2007**, *6*, 3062-3069
22. Wu, J.; Hager, J. W.; Xia, Y.; Londry, F. A.; McLuckey, S. A. Positive ion transmission mode ion/ion reactions in a hybrid linear ion trap *Anal. Chem.* **2004**, *76*, 5006-5015
23. Wells, J. M.; Chrisman, P. A.; McLuckey, S. A. "Dueling" ESI: Instrumentation to study ion/ion reactions of electrospray-generated cations and anions *J. Am. Soc. Mass Spectrom.* **2002**, *13*, 614-622
24. Badman, E. R.; Chrisman, P. A.; McLuckey, S. A. A quadrupole ion trap mass spectrometer with three independent ion sources for the study of gas-phase ion/ion reactions *Anal. Chem.* **2002**, *74*, 6237-6243
25. Zhao, Q.; Soyk, M. W.; Schieffer, G. M.; Houk, R. S.; Badman, E. R.; Fuhrer, K.; Gonin, M. An Ion Trap-Ion Mobility-Time of Flight Mass Spectrometer with Three Ion Sources for Ion/Ion Reactions *J. Am. Soc. Mass Spectrom.* **2008**, *Submitted*

26. Paul, W.; Reinhard, H. P.; Vonzahn, U. The Electric Mass Filter as Mass Spectrometer and Isotope Separator. *Zeitschrift Fur Physik* **1958**, *152*, 143-182
27. McLuckey, S. A.; Reid, G. E.; Wells, J. M. Ion parking during ion/ion reactions in electrodynamic ion traps *Anal. Chem.* **2002**, *74*, 336-346
28. Chrisman, P. A.; Pitteri, S. J.; McLuckey, S. A. Parallel ion parking: Improving conversion of parents to first-generation products in electron transfer dissociation *Anal. Chem.* **2005**, *77*, 3411-3414
29. Chrisman, P. A.; Pitteri, S. J.; McLuckey, S. A. Parallel ion parking of protein mixtures *Anal. Chem.* **2006**, *78*, 310-316
30. Moradian, A.; Douglas, D. J. Mass selective axial ion ejection from linear quadrupoles with added octopole fields *J. Am. Soc. Mass Spectrom.* **2008**, *19*, 270-280
31. Stephenson, J. L.; McLuckey, S. A. Adaptation of the Paul Trap for study of the reaction of multiply charged cations with singly charged anions *Int. J. Mass Spectrom. Ion Process.* **1997**, *162*, 89-106
32. Mo, W.; Langford, M. L.; Todd, J. F. J. Investigation of 'Ghost' Peaks Caused by Non-Linear Fields in the Ion Trap Mass Spectrometer *Rapid Commun. Mass Spectrom.* **1995**, *9*, 107-113
33. Franzen, J.; Gabling, R. H.; Schubert, M.; Wang, Y. In *Practical Aspects of Ion Trap Mass Spectrometry*; March, R. E.;Todd, J. F. J., Eds.; CRC Press: Boca Raton, FL, 1995; Vol. 1, pp 49-167.

Table 1. Typical LIT conditions used to trap and eject ions over 1100-1800 m/z range.

Scan Step	IQ1 (V)	IQ2 (V)	RF Amplitude (V_{0-p})	Resonance Amplitude (V_{0-p})	Resonance Frequency (kHz)	Scan Rate (Da/s)
Fill (10-20 ms)	-10	10	360	--	--	--
Cool (30 ms)	10	10	360	--	--	--
Heating Ramp (100 ms)	10	10	540 to 1260	1.9	150 (q=0.46)	12,300
Cool (30 ms)	10	10	1080	--	--	--
Mass Scan (250 ms)	10	2	1080 to 1800	2.8 to 3.7	275 (q=0.75)	3000

Table 2. Trapping efficiency and MSAE efficiency at various ion fill times for cytochrome *c* and trypsin ions. Uncertainties represent the standard deviations of four to six such measurements.

Fill Time (ms)	Trapping Efficiency (%)	MSAE Efficiency (%)
5	68.9 ± 11.1	9.6 ± 1.8
10	85.3 ± 4.6	7.7 ± 1.6
15	84.9 ± 8.2	6.4 ± 1.7
20	92.0 ± 4.8	5.1 ± 0.86

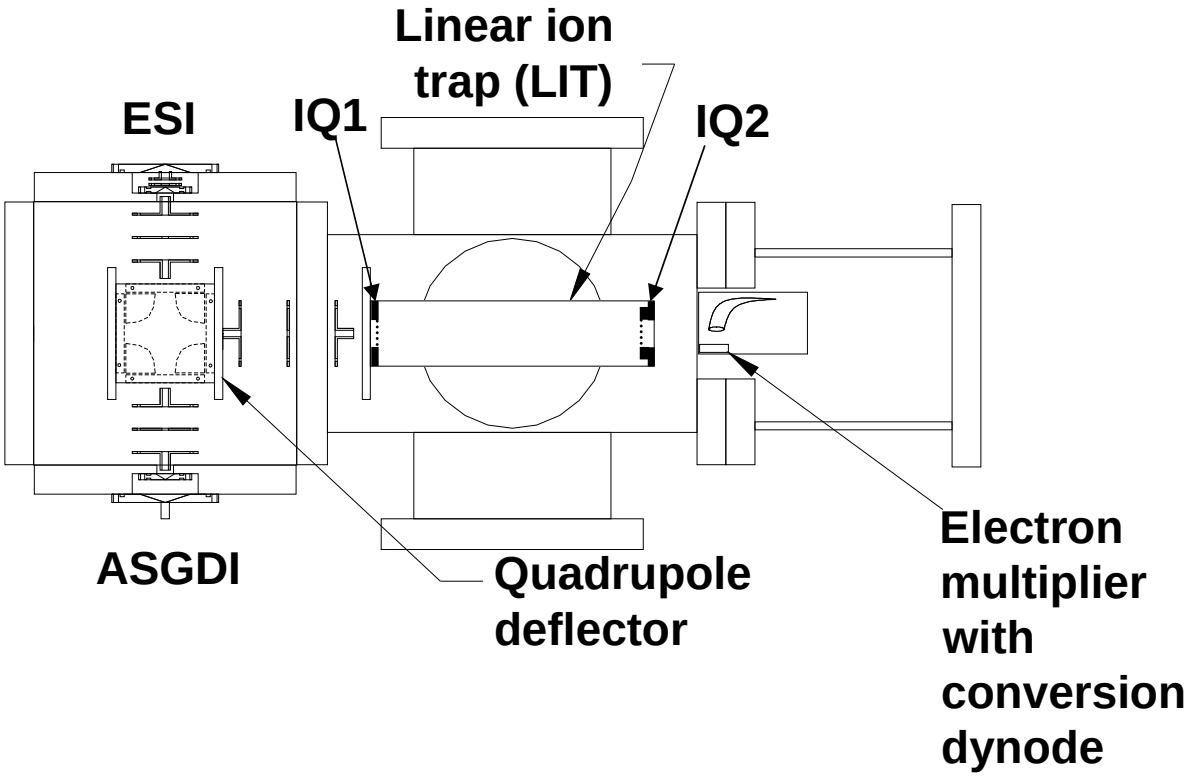

Figure 1. Instrument hardware schematic drawn to scale.

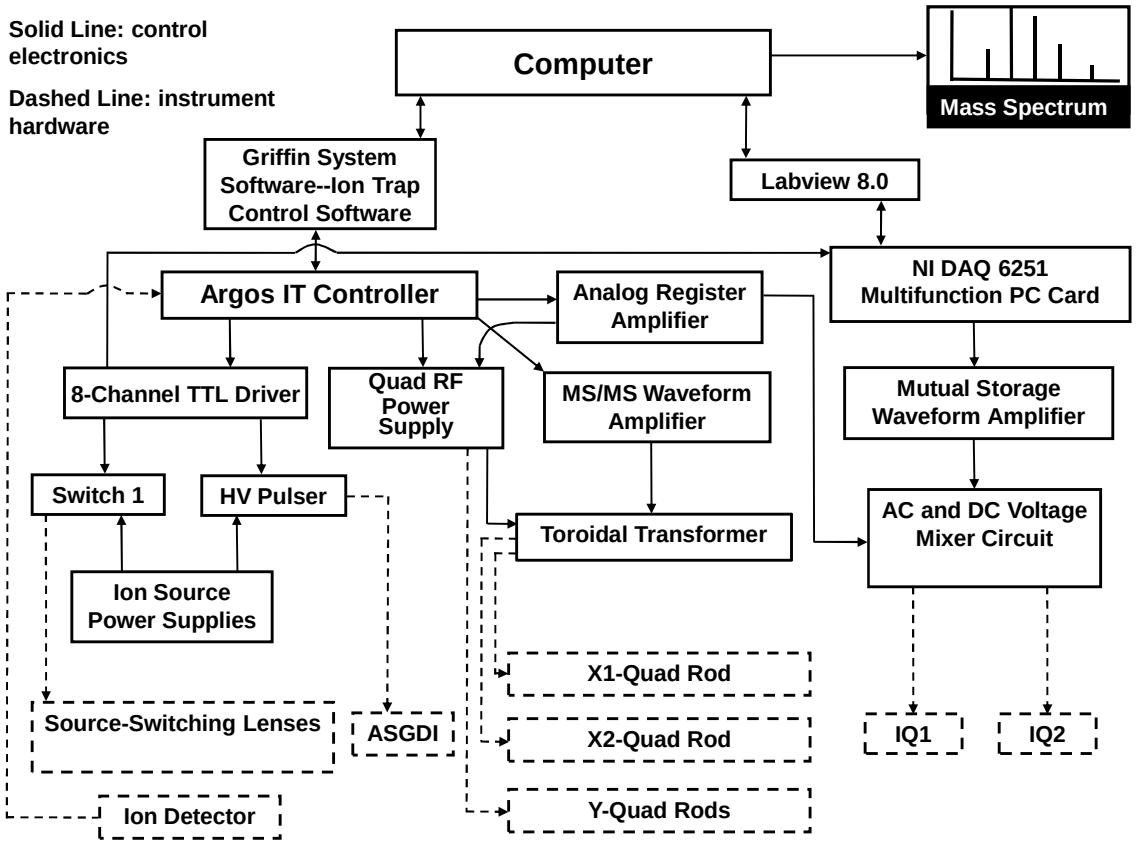

Figure 2. Instrument communication and control diagram.

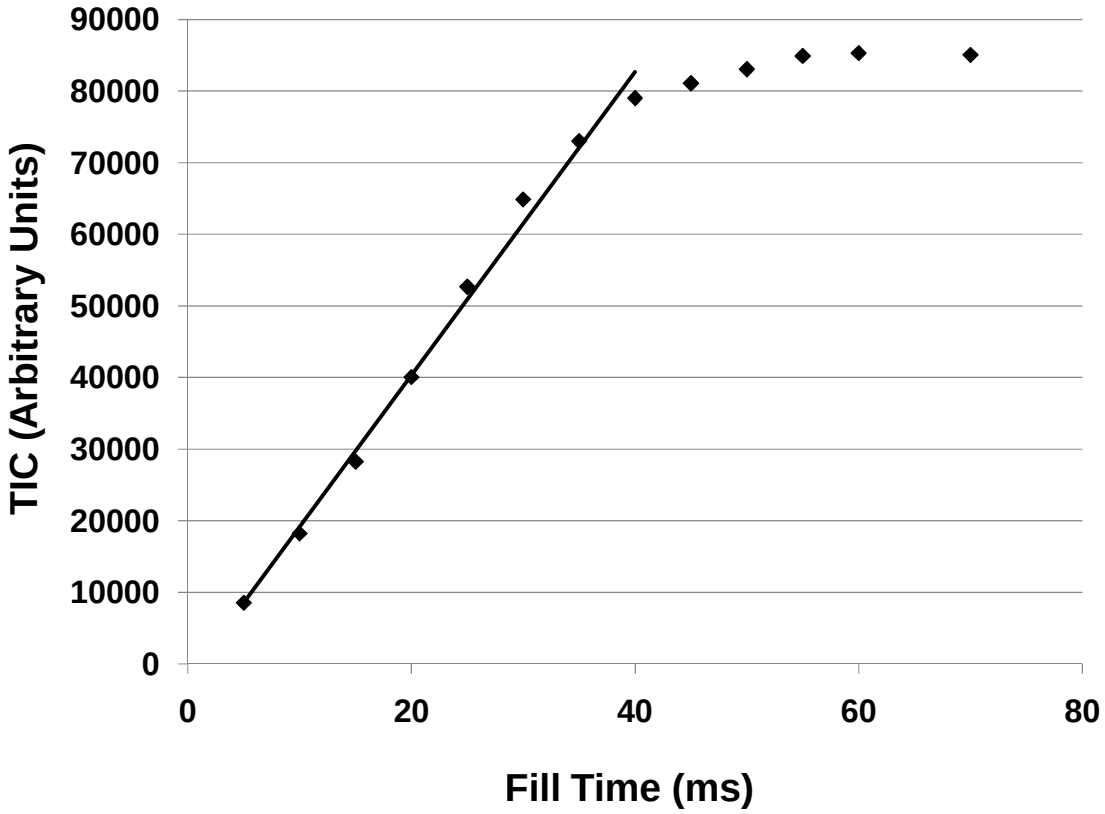

Figure 3. Plot of total ion current vs fill time used to measure the ion capacity of the LIT.

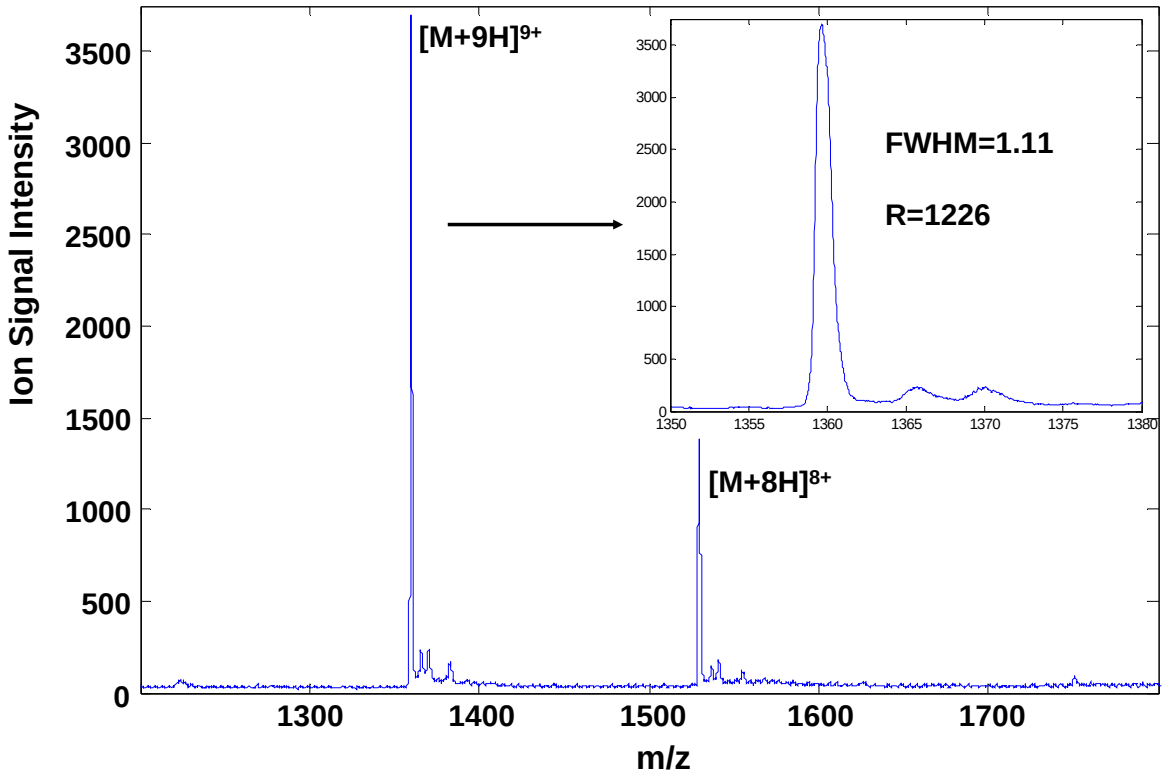

Figure 4. Cytochrome *c* mass spectrum. A heating ramp (100 ms, 540 to 1260 $V_{0\text{-}p}$ rf, 1.9 $V_{0\text{-}p}$, 150 kHz sine wave) reduced the intensity of the adduct peaks that are visible at 54 Da, 90 Da, and 130 Da above each protein peak.

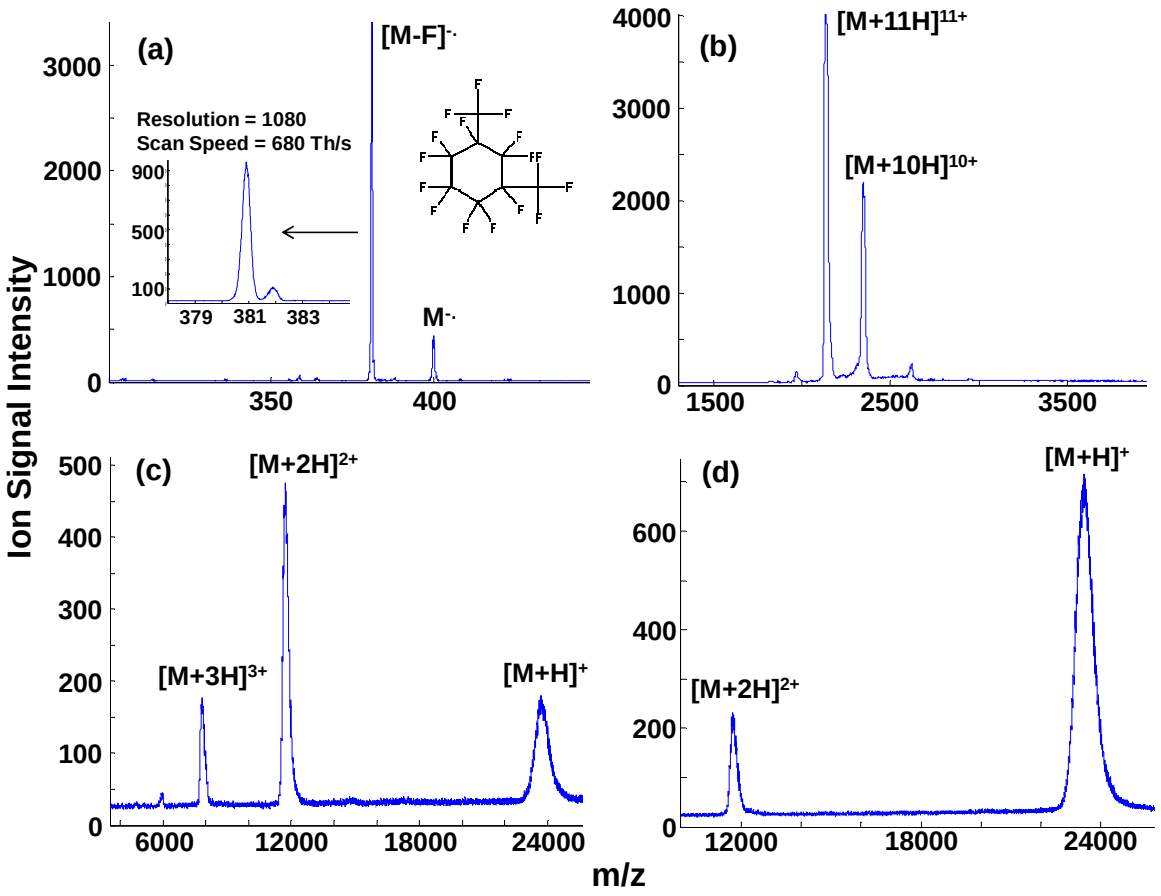

Figure 5. Mass spectra taken from dual polarity storage mode proton transfer ion/ion reactions of intact protein trypsin. (a) Negative ion mode spectrum of the proton transfer reagent ion, PDCH. (b) Pre-ion/ion reaction spectrum of trypsin ions generated directly from ESI. (c) Post-ion/ion reaction spectrum of ions shown in (a) and (b) with a 15 ms PDCH fill and 100 ms reaction. (d) Post-ion/ion reaction spectrum of ions shown in (a) and (b) with a 20 ms PDCH fill and 100 ms reaction.

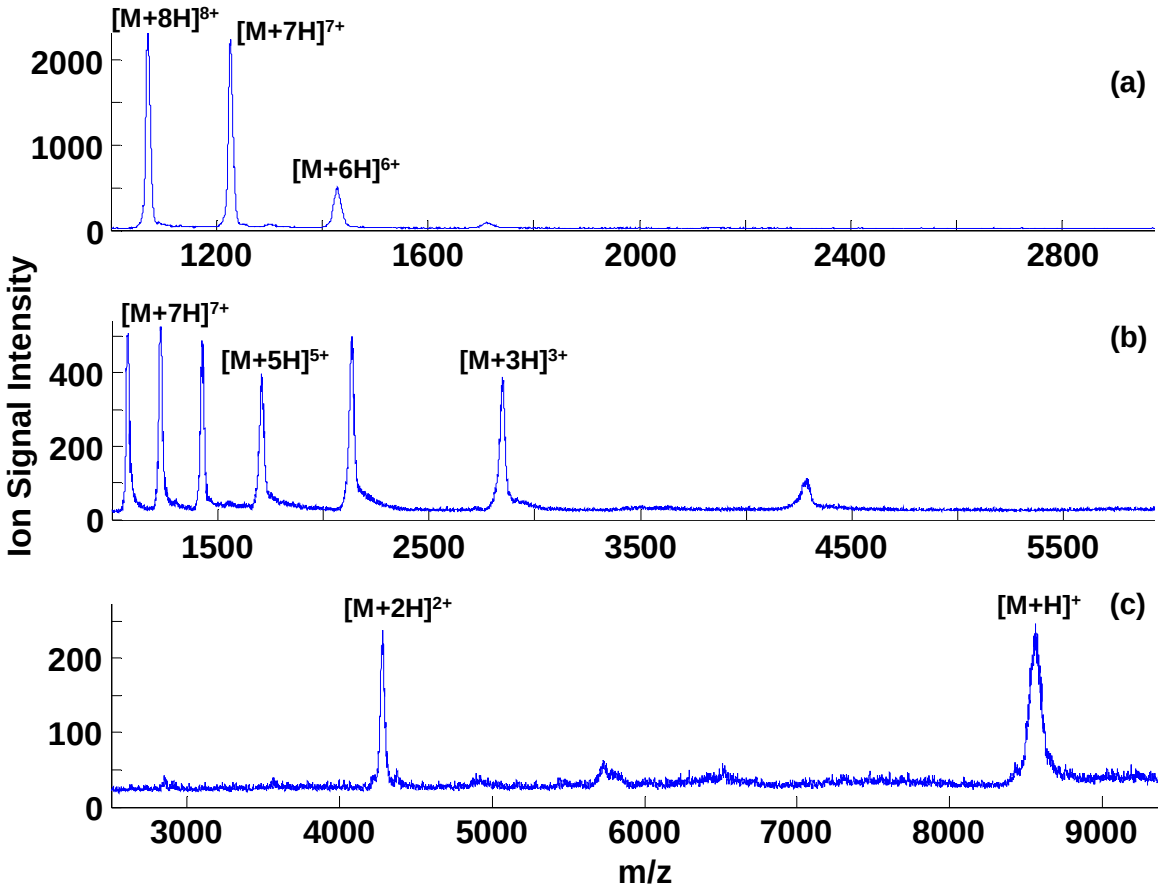

Figure 6. Mass spectra taken from transmission mode proton transfer ion/ion reactions of intact protein ubiquitin. (a) Pre-ion/ion reaction spectrum of ubiquitin ions generated directly from ESI. (b) Mass spectrum resulting from a transmission mode proton transfer ion/ion reaction enabled by passing PDCH anions through the population of trapped ubiquitin ions from (a) for 40 ms. (c) Mass spectrum resulting from a transmission mode proton transfer ion/ion reaction enabled by passing PDCH anions through the population of trapped ubiquitin ions from (a) for 70 ms.

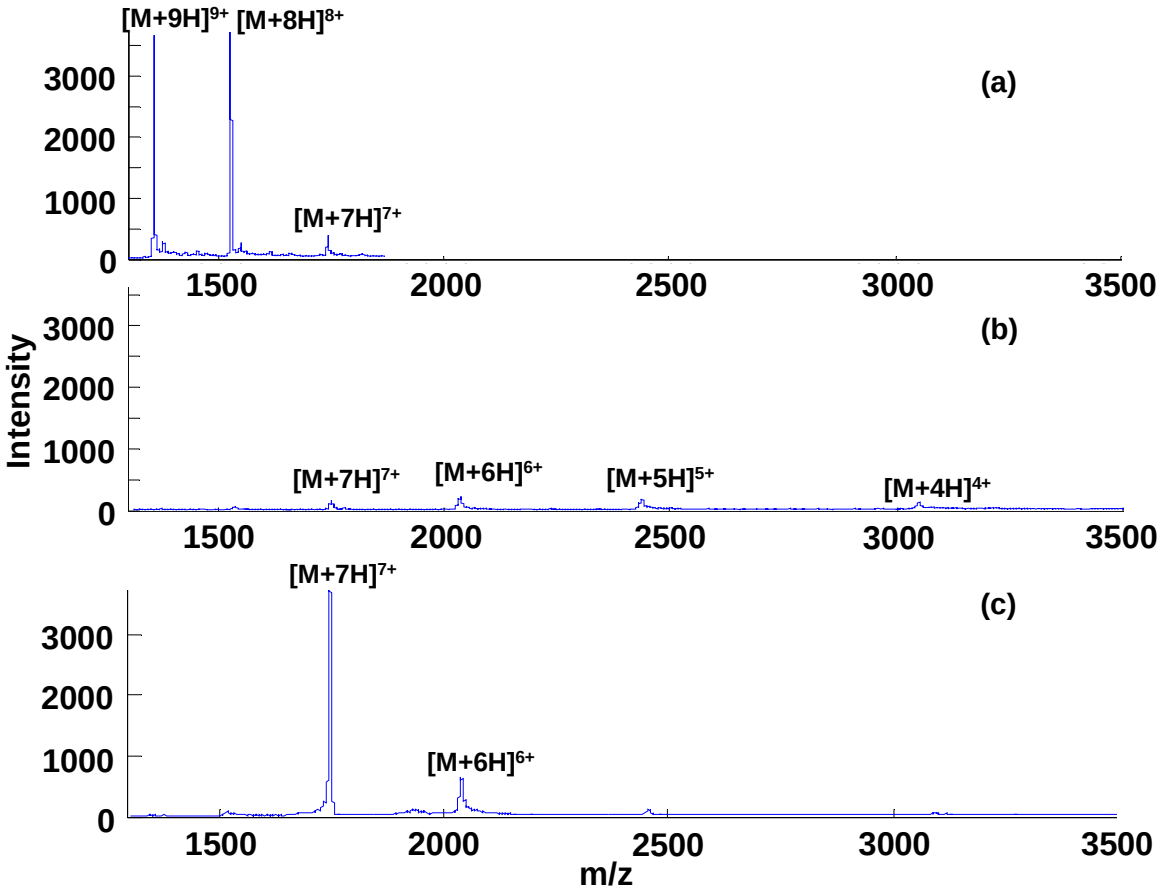

Figure 7. Mass spectra taken from an ion parking experiment during a transmission mode proton transfer ion/ion reaction. (a) Pre-ion/ion reaction spectrum of cytochrome *c* ions generated directly from ESI. (b) Mass spectrum resulting from a transmission mode proton transfer ion/ion reaction enabled by passing PDCH anions through the population of trapped cytochrome *c* from (a) for 20 ms. (c) Mass spectrum resulting from a transmission mode proton transfer ion/ion reaction enabled by passing PDCH anions through the population of trapped cytochrome *c* ion from (a) for 20 ms, during which a 1.8 $V_{0\text{-}p}$, 42 kHz sine wave was added to the x-rods of the LIT, enabling the $[M+7H]^{7+}$ ion to be "parked".

CHAPTER 3.

An Ion Trap - Ion Mobility – Time of Flight Mass Spectrometer with Three Ion Sources for Ion-Ion Reactions

Qin Zhao*, Matthew W. Soyk*†, Gregg M. Schieffer*†, R.S. Houk*†, Ethan R. Badman‡

*Iowa State University, Department of Chemistry, Ames, IA, 50011 USA

†Ames Laboratory, U. S. Department of Energy, Ames, IA 50011 USA

‡ Hoffman-La Roche Inc., Non-Clinical Safety, 340 Kingsland St., Nutley, NJ, 07100 USA

Katrin Fuhrer, Marc Gonin

TOFWerk AG, Feuerwerkerstrasse 39, CH-3602 Thune, Switzerland

A manuscript to be submitted to the *Journal of the American Society for Mass Spectrometry*, 2008.

Abstract

The instrument described here combines the capabilities of ion-ion reactions with ion mobility (IM) and time-of-flight (TOF) measurements for conformation studies and top-down analysis of large biomolecules. Ubiquitin ions from either of two electrospray ionization (ESI) sources are combined in a 3D ion trap with negative ions from atmospheric sampling glow discharge ionization (ASGDI). The ion-ion reaction products are then separated by IM and analyzed via a TOF mass analyzer. Alternatively, protein ions are fragmented by collision-induced dissociation (CID) in the 3D ion trap, followed by ion-ion

reactions to reduce the charge states of the CID product ions, thus simplifying the tandem mass spectrum. Instrument characteristics and the use of a new ion trap controller and software modifications to control the entire instrument are described.

Introduction

Despite the widespread use of mass spectrometry (MS) for biological analyses, further improvements in MS instrumentation are desirable, particularly in areas like proteomics [1] and characterization of large macromolecular complexes [2, 3]. These instrumentation improvements provide analytical capabilities that enable new biological studies not envisioned previously.

Ion mobility (IM) [4, 5] has become a very useful technique for analysis of biological ions in the gas phase. IM provides information about ion size and structure [6], as it rapidly separates ions based on collision cross-section, rather than just m/z ratio. The use of IM to disperse a mixture of ions in time prior to analysis via a time-of-flight (TOF) MS, i.e, nested drift (flight) time measurements, is an important recent advance. These experiments [7] were pioneered by Clemmer and coworkers in the mid-1990's and have now been used by several other groups [8, 9]. In a series of instrumental designs, the Clemmer group has made various modifications to the initial ESI-IM-TOF, including the insertion of a collision cell between the IM drift tube and the TOF for mobility labeling experiments [10, 11], and the addition of an ion trap prior to the mobility drift tube to improve the duty cycle from the continuous ESI source [12, 13]. One publication demonstrated MS/MS capabilities with an ion trap prior to IM-TOF [14], but not with the entire instrument under computer control. Therefore, only relatively simple experiments were possible.

IM has been used to analyze the products of ion-molecule reactions [15] including proton transfer [16, 17], H/D exchange [18], and salvation [19-22]. In these studies the desired reactions take place either in the atmospheric pressure ion source interface region or in the drift tube itself. Thus, only long reaction times and certain reagent ions can be used. In addition, performing reactions in the IM cell can make spectral interpretation difficult because the fragmentation and chemistry occur at the same time. In the current experiments, the ion/ion reaction chemistry is decoupled from the subsequent mobility and mass analysis. Therefore, the reaction time and chemistry of reagent ions are controlled more effectively, including a wider selection of reagent ions from independent ion sources.

Gas-phase ion-ion reactions provide another dimension for gas-phase bioanalysis. Pioneering work by Smith and coworkers [23, 24] were followed by a continuing series of experiments by McLuckey's group [25]. Ion-ion reactions are rapid, versatile, and can be controlled via various ion manipulation schemes. To date, the most common type of reaction has been proton-transfer to manipulate the charge states of multiply-charged ions [26] and simplify complex MS/MS spectra [27, 28]. Use of product ions in low charge states can improve mass accuracy and resolution, especially with low resolution mass analyzers. Other useful reactions include electron transfer, most notably electron transfer dissociation (ETD) [29-31], electron capture dissociation (ECD) [32, 33], and complex formation [34, 35]. Ion-ion reactions can also be used to measure chemical properties of gas-phase biomolecules. Various instruments specifically for ion-ion reactions include two [29, 36-38], three[39], or four [40] independent ion sources arranged around an ion trap, although use of pulsed sources and a single ion extraction system is also possible [41, 42].

Here, we describe the first instrument to include capabilities for both ion-ion reactions and IM-TOF-MS measurements. Initial experiments and instrument characteristics are described, including use of a new ion trap controller and software to control the entire instrument.

Experimental

Bovine ubiquitin (Sigma-Aldrich, St. Louis, MO) was used without further purification. Protein solutions were 20 to 30 µM in 1% aqueous acetic acid for positive ion mode. Nano-ESI emitters were pulled from glass capillaries (1.5 mm o.d., 0.86 mm i.d.) by a micropipette puller (P-97, Sutter Instruments, Novato, CA). Nano-ESI was performed by applying +1 kV to +1.2 kV to the protein solution via a stainless steel wire through the back of the sample capillary. Negative ions from perfluoro-1,3-dimethylcyclohexane (PDCH, Sigma-Aldrich , St. Louis, MO) were used as the proton acceptor reagent.

Instrumentation

General. The instrument is shown to scale in Figure 1. It contains three independent ion sources: two for ESI and one for ASGDI [43]. Ions from these sources are stored in the 3D quadrupole IT for reaction. The products are separated by the IM drift tube, followed by a quadrupole-time-of-flight mass spectrometer (q-TOF).

The vacuum chamber consists of an 8” Conflat cube, which houses the three ion sources, ion optics, and turning quadrupole deflector (TQ, Extrel, Pittsburgh, PA). The cube is evacuated by a turbo pump (Turbo-V550 MacroTorr, 550 l/s N_2, Varian Inc., Palo Alto, CA) backed by a mechanical pump (SD-30, Varian, Palo Alto, CA) and is attached to a

custom built rectangular chamber (304 stainless steel, 35.6 cm wide ×76.2 cm long × 33.0 cm high) that also houses the IT, drift tube, and quadrupole collision cell. The TOF is in an aluminum housing (8.90 cm × 25.4 cm × 66.7 cm) attached to the back of the chamber; the TOF tube is oriented vertically. The main vacuum chamber is evacuated by two diffusion pumps (Diffstak 250/2000M and 160/700M, BOC Edwards) backed by mechanical pumps (E2M40 and RV12, respectively, BOC Edwards, Wilmington, MA). The TOF is pumped by a turbomolecular pump (Turbo-V550 MacroTorr, 550 l/s N_2, Varian Inc., Palo Alto, CA), backed by a mechanical pump (RV12, BOC Edwards). Convectron and ion gauges (Series 375 and 358, Helix Technology Corporation, Mansfield, MA) measure the ion source and chamber pressures (all are uncorrected). The base pressures are 7.5×10^{-8} mbar in the main chamber and 3.3×10^{-7} mbar in the TOF when the sources are closed. In normal operation, one ESI source and the ASGDI source are open, and helium is added to the drift tube (~1.3 to 2.0 mbar) through a precision leak valve (Model 203, Granville Phillips, Boulder, CO). The main chamber pressure is then $\sim1\times10^{-4}$ mbar and the pressure in the TOF region is 9×10^{-7} mbar.

Ion Sources. The basic design for a three ion source interface has been described previously [40]. The three sources are arranged around three faces of the 8” Conflat cube; one source is on the ion optical axis of the instrument, and the other two are orthogonal to it. The two ESI sources are identical in design. The interface region, which is 5.08 cm in diameter and 1.59 cm deep, is machined out of an 8” ConFlat flange. A 254 μm diameter aperture separates the interface region from atmosphere, and a 381 μm diameter aperture separates the interface region from the high vacuum region. Two lenses between the

apertures focus ions through the interface region. Negative ions from perfluoro-1,3-dimethylcyclohexane (PDCH, Sigma-Aldrich, St. Louis, MO) were used as the proton acceptor reagent. Each ESI interface region operates at ~1 mbar during the experiment and is pumped by a mechanical pump (E2M40, BOC Edwards). The nano-ESI voltages are provided by 5 kV power supplies (ORTEC 659, Oak Ridge, TN).

The ASGDI source interface region has the same design and dimensions as the ESI sources but without the interface lenses. It is pumped by a mechanical pump (E2M40, BOC Edwards). PDCH headspace vapors are sampled via a 0.64 cm diameter Nylon tube connecting the sample container and the outer aperture plate. The source pressure (~0.786 mbar) is regulated by a bellows valve (SS-4BMW, Swagelok) inserted in the tubing between the compound headspace and the source region. The ASGDI source uses a 3 kV power supply (ORTEC 556, Oak Ridge, TN) and a high voltage pulser (PVX-4150, Directed Energy Corp., Fort Collins, CO) that is trigged by a TTL pulse from the Argos IT controller (Griffin Analytical Technologies, West Lafayette, IN), to apply a ~420 V pulse between the outer and inner (grounded) aperture plates. This ASGDI pulse lasts for the time required to add reagent anions to the IT, typically 5 to 20 ms.

Each ion source has three lenses attached to the vacuum side of the flange to focus the ions from the exit aperture of the source into the TQ. The second lens is split and serves as a deflector for direction focusing. The TQ was modified by severing the electrical connection between diagonally opposing rods and by applying four independent DC potentials to the four TQ rods. This allows ions to either be deflected 90^{o} onto the axis of the instrument or to be passed straight through.

After the TQ, three lenses focus the ions into the IT. Two home-built high-voltage switches, controlled by TTL signals from the Argos IT controller, switch the voltages applied to the TQ and three subsequent lenses to allow ions from the desired ion source into the IT. Six nine-channel DC power supplies (±500 V, TD9500, Spectrum Solutions, Russellton, PA) generate the potentials for the ion optics from the sources to the ion trap.

Ion Trap. The 3D quadrupole IT (ideal geometry, r_0 = 1.0 cm, z_0 = 0.707 cm, RM Jordan, Grass Valley, CA) is attached to the drift tube; the exit is mounted 0.635 cm from the front plate of the drift tube. The end caps are at ground, and the DC potential on the ring electrode is zero to prevent any asymmetric fields during ion trapping. The 665 kHz ion trapping voltage is generated by a home-built LC circuit that provides up to 5000 V_{0p}. The maximum low mass cutoff value is ~m/z 1220 (calculated assuming an ideal ion trap geometry). A 0 to 10 V dc control signal from the Argos IT controller determines the rf trapping voltage. A custom control generates the initial low-level rf voltage, measures feedback to stabilize the rf voltage, and contains calibration data. The initial rf voltage is first amplified to 0 to 200 V_{0p} by a 50 W commercial amplifier (AG1020, T&C Power Conversion Inc., Rochester, NY) and finally by the custom LC circuit to the full 0 to 5000 V_{0p}. Measured stabilities of the full rf voltage are better than ±1%. A TTL input allows the rf wave to be shut off in ~15 µs at any rf amplitude. The shutoff is not locked to the rf phase.

The ion trap timing and voltages are controlled by an Argos IT controller and software (Figure 2). The Argos provides the master clock for the entire instrument, as well as two independent arbitrary waveform outputs, digital TTL triggers, and analog control outputs (0-4 V). One arbitrary waveform output provides the 0-10 V dc control signal for the ion

trap rf; the other is applied to the front endcap electrode (after being amplified by x17 to 85 V_{p-p}) to perform mass selection and resonance excitation. The TTL triggers are used to start the ASGDI source, control the high voltage switches for the ion sources, and start the ion injection pulse for the mobility experiment. A custom 8-channel driver is used to increase the power of the TTL signals to enable them to trigger 50 Ω loads. The ion injection TTL pulse also enables the high voltage pulser (PVX-4150, Directed Energy Corp., Fort Collins, CO, applied to the exit endcap) to eject ions from the ion trap. Typically this ejection pulse is 80 to 400V applied for 3 to 5 μs. Two analog signals are used to control the quadrupole collision cell, described below.

Drift Tube. The drift tube (modified from a design provided by Valentine et al [44, 45]) consists of alternating 12.7 cm diameter 304 stainless steel lenses (0.16-cm thick, 12.7-cm o.d. 4.40-cm i.d.) and Delrin insulating rings (1.27 cm thick, 12.7 cm o.d., 8.26 cm i.d.). The drift tube is 44.45 cm long (together with the ion funnel) with a 0.5 mm diameter entrance aperture. A chain of 2 MΩ resistors connects the lenses, creating an electric field (typically 11 to 13 V/cm) down the drift tube. The voltage applied to the front of the drift tube is typically 30 to 100 V lower—for positive ions—than that of the ion trap. A capacitance manometer (690A13TRC, MKS Instrument, Methuen, MA) measures the He pressure inside the drift tube, which is typically ~1.33 to 2.00 mbar, controlled via another precision leak valve.

Ion Funnel. To improve ion transmission efficiency, an ion funnel [45, 46] is integrated into the back of the drift tube (Figure 1). The funnel is based on the device

described by the Smith [46] and Jarrold groups [47]. After the last ring of the drift tube, a series of 25 stainless steel electrodes (0.0794 cm thick, 12.7 cm o.d.) with circular apertures whose inner diameters decrease linearly from 4.293 to 0.483 cm is attached. The ion funnel electrodes are sealed together using 0.3175 cm thick Delrin spacers and Viton o-rings giving a funnel length of 11.11 cm. Thus, the helium pressure in the drift tube and ion funnel are the same. The electrodes are connected to each other with a series of resistors (Vishay, 500 kΩ, 0.6 W, ±1%). One voltage applied to the entrance of the drift tube, and a second voltage is applied to the exit of the ion funnel to set the axial electric field down the drift tube-ion funnel assembly.

In the ion funnel, alternate lenses are capacitively coupled (Vishay, 1000 pF, 1.5 kV_{rms}, ±20%) to form two lens chains. RF voltages (Ardara Technologies, North Huntingdon, PA) that are 180° degrees out of phase from each other are applied to each chain with amplitudes ~90 V_{pp} at 360 kHz. A capacitor to ground decouples the RF voltage from the drift tube lenses. There is one DC electrode after the exit of the ion funnel with a pressure-limiting aperture (1.0 mm diam).

In this instrument, the ion funnel increases the overall total ion signal by a factor of ~7. Here, the basis of comparison is the same number of electrodes at the end of the drift tube all with the same ID and no rf voltage. In this experiment, signal is measured by extracting ions from the TOF source directly to the TOF microchannel plate (MCP) detectors.

Another set of three lenses behind the drift tube-ion funnel focuses ions into the quadrupole collision cell (Figure 1). The voltages supplied to the ion funnel dc lens, the lenses before the collision cell, the entrance and exit lenses of the collision cell, and the

lenses between the collision cell and the TOF are floated on the drift tube exit voltage using a nine-output floating power supply (TD9500HV, Spectrum Solutions Inc., Russellton, PA).

Quadrupole-TOF. The quadrupole collision cell (Figure 1) transmits ions from the ion funnel to the TOF. It also provides for CID of ions labeled by mobility (i.e., a pseudo MS/MS step) [10, 11], although this capability is not shown in this paper. The quadrupole (r_0 = 9.5 mm, 880 kHz, 3600 V_{0p} per pole, Extrel, Pittsburgh, PA) is followed by an orthogonal W-reflectron TOF (TOFWerk, Thun, Switzerland). The collision cell and its electronics are floated using an isolation transformer (SIT 30-1000, Stangenes Industries Inc., Palo Alto, CA). The collision cell is mounted to the vacuum side of an 8" conflat flange that is attached to the back of the main vacuum chamber. A capacitance manometer (Model 690A01TRC, MKS Instrument, Methuen, MA) measures the pressure inside the collision cell, which is typically He at ~8×10^{-4} mbar of He and is controlled via another precision leak valve. The Argos IT controller (Figure 2) supplies two 0 to 4 V analog signals that are amplified to 0 to 10 and -200 to 200 V, respectively, and used by the quadrupole power supply to control the rf amplitude and to supply the dc bias to the collision cell rods to set the collision energy.

After the ions exit the collision cell, they are focused into the source region of the TOF by a series of 10 lenses mounted in the hole machined out of the 8" conflat flange between the collision cell and the TOF, which is mounted vertically on the air side of the flange. One lens is split into half-plates for vertical direction focusing. The ions are pulsed upwards into the TOF drift region by a 2 μs pulse, and are then accelerated into the drift region by ~5800V. The voltages on the TOF electrodes and detector are controlled by the TOF software, which communicates directly with the TOF power supply. The TOF has a W-

reflectron configuration and can be operated in V-mode or in W-mode. Only the V-mode is used in this paper; the effective flight path is ~1.5 m.

The ion detector is an eight-anode microchannel plate (MCP, Ionwerks, Houston, TX) that has post acceleration voltage of ~6000 V. The signal is amplified ×100 by two four-channel preamplifiers (XCD quad amplifier/discriminator, Ionwerks, Houston, TX) and then sent to an 8 channel time-to-digital converter (TDC×8, Ionwerks, Houston, TX). The TOF software reads the data from the TDC to create 2D data that contain both mobility time and mass spectral information.

The timing of the TOF data acquisition is similar to methods described previously[7, 12]. As shown by the bottom three traces in Figure 3, the TOF timing controller gets signals from the software and an external trigger and sends TTL triggers to the TDC×8 and to the TOF pulser. The mobility acquisition is started by the ion injection pulse (a trigger from the Argos), after which the TOF timing controller starts sending TTL triggers—at specific intervals depending on the mass range being acquired—simultaneously to the TDC×8 and the TOF extraction lenses. In a typical experiment 100 mass spectra are taken within each 10 ms mobility spectrum, up to a maximum m/z value of 2400.

Results and Discussion

IM-TOF after Ion/Ion Reactions. In early research on proton transfer reactions with IM, a basic gas was introduced into the source region to create lower charge state ions through an in-source proton transfer reaction. In the present instrument, the total reaction time and reagent ion identity can be controlled. The experimental timing diagram (Figure 3) is similar to those previously shown for ion/ion reactions [40], except the usual ion trap mass

analysis step is replaced by injection of product ions into the IM drift tube. The experiment scan function shown in Figure 3 includes acquisition of nested flight time - mobility data.

These capabilities are illustrated using charge reduction reactions of multiply charged ubiquitin ions with PDCH anions. The spectrum of the anions from the ASGDI is shown in Figure 4; note that the main reagent ions are $[M-F]^{-\cdot}$ and $[M-CF_3]^{-\cdot}$.

Charge reduction reactions can be used to produce ions in lower charge states than the usual ions generated solely by the ESI process. Additionally, by reducing the charge states of the protein ions, the IM resolution for ions in different charge states can be improved. Figure 5a shows a 3D mobility-m/z spectrum of ubiquitin before proton transfer reactions. The main charge states observed for ubiquitin under these solution and source conditions are +8 and +9. The mass resolution shown is $m/\Delta m = 930$ at m/z 1071.6. Mass accuracies are within 28 ppm, using an external calibration.

For a typical ion/ion reaction-IM experiment, ubiquitin ions are injected for 50 to 100 ms, $PDCH^-$ ions are injected for 20 to 40 ms, and both polarity ions are trapped in the IT to react for 50 to 150 ms depending on the product ion charge states desired. A 3 to 5 µs pulse at -100V is then applied to the back endcap of the ion trap to inject ions into the drift tube. For the IM separation the He pressure in the drift tube is 1.3 to 1.8 mbar, and the applied voltages are -150V on the entrance of the drift tube and -700 V on the last electrode of the ion funnel.

Figure 5b and 5c show spectra after ion/ion charge reduction reaction of ubiquitin with PDCH. Ubiquitin ions are converted to lower charge states, and the +1, +2 and +3 ubiquitin ions can now be resolved in the IM dimension. Previous attempts at analysis of

protein mixtures by CID after IM separation suffered because higher charge states of the proteins were not resolved in the mobility separation [48]. Thus, mobility labeling for proteins is not as useful as for peptides. Ion/ion reaction combined with IM separations provides a new technique to make mobility labeling (for on-the-fly MS/MS) possible for intact proteins. The capability to effectively fragment proteins behind the drift tube, especially at these lower charge states, is still under development.

Of course, ion cross-sections can be determined from the IM drift times:[49]

$$\Omega = \frac{(18\pi)^{1/2}}{16}\frac{ze}{(k_b T)^{1/2}}\left[\frac{1}{m_i}+\frac{1}{m_b}\right]^{1/2}\frac{1}{N}\frac{t_D E}{L}\frac{760}{P}\frac{T}{273.2}$$

where z is the charge state of ions, m_i is the mass of ions, m_b is the mass of the buffer gas, E is the electric field through the drift cell, L is the length of the drift cell, t_D is the flight time through the drift cell, P is the pressure of the buffer gas, and T is the temperature of the buffer gas.

Such cross-section measurements for ubiquitin ions are listed in Table 1. These data show that reducing charge state from +8 through +4 induces folding, i.e., lower measured cross sections. Further charge reduction from +4 to +1 does not change the cross sections appreciably, as if the protein then remains in a folded state.

The effects of ion-ion reactions and charge state on measured cross sections and folding are discussed in more detail in other papers [50, 51].

CID on Intact Proteins followed by Charge Reduction. Figure 6a shows a spectrum obtained after storing only the +7 charge state of ubiquitin. Additional peaks are seen at m/z

values above that of the protein. The abundances of these "extra" ions vary from day to day. They are also observed at similar abundances when the same sample is analyzed on a commercial triple quadrupole instrument, so we believe they are mainly impurities in the sample, rather than adducts formed inside the instrument. We discriminate against these "extra" ions by trapping only the +7 ubiquitin ions in the results presented below.

The +7 ubiquitin ions can readily be fragmented in the ion trap (Figure 6b). These CID product ions are in a variety of relatively high charge states and are only moderately resolved in the IM dimension. Thus, it is not easy to assign them at first.

Figure 6c shows the spectrum resulting from charge reduction of the fragment ions in the ion trap after CID. The spectrum shifts to higher m/z, and the dispersion in the IM dimension is greatly improved. Many of the charge-reduced CID fragments can now be assigned by comparing the observed m/z values with that of fragments generated from the known sequence of ubiquitin. The assumption that the fragment ions in Figure 6c are in low charge states greatly simplifies these assignments. Most of the fragments observed here are b and y ions, in agreement with those found in other studies [40, 52]; a few c ions may be present.

The IM plot for the charge-reduced fragments (Figure 6c) shows distinct groups that fall along slanted lines of different slopes for peptide fragment ions in +1, +2 and +3 charge states, as noted by Clemmer and co-workers. This phenomenon provides additional evidence to help assign charge states. These groups merge closer together at higher charge states (Figure 6b)[13], which is one reason they are poorly resolved in Figure 6a.

Armed with the identities of the charge-reduced fragments (Figure 6c), many of the original, more highly charged fragments in Figure 6b can now be assigned. For example,

y_{58}^{2+} is in the charge-reduced spectrum, so a more highly charged version (y_{58}^{5+} in this case) should appear in the original CID spectrum (Figure 6b). Here we assume that the peptide fragment ions do not dissociate further during the charge reduction reactions, as shown by McLuckey [27] . A number of other, similar cases are identified in Figure 6b. The unusual c_{52}^{2+} and c_{59}^{2+} ions tentatively identified in the charge reduced spectrum can also be found in higher charge states in the original CID spectrum, which helps validate their assignment.

Summary of the Instrument:

From the above instrumentation description and result demonstration, this instrument combines ion mobility and ion/ion reaction capabilities, and it can be operated in variety of ways for different purposes. Firstly, it is very powerful to manipulate charge state and study the conformation change (folding and unfolding) of the large biomolecules. We have done work on this, and a publication will follow this instrument paper. Secondly, multiple stage MS/MS with charge reduction reaction makes top down analysis more efficient because it helps to assign fragments by both ion mobility dispersion and charge reduction. Thirdly, other types of ion/ion reaction (ETD, protein and metal ions, protein complexes formation) can also be done on this instrument.

There is a lot of room for instrument development, such as replacing the 3-D ion trap with a linear ion trap, exploring the w-mode of the time-of-flight, and performing one more step of CID or adding a high-energy CID collision cell after ion mobility separation. Though the sensitivity of this instrument is not very high, we believe it is a start of a new research area and will open a broad space to explore.

Acknowledgements

The authors acknowledge helpful discussions with Steve Valentine (Indiana Univ.); Scott McLuckey for the design of high-voltage switches; Brent Knecht, Garth Patterson, Brent Rardin, and Mitch Wells (Griffin Analytical) for assistance with the Argos and software; David Prior (Pacific Northwest National Lab) for design of the IT rf amplifier; and Randy Pedder (Ardara Technologies, North Huntingdon, PA) for advice on use of the rf supply for the ion funnel. Other custom electronics were designed and constructed by Lee Harker (Ames Lab Engineering Services Group); vacuum welding by Charlie Burg (Ames Lab); precision machining by Richard Egger, the late Steve Lee, and Terry Soseman (ISU Chemistry Machine Shop). Derrick Morast analyzed the ubiquitin sample with another ESI instrument to help determine the origin of the "extra" peaks. ERB acknowledges funding from Waters Corp. via an ASMS Research Award. Funding from Iowa State University: College of Liberal Arts and Sciences, Office of Biotechnology, Plant Sciences Institute, and the Carver Trust are gratefully acknowledged.

References

1. Pandey, A.; Mann, M. Proteomics to study genes and genomes *Nature* **2000**, *405*, 837-846
2. Loo, J. A.; Berhane, B.; Kaddis, C. S.; Wooding, K. M.; Xie, Y. M.; Kaufman, S. L.; Chernushevich, I. V. Electrospray ionization mass spectrometry and ion mobility analysis of the 20S proteasome complex *J. Am. Soc. Mass Spectrom.* **2005**, *16*, 998-1008
3. Sobott, F.; McCammon, M. G.; Hernandez, H.; Robinson, C. V. The flight of macromolecular complexes in a mass spectrometer *Philos. Trans. R. Soc. Lond. Ser. A-Math. Phys. Eng. Sci.* **2005**, *363*, 379-389
4. St Louis, R. H.; Hill, H. H. Ion Mobility Spectrometry in Analytical-Chemistry *Crit. Rev. Anal. Chem.* **1990**, *21*, 321-355

5. Collins, D. C.; Lee, M. L. Developments in ion mobility spectrometry-mass spectrometry *Anal. Bioanal. Chem.* **2002**, *372*, 66-73
6. Jarrold, M. F. Peptides and proteins in the vapor phase *Annu. Rev. Phys. Chem.* **2000**, *51*, 179-207
7. Hoaglund, C. S.; Valentine, S. J.; Sporleder, C. R.; Reilly, J. P.; Clemmer, D. E. Three-dimensional ion mobility TOFMS analysis of electrosprayed biomolecules *Anal. Chem.* **1998**, *70*, 2236-2242
8. Stone, E.; Gillig, K. J.; Ruotolo, B.; Fuhrer, K.; Gonin, M.; Schultz, A.; Russell, D. H. Surface-induced dissociation on a MALDI-ion mobility-orthogonal time-of-flight mass spectrometer: Sequencing peptides from an "in-solution" protein digest *Anal. Chem.* **2001**, *73*, 2233-2238
9. Steiner, W. E.; Clowers, B. H.; English, W. A.; Hill, H. H. Atmospheric pressure matrix-assisted laser desorption/ionization with analysis by ion mobility time-of-flight mass spectrometry *Rapid Commun. Mass Spectrom.* **2004**, *18*, 882-888
10. Hoaglund-Hyzer, C. S.; Li, J. W.; Clemmer, D. E. Mobility labeling for parallel CID of ion mixtures *Anal. Chem.* **2000**, *72*, 2737-2740
11. Hoaglund-Hyzer, C. S.; Clemmer, D. E. Ion trap/ion mobility/quadrupole/time of flight mass spectrometry for peptide mixture analysis *Anal. Chem.* **2001**, *73*, 177-184
12. Henderson, S. C.; Valentine, S. J.; Counterman, A. E.; Clemmer, D. E. ESI/ion trap/ion mobility/time-of-flight mass spectrometry for rapid and sensitive analysis of biomolecular mixtures *Anal. Chem.* **1999**, *71*, 291-301
13. Myung, S.; Lee, Y. J.; Moon, M. H.; Taraszka, J.; Sowell, R.; Koeniger, S.; Hilderbrand, A. E.; Valentine, S. J.; Cherbas, L.; Cherbas, P.; Kaufmann, T. C.; Miller, D. F.; Mechref, Y.; Novotny, M. V.; Ewing, M. A.; Sporleder, C. R.; Clemmer, D. E. Development of high-sensitivity ion trap ion mobility spectrometry time-of-flight techniques: A high-throughput nano-LC-IMS-TOF separation of peptides arising from a Drosophila protein extract *Anal. Chem.* **2003**, *75*, 5137-5145
14. Badman, E. R.; Myung, S.; Clemmer, D. E. Gas-phase separations of protein and peptide ion fragments generated by collision-induced dissociation in an ion trap *Anal. Chem.* **2002**, *74*, 4889-4894
15. Green, M. K.; Lebrilla, C. B. Ion-molecule reactions as probes of gas-phase structures of peptides and proteins *Mass Spectrom. Rev.* **1997**, *16*, 53-71
16. Valentine, S. J.; Counterman, A. E.; Clemmer, D. E. Conformer-dependent proton-transfer reactions of ubiquitin ions *J. Am. Soc. Mass Spectrom.* **1997**, *8*, 954-961
17. Valentine, S. J.; Anderson, J. G.; Ellington, A. D.; Clemmer, D. E. Disulfide-intact and -reduced lysozyme in the gas phase: Conformations and pathways of folding and unfolding *J. Phys. Chem. B* **1997**, *101*, 3891-3900
18. Valentine, S. J.; Clemmer, D. E. H/D exchange levels of shape-resolved cytochrome c conformers in the gas phase *J. Am. Chem. Soc.* **1997**, *119*, 3558-3566

19. Woenckhaus, J.; Mao, Y.; Jarrold, M. F. Hydration of gas phase proteins: Folded +5 and unfolded +7 charge states of cytochrome c *J. Phys. Chem. B* **1997**, *101*, 847-851
20. Fye, J. L.; Woenckhaus, J.; Jarrold, M. F. Hydration of folded and unfolded gas-phase proteins: Saturation of cytochrome c and apomyoglobin *Journal of the American Chemical Society* **1998**, *120*, 1327-1328
21. Woenckhaus, J. Drift time mass spectrometric protein hydration experiments *Int. J. Mass Spectrom.* **2002**, *213*, 9-24
22. Wyttenbach, T.; Liu, D. F.; Bowers, M. T. Hydration of small peptides *International Journal of Mass Spectrometry* **2005**, *240*, 221-232
23. Loo, R. R. O.; Udseth, H. R.; Smith, R. D. Evidence of Charge Inversion in the Reaction of Singly Charged Anions with Multiply Charged Macroions *J. Phys. Chem.* **1991**, *95*, 6412-6415
24. Loo, R. R. O.; Udseth, H. R.; Smith, R. D. A New Approach for the Study of Gas-Phase Ion-Ion Reactions Using Electrospray Ionization *J. Am. Soc. Mass Spectrom.* **1992**, *3*, 695-705
25. Pitteri, S. J.; McLuckey, S. A. Recent developments in the ion/ion chemistry of high-mass multiply charged ions *Mass Spectrom. Rev.* **2005**, *24*, 931-958
26. Stephenson, J. L.; McLuckey, S. A. Ion/ion proton transfer reactions for protein mixture analysis *Anal. Chem.* **1996**, *68*, 4026-4032
27. Stephenson, J. L.; McLuckey, S. A. Simplification of product ion spectra derived from multiply charged parent ions via ion/ion chemistry *Anal. Chem.* **1998**, *70*, 3533-3544
28. McLuckey, S. A.; Reid, G. E.; Wells, J. M. Ion parking during ion/ion reactions in electrodynamic ion traps *Anal. Chem.* **2002**, *74*, 336-346
29. Syka, J. E. P.; Coon, J. J.; Schroeder, M. J.; Shabanowitz, J.; Hunt, D. F. Peptide and protein sequence analysis by electron transfer dissociation mass spectrometry *Proc. Natl. Acad. Sci. U. S. A.* **2004**, *101*, 9528-9533
30. Pitteri, S. J.; Chrisman, P. A.; Hogan, J. M.; McLuckey, S. A. Electron transfer ion/ion reactions in a three-dimensional quadrupole ion trap: Reactions of doubly and triply protonated peptides with SO2 center dot *Anal. Chem.* **2005**, *77*, 1831-1839
31. Chrisman, P. A.; Pitteri, S. J.; Hogan, J. M.; McLuckey, S. A. SO2- electron transfer ion/ion reactions with disulfide linked polypeptide ions *J. Am. Soc. Mass Spectrom.* **2005**, *16*, 1020-1030
32. Breuker, K.; Oh, H. B.; Lin, C.; Carpenter, B. K.; McLafferty, F. W. Nonergodic and conformational control of the electron capture dissociation of protein cations *Proc. Natl. Acad. Sci. U. S. A.* **2004**, *101*, 14011-14016
33. Ge, Y.; Lawhorn, B. G.; ElNaggar, M.; Strauss, E.; Park, J. H.; Begley, T. P.; McLafferty, F. W. Top down characterization of larger proteins (45 kDa) by electron capture dissociation mass spectrometry *J. Am. Chem. Soc.* **2002**, *124*, 672-678

34. Wells, J. M.; Chrisman, P. A.; McLuckey, S. A. Formation of protein-protein complexes in vacuo *J. Am. Chem. Soc.* **2001**, *123*, 12428-12429
35. Newton, K. A.; McLuckey, S. A. Generation and manipulation of sodium cationized peptides in the gas phase *J. Am. Soc. Mass Spectrom.* **2004**, *15*, 607-615
36. Stephenson, J. L.; McLuckey, S. A. Adaptation of the Paul Trap for study of the reaction of multiply charged cations with singly charged anions *Int. J. Mass Spectrom. Ion Process.* **1997**, *162*, 89-106
37. Reid, G. E.; Wells, J. M.; Badman, E. R.; McLuckey, S. A. Performance of a quadrupole ion trap mass spectrometer adapted for ion/ion reaction studies *Int. J. Mass Spectrom.* **2003**, *222*, 243-258
38. Wu, J.; Hager, J. W.; Xia, Y.; Londry, F. A.; McLuckey, S. A. Positive ion transmission mode ion/ion reactions in a hybrid linear ion trap *Anal. Chem.* **2004**, *76*, 5006-5015
39. Xia, Y.; Liang, X.; McLuckey, S. A. Pulsed Dual Electrospray Ionization for Ion/Ion Reactions *Journal of the American Society for Mass Spectrometry* **2005**, *16*, 1750-1756
40. Badman, E. R.; Chrisman, P. A.; McLuckey, S. A. A quadrupole ion trap mass spectrometer with three independent ion sources for the study of gas-phase ion/ion reactions *Anal. Chem.* **2002**, *74*, 6237-6243
41. Liang, X. R.; Xia, Y.; McLuckey, S. A. Alternately pulsed nanoelectrospray ionization/atmospheric pressure chemical ionization for ion/ion reactions in an electrodynamic ion trap *Analytical Chemistry* **2006**, *78*, 3208-3212
42. Liang, X. R.; Han, H. L.; Xia, Y.; McLuckey, S. A. A pulsed triple ionization source for sequential ion/ion reactions in an electrodynamic ion trap *Journal of the American Society for Mass Spectrometry* **2007**, *18*, 369-376
43. McLuckey, S. A.; Glish, G. L.; Asano, K. G.; Grant, B. C. Atmospheric Sampling Glow-Discharge Ionization Source for the Determination of Trace Organic-Compounds in Ambient Air *Analytical Chemistry* **1988**, *60*, 2220-2227
44. Valentine, S. J.; Koeniger, S. L.; Clemmer, D. E. A split-field drift tube for separation and efficient fragmentation of biomolecular ions *Anal. Chem.* **2003**, *75*, 6202-6208
45. Him, T.; Tolmachev, A. V.; Harkewicz, R.; Prior, D. C.; Anderson, G.; Udseth, H. R.; Smith, R. D.; Bailey, T. H.; Rakov, S.; Futrell, J. H. Design and implementation of a new electrodynamic ion funnel *Anal. Chem.* **2000**, *72*, 2247-2255
46. Tang, K.; Shvartsburg, A. A.; Lee, H. N.; Prior, D. C.; Buschbach, M. A.; Li, F. M.; Tolmachev, A. V.; Anderson, G. A.; Smith, R. D. High-sensitivity ion mobility spectrometry/mass spectrometry using electrodynamic ion funnel interfaces *Analytical Chemistry* **2005**, *77*, 3330-3339

47. Julian, R. R.; Mabbett, S. R.; Jarrold, M. F. Ion funnels for the masses: Experiments and simulations with a simplified ion funnel *Journal of the American Society for Mass Spectrometry* **2005**, *16*, 1708-1712
48. Badman, E. R.; Hoaglund-Hyzer, C. S.; Clemmer, D. E. Dissociation of different conformations of ubiquitin ions *J. Am. Soc. Mass Spectrom.* **2002**, *13*, 719-723
49. Clemmer, D. E.; Jarrold, M. F. Ion mobility measurements and their applications to clusters and biomolecules *J. Mass Spectrom.* **1997**, *32*, 577-592
50. Rachel R. Ogorzalek Loo, B. E. W., and Richard D. Smith Proton Transfer Reaction Studies of Multiply Charged Proteins in a High Mass-to-Charge Ratio Quadrupole Mass Spectrometer *Journal of American Society for Mass Spectrometry* **1994**, *5*, 1064-1071
51. Stephen J. Valentine, J. G. A., Andrew D. Ellington, and David E. Clemmer Disulfide-Intact and -Reduced Lysozyme in the Gas Phase: Conformations and Pathways of Folding and Unfolding *Journal of Physical Chemestry B* **1997**, *101*, 3891-3900
52. Xia, Y.; Liang, X. R.; McLuckey, S. A. Ion trap versus low-energy beam-type collision-induced dissociation of protonated ubiquitin ions *Analytical Chemistry* **2006**, *78*, 1218-1227

Table 1. Measured cross-sections for ubiquitin ions in different charge states.

Charge state	m/z	Cross-section ($Å^2$)
+8	1071.6	1444.0
+7	1224.7	1405.3
+6	1482.5	1365.1
+5	1714.0	1054.5
+4	2142.2	960.5
+3	2856.0	938.2
+2	4283.5	945.4
+1	8565.9	944.7

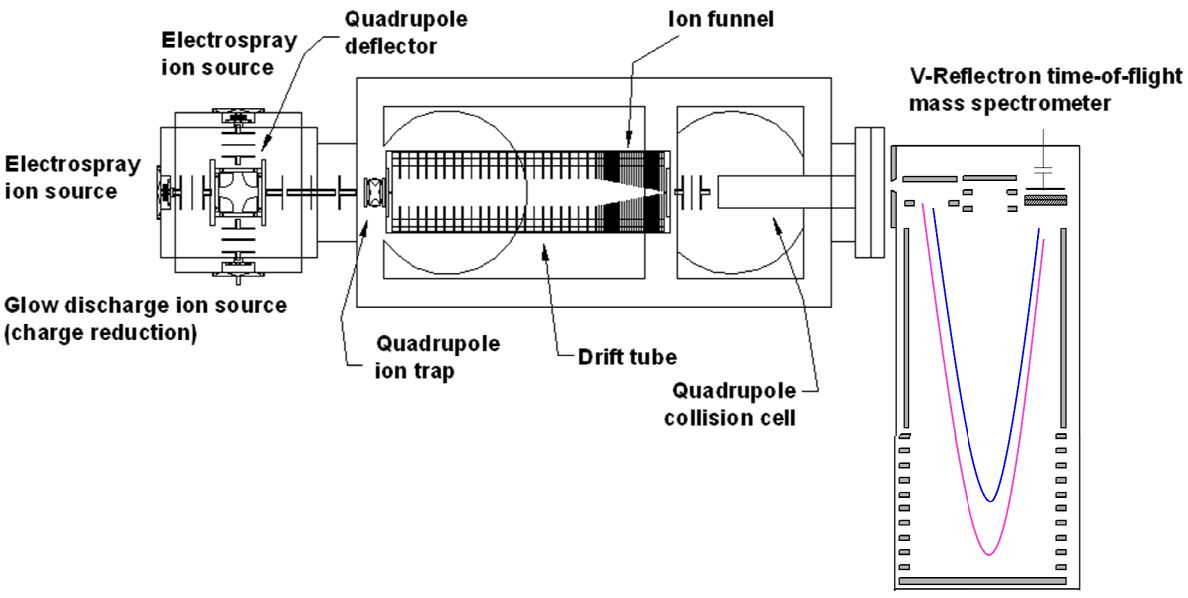

Figure 1. Scale diagram showing overall instrument, including two ESI and one ASGDI sources, ion optics, quadrupole deflector, IT, IM drift tube with ion funnel and q-TOF.

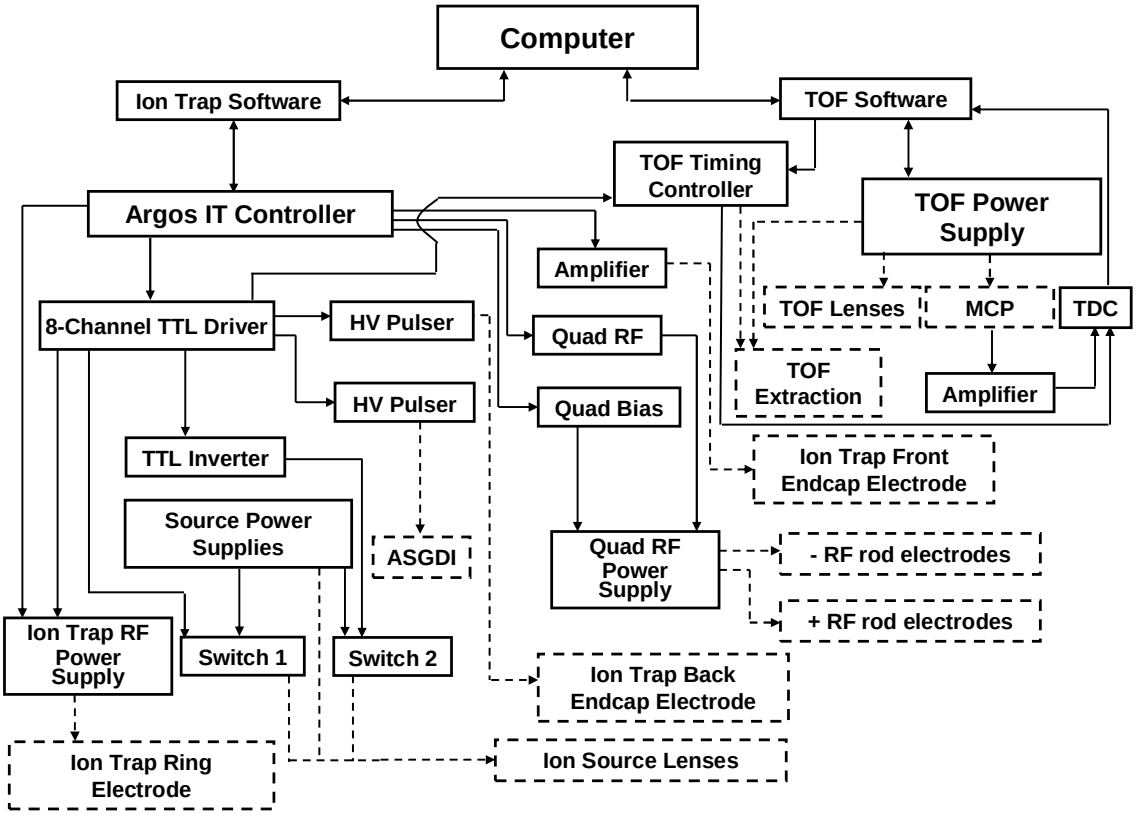

Figure 2. Block diagram of instrument control electronics (see text for details). The solid lines indicate instrument control electronics, and the dashed lines indicate hardware in the vacuum chamber.

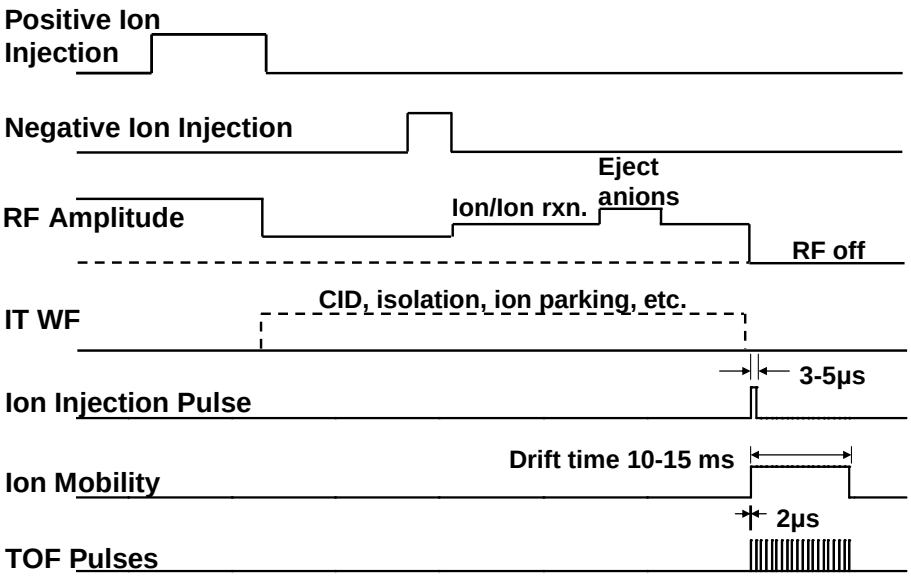

Figure 3. A generic scan function for an ion/ion reaction followed by nested flight time/ion mobility experiment. The top and second plots show the time during which positive and negative ions are injected. The third plot shows the amplitude of the rf trapping voltage applied to the ring electrode of the ion trap. The lower three plots show the times when ions after ion/ion reaction are injected into the drift tube, ion mobility data acquisition and TOF extraction pulses.

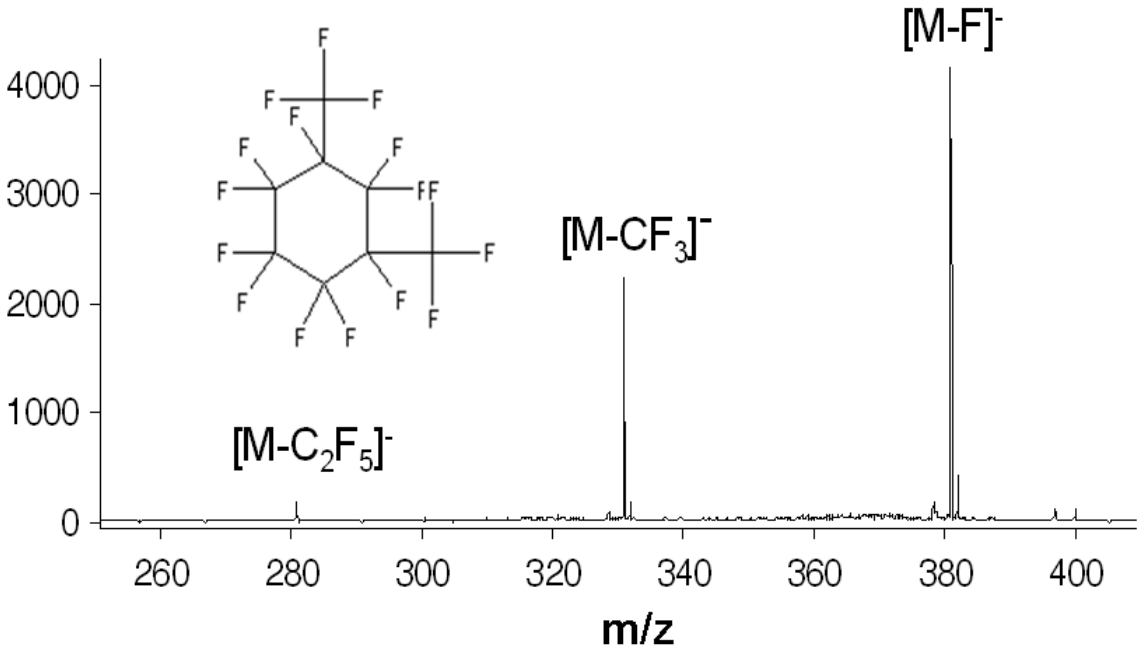

Figure 4. Mass spectrum of PDCH reagent ions from ASGDI.

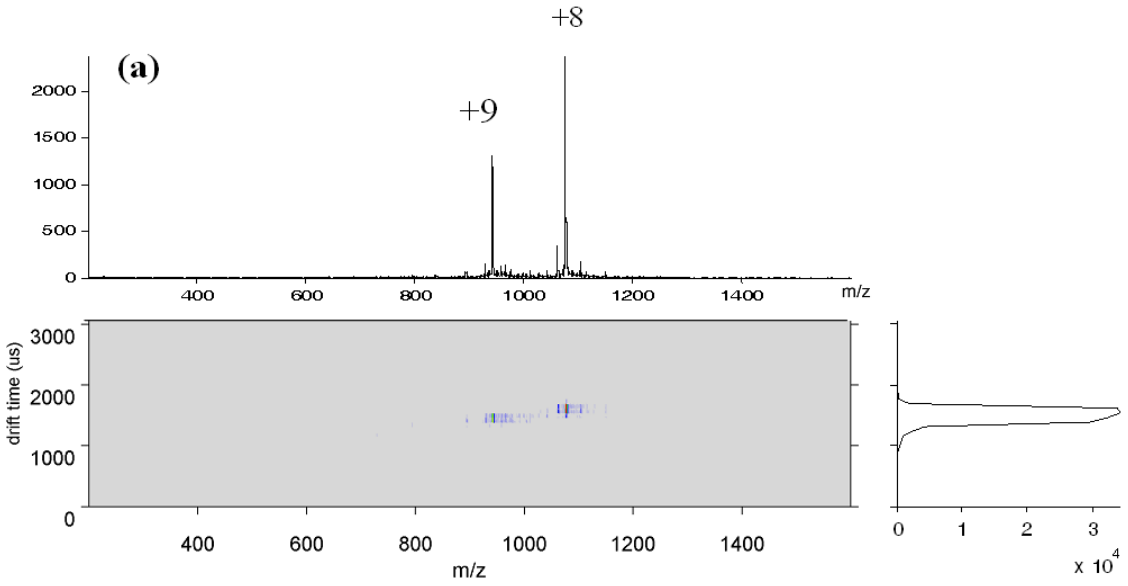

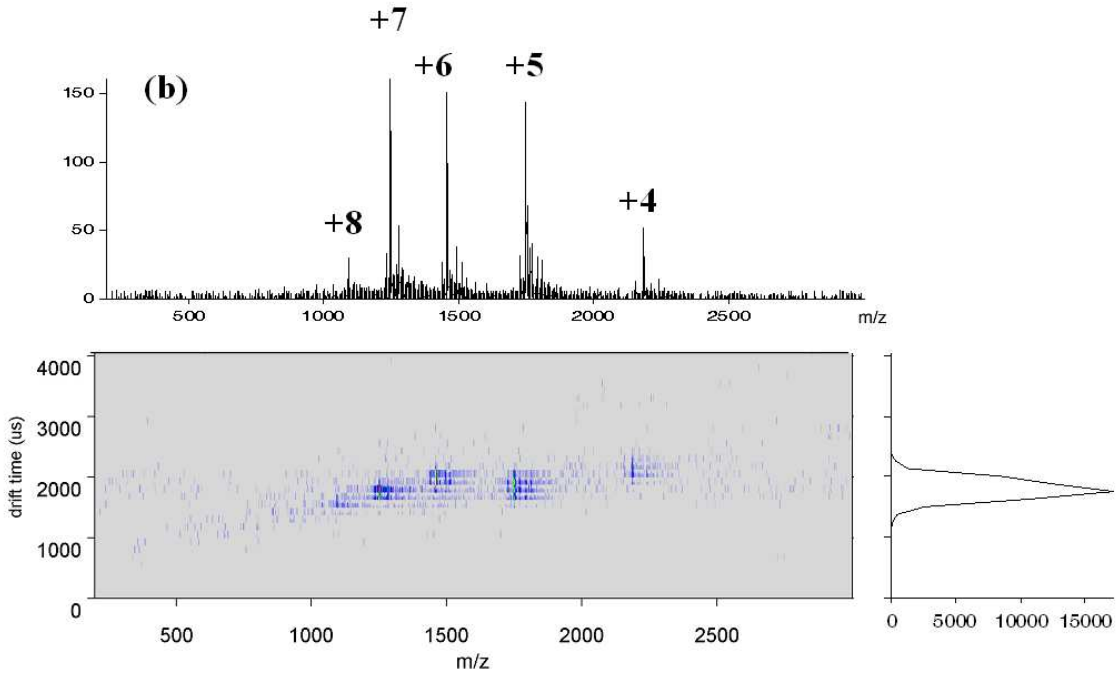

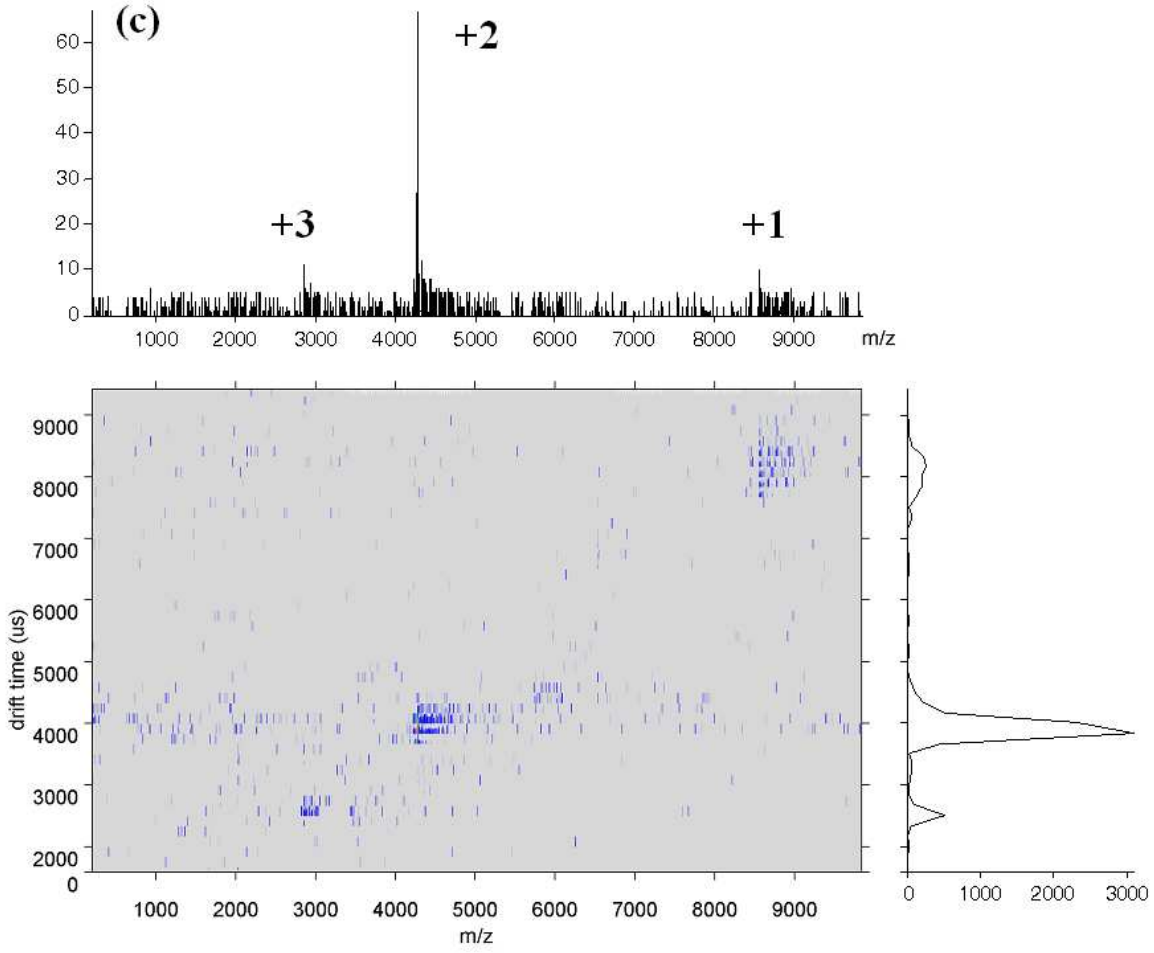

Figure 5. a) 3D mobility mass spectrum of ubiquitin; b) 3D mobility mass spectrum of ubiquitin after ion/ion reaction with PDCH negative ions for 20 ms; and c) spectrum after reaction for 200 ms. The ions in lower charge states are more readily resolved by IM. Conditions: 0.30mg/ml ubiquitin aqueous solution with 1% acetic acid, drift voltage -150V to -700V, drift pressure 1.045 Torr, IT fill time 50 ms for ubiquitin.

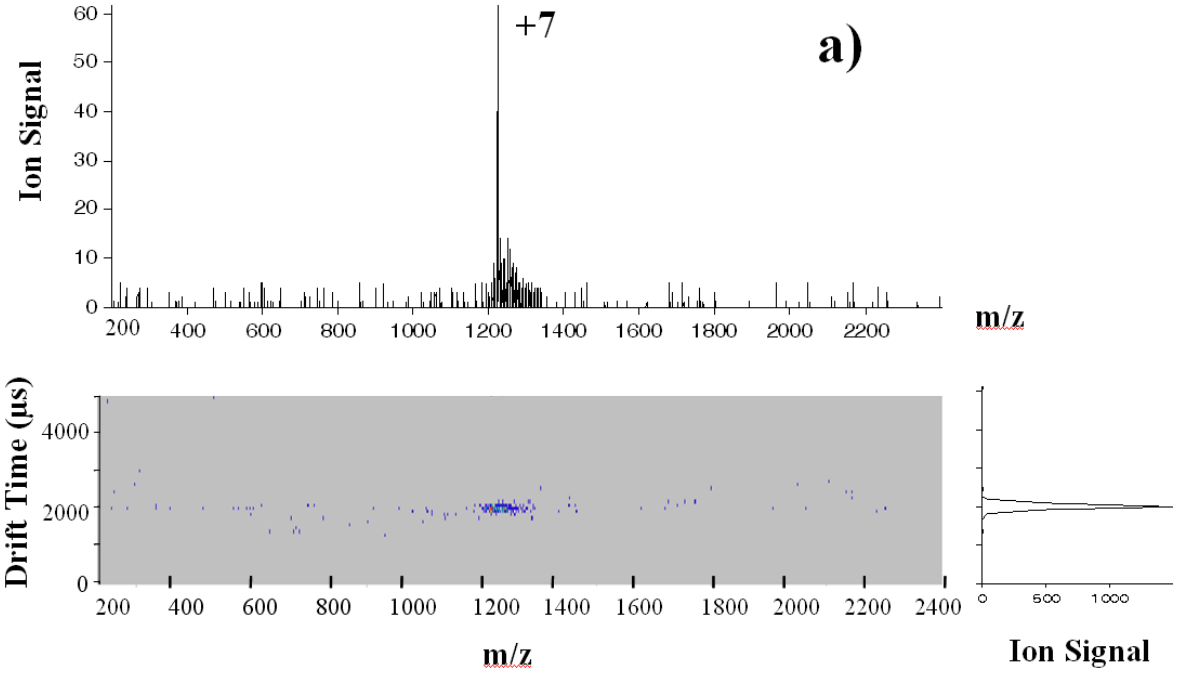

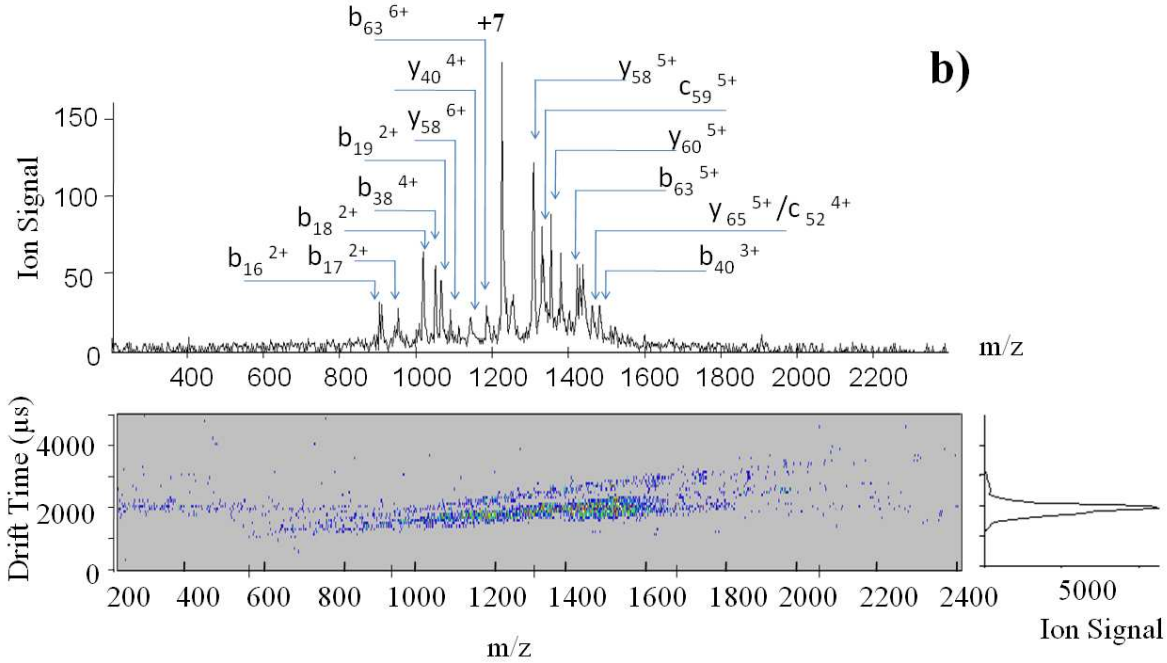

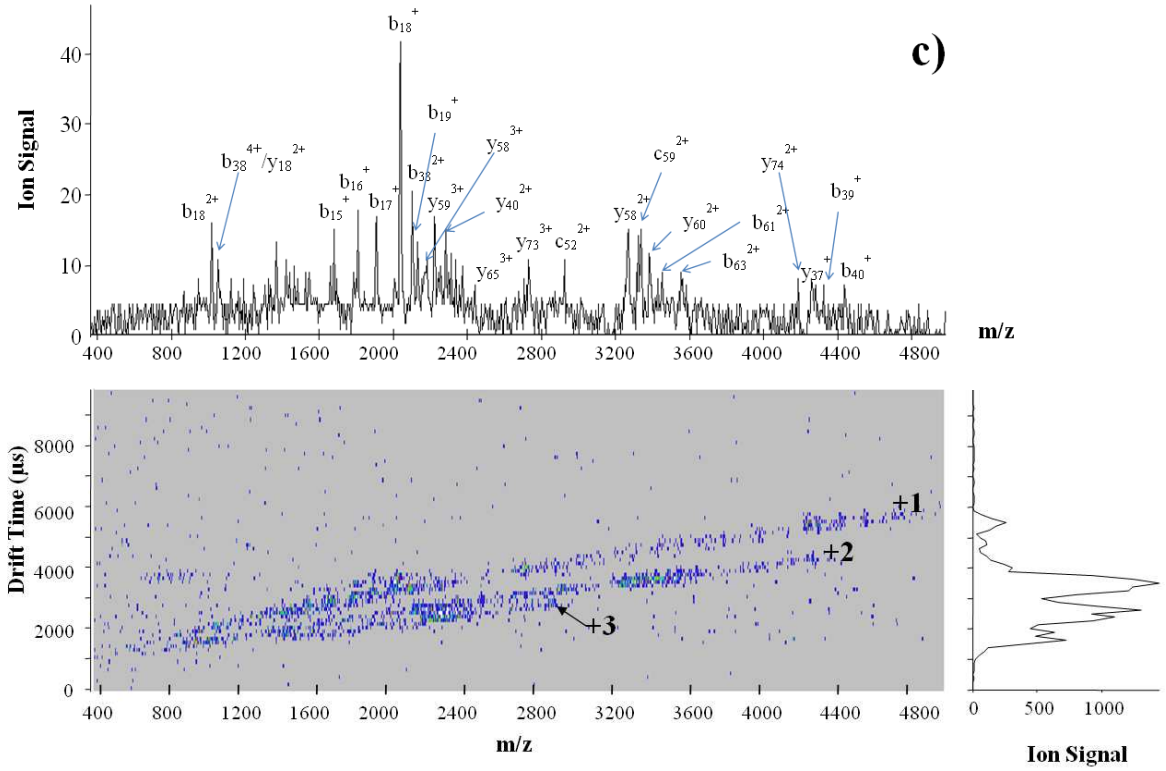

Figure 6**.** a) 3-D ion mobility spectrum of isolated ubiquitin +7 ions from 3-D ion trap; b) CID fragments from ubiquitin +7 ions generated in 3-D ion trap; c) CID fragments from ubiquitin +7 ions after charge reduction with PDCH ions for 30 ms.

CHAPTER 4.

Effects of Ion/Ion Reactions on Conformation of Gas-Phase Cytochrome *c* Ions

Qin Zhao*, Mathew W. Soyk*†, Gregg M. Schieffer*†, R. S. Houk*† and Ethan R. Badman‡

*Department of Chemistry, Iowa State University, Ames, IA, 50011 USA

†Ames Laboratory USDOE, Iowa State University, Ames IA 50011 USA

‡ Hoffman-La Roche Inc., Non-Clinical Safety, Nutley, NJ, 07110, USA

A manuscript to be submitted to the *Journal of the American Society for Mass Spectrometry*, 2008.

Abstract

Positive ions from cytochrome *c* are studied in a 3-D ion trap/ion mobility (IM)/quadrupole-time-of-flight (TOF) instrument with three independent ion sources. The IM separation allows measurement of the cross section of the ions. Ion/ion reactions in the 3-D ion trap that remove protons cause the cytochrome *c* ions to refold gently without other degradation of protein structure. The conformation(s) of the product ions generated by ion/ion reactions in a given charge state are independent of the original charge state of the cytochrome *c* ions. In the lower charge states (+1 to +5) cytochrome *c* ions made by the ion/ion reaction have a single conformation with cross section of ~ 1110 to 1180 $Å^2$, even if the original +8 ion started with two conformations. These cross section values are close to those of the "most folded" conformation found previously. The conformation expands slightly when the charge state is reduced from +5 to +1. In a given charge state, ions created

by ion/ion reaction prefer to produce the more compact conformation in somewhat higher abundances, compared to those produced by the electrospray ionization (ESI) source alone. A variety of related studies that employ ion/ion reactions and IM to probe conformations of biomolecular ions should be possible by these methods.

Introduction

The determination of protein conformation is important in many biological applications. Of the various methods for these measurements, mass spectrometry (MS) has certain advantages such as speed and the need for only small amounts of sample. The variations of MS for the study of protein conformation include ion mobility (IM)[1-3], H/D exchange [4-8], and native electron capture dissociation (NECD)[9, 10]. Of these methods, IM provides a direct way to examine the gas-phase conformation of the ions by probing the average cross-section of the protein ions via collisions with buffer gas [3]. Early research on protein folding and unfolding was done with an IM-quadrupole instrument[1]. To study ions in lower charge states than those made directly from the electrospray ionization (ESI) source, a basic collision gas (e.g., acetophenone or 7-methyl-1, 3, 5-triazabicyclo [4,4,0] dec-5-ene(MTBD)) [11] was introduced into the source region. The collision gas extracted protons from the protein ion and created lower charge state ions through proton transfer reactions in the source. In these studies, the reactions took place only in the atmospheric pressure ion source interface region. Thus, control and variation of the reaction time and extent of reaction were difficult, and only certain reagent ions were available.

Recent instrumentation improvements have greatly extended the type of structural information and number of possible experiments available in this area. The development of a 3-D trap-IM-time of flight (TOF) instrument allows time dependent studies of gas-phase protein ions, including folding, unfolding and structural transitions[12-15]. A multi-stage IMS-MS instrument[16, 17] provides two important new functions. First, a protein ion in a specific structure can be selected by IMS, then activated and separated in the next drift region. Second, "state- to- state" structural transitions can be studied by "structure selection-activation" cycles.

Gas-phase ion-ion reactions provide another dimension for gas-phase bioanalysis by MS. To date, these reactions have been mainly used to simplify complex MS/MS spectra[18, 19] or provide fragments for structural assignment [20, 21] by methods like electron transfer dissociation (ETD)[22-24]. A three-source-ion trap-drift tube-q-TOF instrument was recently developed by our group to combine ion-ion reactions with IM-TOF measurements[25, 26]. The present paper describes how proton transfer ion/ion reactions can be used to manipulate charge state and study the effect of ion/ion reactions on the conformation change of cytochrome *c* ions.

Experimental

The design and general operating conditions for the home-built three source-3-D trap-IM-TOFMS are described in another paper [25]. Bovine heart cytochrome *c* (Sigma-Aldrich, St. Louis, MO) is the test protein because the behavior of its gas-phase ions has been studied extensively [12, 15, 27]. In most experiments, the protein was dissolved without further purification at 20 to 30 μM in water with 1% aqueous acetic acid; water alone was used for

some of the results shown in the last figure. These samples were introduced through one nano-ESI source in positive mode. Perfluoro-1,3-dimethylcyclohexane (PDCH, Sigma-Aldrich, St. Louis MO) was used as the proton transfer reagent. Negative PDCH ions were created by atmospheric sampling glow discharge ionization (ASGDI) in a second source. Both positive cytochrome *c* ions and negative PDCH ions were trapped together in the 3-D trap and allowed to react for selected times between 50 ms to 200 ms. The product ions were then injected into the drift tube for IM separation, followed by m/z analysis and detection by TOF-MS. The drift tube is 44.45 cm long, filled with helium gas at a pressure of 1 to 1.5 Torr, and the axial electric field in the drift tube is 12 to 13 V/cm. Cross sections are calculated from the mass resolved mobility spectra in the usual fashion[3, 28].

Results and Discussion

Effect of Charge Reduction Reaction on the Conformation of Cytochrome c Ions.

In 1% acetic acid/water solution, ESI produces cytochrome *c* ions in two main charge states (+8 and +9), as seen in the 3-D nested drift/flight [1] IM-TOF mass spectrum (Figure 1). Although their IM drift times overlap, resolved mobility peaks for the +8 and +9 ions can be extracted because these ions are m/z resolved. Note that the +8 ion has two resolvable cross sections, which are generally attributed to different gas-phase conformations.

To study how ion/ion reactions affect the conformation of protein ions, either +8 or +9 ions are isolated in the 3-D ion trap first. The mass spectra of isolated +8 and +9 ions and their cross section distributions are shown in Figure 2. The cross section plots are similar to those obtained when both +8 and +9 ions are stored and ejected into the drift tube before m/z

resolution. Isolation in the 3-D trap does not heat and unfold the ions appreciably, at least at time scales up to ~ 200 ms.

PDCH anions are then injected into the ion trap from the ASGDI source and react with cytochrome *c* ions to remove protons for the desired time. A typical spectrum after ion/ion reaction is shown in Figure 3. The resulting cross sections (Table 1) agree well with those reported in the literature [12]. The proton transfer reactions leave the protein ions in a range of charge states, which can be as low as +1. These reactions do not remove the covalently-bound heme group, in agreement with other reports on myoglobin, which does not lose its noncovalently-bound heme group after proton transfer reactions [29].

Cross-section values for cytochrome *c* ions in each charge state, produced by reaction of either isolated +8 or +9 ions with PDCH anions in the trap, are summarized in Table 1. The distributions of cross section observed for each charge state are indicated in Figure 4. These distribution plots indicate the relative abundances of the various folded conformations of the cytochrome *c* ion in a given charge state.

In general, the distributions of conformations for a given charge state are similar whether the ions started as +8 or +9. The distribution for the +7 ion made from +8 (i.e., in the left plot in Figure 4) has an additional, partly resolved peak at low cross section that is not seen in the distribution for the +7 ion made from +9. The wider peaks seen for +7 and +6 ions after ion/ion reaction suggest that there may be several additional conformations not fully resolved by ion mobility. The ions in lower charge states (+5 to +1) have only one mobility peak, even when the reactant ion was the +8 form with two mobility peaks originally.

It is tempting to assert that observation of just one mobility peak means the ions have only one conformation. The narrowest mobility peak seen for the +9 ion of cytochrome *c* has a full width at half maximum (fwhm) of ~180 µs (Figure 1). Calculations indicate the contribution to the fwhm of this peak from diffusion to be only ~ 16 µs. Under these experimental conditions, $Cs_7I_6^+$ ions or protonated reserpine ions (from ESI of CsI or reserpine in water) yield single mobility peaks ~80 µs fwhm, roughly half the width of the narrowest protein peaks. Thus, each of the "single" mobility peaks seen for cytochrome *c* may actually correspond to the juxtaposition of unresolved peaks from ions in several conformations of similar size. For brevity, we use phrases like "one conformation" or "a single conformation" in the discussion below, with this caveat in mind.

These results show that the protein ions can fold to one or more compact conformations during the charge reduction reaction. This observation is explained as follows. When the protein ions pass into the vacuum system, the solvent molecules evaporate, and the attraction between hydrophobic portions of the molecules diminishes. Thus, the highly charged protein ion opens rapidly to an "unfolded" conformation [11, 12]. The ion/ion reaction then removes protons, whose charges keep the protein unfolded. Intramolecular charge repulsion becomes weaker, hydrogen bonds become more important, so the protein gradually refolds as more protons are removed.

The cross-section of cytochrome *c* in the crystal structure is 1090 $Å^2$ [12, 30] . In the gas phase, ions with cross-sections from 1050 $Å^2$ to 1350 $Å^2$ are generally assigned to this "most compact" conformation[12, 30]. Thus, Figure 4 shows that the proton transfer reactions in the 3-D ion trap allow the original "unfolded" protein to pass gradually through

several partially folded conformations and eventually assume the most compact conformation, with a cross section close to that of cytochrome *c* in its crystal structure.

Close examination of the mobility plots in Figure 4 shows that the +5 ion has the smallest cross section, and cross sections for those ions in the "most compact" conformation increase slightly as charge state is reduced from +5 to +1. Apparently, as more protons are removed from the +5 ion, cytochrome *c* stays in one conformation, but the size of the molecule expands by a measurable amount. This effect has not been seen previously.

Conformation of Ions Made by Ion/Ion Reaction Compared to Those Produced Directly by ESI. To generate ions in lower original charge states, cytochrome *c* is sprayed from water without acetic acid. These ions are then measured without ion/ion reaction, and the results are compared to those obtained by charge reduction reactions of more highly charged ions from water/acetic acid solutions.

Figure 5 compares cross section distributions for ions in a given charge state, prepared either by ion/ion reaction or by ESI directly. First, consider the results for the +7 and +6 charge states. Within a given charge state, either +7 or +6, the number of conformations seen and their cross sections are almost the same, but the relative abundances of the various conformations can be different. More compact conformations are more abundant for the +5, +6 and +7 ions made by ion/ion reaction than by ESI directly. For the +5 ions, the "most compact" conformation is most abundant, and at least one entirely different, more open conformation is seen only for the +5 ions made by ESI directly from water. The "closed" +5 conformer made by ion/ion reaction could not be converted to the more "open" structure by heating the +5 ions, i.e., by increasing the trapping time (as far as 4 s) or by increasing the

kinetic energy used to inject ions into the drift tube. For the +4 ions in Figure 5, a "single" conformation with cross section ~ 1200 $Å^2$ predominates, although there is some of an even smaller conformation for the ions produced directly by ESI.

Conclusions

Gas-phase ion-ion reactions combined with IM measurements provide a new way to study conformation changes in protein ions. Exothermic processes like these multiple proton transfer reactions might be expected to simply heat the ions and unfold them[31] . The observation of the protein ions in folded states after ion/ion reaction agrees with McLuckey's findings that collisions with the bath gas in the 3-D trap cool the ions[32]. Thus, ion/ion reactions can be performed while the ions remain in, or perhaps re-fold into, biologically-interesting conformations.

In addition to the charge reduction reactions described here, this three source-ion trap-IM-TOFMS should facilitate a variety of ion/ion reaction studies pertinent to bioanalysis. The identity and amount of reagent ion and the reaction time can be controlled over wide ranges. Other reactions such as electron transfer dissociation [22, 23], metal addition [33] , and some sequential reactions (e.g., ETD followed by charge reduction to simplify assignment of the ETD fragments) should be possible. The time progression of kinetic processes that change either the m/z value or the conformation of the ions should be measurable, at least for processes that occur on time scales long compared to the duration of the measurement (~ 1 s). These and other studies are underway in our laboratory.

Acknowledgments

This work was funded by a grant from the Vice Provost for Research, Iowa State University. QZ and MS acknowledge the Conoco-Phillips Fellowship (Iowa State University, 2006-2007 and 2007-2008) for financial support. MS also acknowledges the GAANN Fellowship (Iowa State University, 2008) and the Velmer A. and Mary K. Fassel Fellowship (Iowa State University, 2006-2007).

References

1. Hoaglund, C.S., Valentine, S. J., Sporleder, C. R., Reilly, J. P., Clemmer, D. E., *Three-dimensional ion mobility TOFMS analysis of electrosprayed biomolecules.* Analytical Chemistry, 1998. **70**(11): p. 2236-2242.
2. Clemmer, D.E., Hudgins, R. R., Jarrold, M. F., *Naked Protein Conformations - Cytochrome-C in the Gas-Phase.* Journal of the American Chemical Society, 1995. **117**(40): p. 10141-10142.
3. Clemmer, D.E., Jarrold, M. F., *Ion mobility measurements and their applications to clusters and biomolecules.* Journal of Mass Spectrometry, 1997. **32**(6): p. 577-592.
4. Wood, T.D., Chorush, R. A., Wampler, F. M., Little, D. P., Oconnor, P. B., McLafferty, F. W., *Gas-Phase Folding and Unfolding of Cytochrome-C Cations.* Proceedings of the National Academy of Sciences of the United States of America, 1995. **92**(7): p. 2451-2454.
5. Cassady, C.J., Carr, S. R., *Elucidation of isomeric structures for ubiquitin [M+12H] (12+) ions produced by electrospray ionization mass spectrometry.* Journal of Mass Spectrometry, 1996. **31**(3): p. 247-254.
6. Freitas, M.A., Hendrickson, C. L., Emmett, M. R., Marshall, A. G., *Gas-phase bovine ubiquitin cation conformations resolved by gas-phase hydrogen/deuterium exchange rate and extent.* International Journal of Mass Spectrometry, 1999. **187**: p. 565-575.
7. Freitas, M.A., Hendrickson, C. L., Marshall, A. G., *Correlation Between Solution and Gas-phase Protein Conformation: H/D Exchange, IRMPD, and ESI FT-ICR MS.* Proc. SPIE-Int. Soc. Opt. Eng., 2000. **3926**: p. 61-68.
8. Robinson, E.W. and E.R. Williams, *Multidimensional separations of ubiquitin conformers in the gas phase: Relating ion cross sections to H/D exchange*

measurements. Journal of the American Society for Mass Spectrometry, 2005. **16**(9): p. 1427-1437.

9. Breuker, K., McLafferty, F. W., *Native electron capture dissociation for the structural characterization of noncovalent interactions in native cytochrome c.* Angewandte Chemie-International Edition, 2003. **42**(40): p. 4900-4904.
10. Breuker, K., and McLafferty, Fred W., *The Thermal Unfolding of native Cytochrome c in the Transition from Solution to Gas Phase Probed by Native Electron Capture Dissociation.* Angrew Chem. Int. Ed., 2005. **44**: p. 4911-4914.
11. Valentine, S.J., Counterman, A. E., Clemmer, D. E., *Conformer-dependent proton-transfer reactions of ubiquitin ions.* Journal of the American Society for Mass Spectrometry, 1997. **8**(9): p. 954-961.
12. Badman, E.R., Hoaglund-Hyzer, C. S., Clemmer, D. E., *Monitoring Structural Changes of Proteins in an Ion Trap over ~10 to 200 ms: Unfolding Transitions in Cytochrome c Ions.* Analytical Chemistry, 2001. **73**(24): p. 6000-6007.
13. Badman, E.R., Hoaglund-Hyzer, C. S., Clemmer, D. E., *Dissociation of different conformations of ubiquitin ions.* Journal of the American Society for Mass Spectrometry, 2002. **13**(6): p. 719-723.
14. Myung, S., Badman, E. R., Lee, Y. J., Clemmer, D. E., *Structural transitions of electrosprayed ubiquitin ions stored in an ion trap over similar to 10 ms to 30 s.* Journal of Physical Chemistry A, 2002. **106**(42): p. 9976-9982.
15. Badman, E.R., Myung, S., Clemmer, D. E., *Evidence for Unfolding and Refolding of Gas-Phase Cytochrome c Ions in a Paul Trap.* Journal of the American Society for Mass Spectrometry, 2005. **16**(9): p. 1493-1497.
16. Koeniger S. L., Merenbloom Samuel I., and Clemmer David E., *Evidence for Many Resolvable Structures within Conformation Types of Electrosprayed Ubiquitin Ions.* Journal of Physical Chemstry B, 2006. **110**(7017-7021).
17. Koeniger S. L., M.S.I., Sevugarajan Sundarapandian, Clemmer David E., Hudgins, Robert R., Jamold Martin F., *Transfer of Structural Elements from Compact to Extended States in Unsolvated Ubiquitin.* Journal of American Chemical Society, 2006. **128**(35): p. 11713-11719.
18. Stephenson, J.L., McLuckey, S. A., *Simplification of product ion spectra derived from multiply charged parent ions via ion/ion chemistry.* Analytical Chemistry, 1998. **70**(17): p. 3533-3544.
19. Stephenson, J.L., McLuckey, S. A., Reid, G. E., Wells, J. M., Bundy, J. L., *Ion/ion chemistry as a top-down approach for protein analysis.* Current Opinion in Biotechnology, 2002. **13**(1): p. 57-64.
20. Breuker, K., Oh, H. B., Lin, C., Carpenter, B. K., McLafferty, F. W., *Nonergodic and conformational control of the electron capture dissociation of protein cations.*

Proceedings of the National Academy of Sciences of the United States of America, 2004. **101**(39): p. 14011-14016.

21. Ge, Y., Lawhorn, B. G., ElNaggar, M., Strauss, E., Park, J. H., Begley, T. P., McLafferty, F. W., *Top down characterization of larger proteins (45 kDa) by electron capture dissociation mass spectrometry.* Journal of the American Chemical Society, 2002. **124**(4): p. 672-678.
22. Syka, J.E.P., Coon, J. J., Schroeder, M. J., Shabanowitz, J., Hunt, D. F., *Peptide and protein sequence analysis by electron transfer dissociation mass spectrometry.* Proceedings of the National Academy of Sciences of the United States of America, 2004. **101**(26): p. 9528-9533.
23. Pitteri, S.J., Chrisman, P. A., Hogan, J. M., McLuckey, S. A., *Electron transfer ion/ion reactions in a three-dimensional quadrupole ion trap: Reactions of doubly and triply protonated peptides with SO2 center dot.* Analytical Chemistry, 2005. **77**(6): p. 1831-1839.
24. Chrisman, P.A., Pitteri, S. J., Hogan, J. M., McLuckey, S. A., *SO2- electron transfer ion/ion reactions with disulfide linked polypeptide ions.* Journal of the American Society for Mass Spectrometry, 2005. **16**(7): p. 1020-1030.
25. Zhao, Q., Soyk, M., Schieffer Gregg, Badman, Ethan R. and Houk, R., S., submitted to J. Am. Soc. Mass Spectrum.
26. Badman, E.R., Schieffer, G.M., Soyk, M., Zhao, Q., Anderson, T.J. *An ESI-Ion Trap-Ion Mobility-q-TOF to Study Ion-Ion Reactions of Intact Biopolymers*. in *Proceedings of the 53rd ASMS Conference on Mass Spectrometry and Allied Topics*. 2005. San Antonio, TX.
27. McLafferty, F.W., Guan, Z. Q., Haupts, U., Wood, T. D., Kelleher, N. L., *Gaseous conformational structures of cytochrome c.* Journal of the American Chemical Society, 1998. **120**(19): p. 4732-4740.
28. Chrisman, P.A., Newton, K. A., Reid, G. E., Wells, J. M., McLuckey, S. A., *Loss of charged versus neutral heme from gaseous holomyoglobin ions.* Rapid Communications in Mass Spectrometry, 2001. **15**(23): p. 2334-2340.
29. Stephenson, J.L., VanBerkel, G. J., McLuckey, S. A., *Ion-ion proton transfer reactions of bio-ions involving noncovalent interactions: Holomyoglobin.* Journal of the American Society for Mass Spectrometry, 1997. **8**(6): p. 637-644.
30. David E. Clemmer, R.R.H., and Martin F. Jamold, *Naked Protein Conformations: Cytochrome c in the Gas Phase.* Journal of American Chemical Society, 1995. **117**: p. 10141-10142.
31. Stephenson, J.L., McLuckey, S. A., *Ion/ion reactions in the gas phase: Proton transfer reactions involving multiply-charged proteins.* Journal of the American Chemical Society, 1996. **118**(31): p. 7390-7397.

32. Wells, J.M., Chrisman, P. A., McLuckey, S. A., *Formation and characterization of protein-protein complexes in vacuo.* Journal of the American Chemical Society, 2003. **125**(24): p. 7238-7249.
33. Badman, E.R., P.A. Chrisman, and S.A. McLuckey, *A quadrupole ion trap mass spectrometer with three independent ion sources for the study of gas-phase ion/ion reactions.* Analytical Chemistry, 2002. **74**(24): p. 6237-6243.

Table 1. Average cross-sections of cytochrome *c* in different charge states

*****Cross-section of ions from charge reduction of isolated +9 cytochrome *c* ions

[#]Cross-section of ions from charge reduction of isolated +8 cytochrome *c* ions

Charge State	m/z	*Cross-section ($Å^2$) ± 56$Å^2$	[#]Cross-section ($Å^2$) ± 56$Å^2$
+9	1359.6	2116.3	
+8	1529.6	1601.0, 1847.6	1798.0, 2032.8
+7	1748.0	1616.6, 1832.4	1612.4,1827.6
+6	2039.2	1293.2, 1478.1	1197.6, 1474.3
+5	2446.8	1077.7	1074.9
+4	3058.3	1108.3	1162.4
+3	4077.3	1154.5	1151.5
+2	6115.5	1120.8	1179.2
+1	12230	1185.4	1182.3

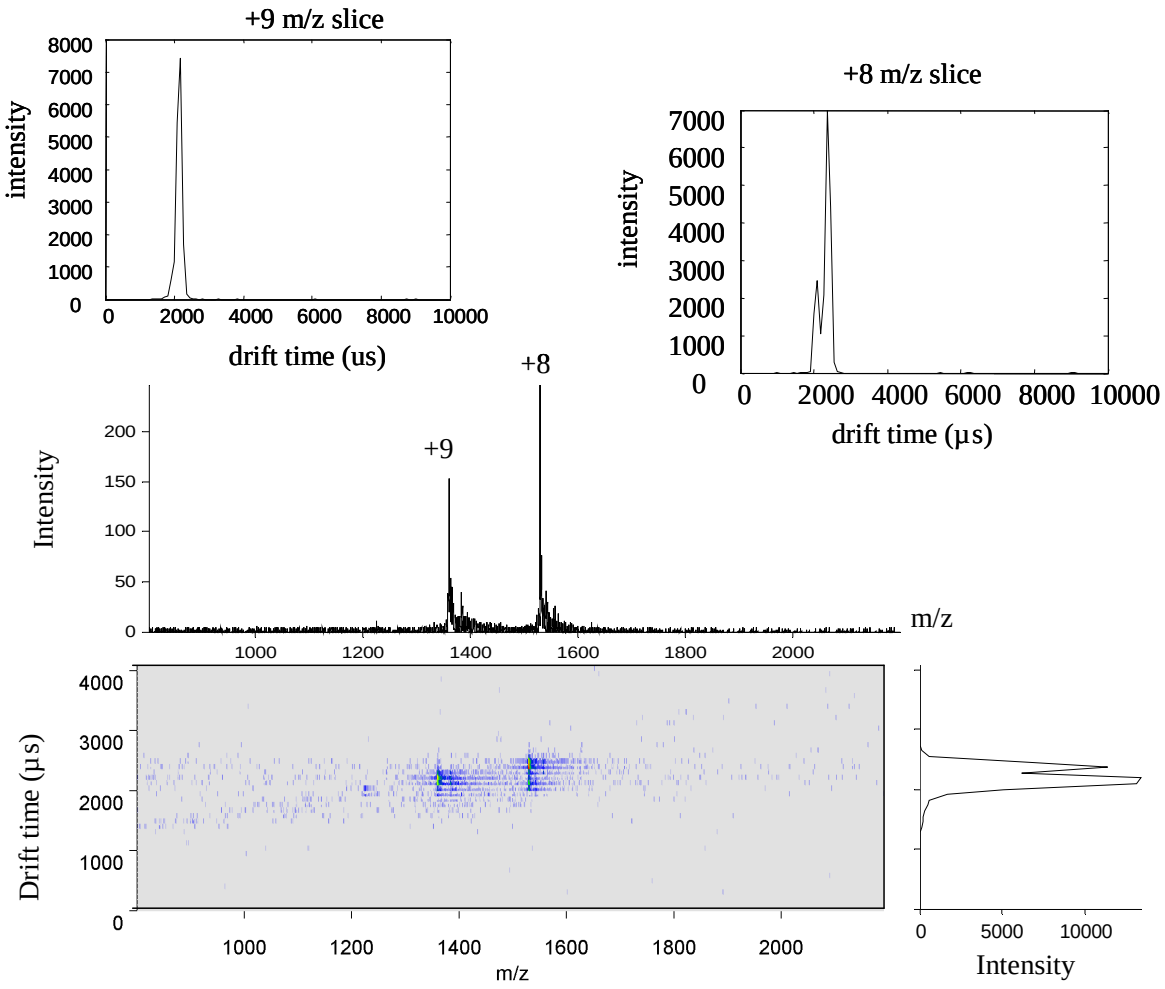

Figure 1. Nested 3-D IM-TOF mass spectrum of 30 µM cytochrome *c* in water with 1% acetic acid. The summed mass and ion mobility spectra are in the middle and at the lower right, respectively. The extracted IM spectra for cytochrome *c* +8 and +9 ions are displayed at the top.

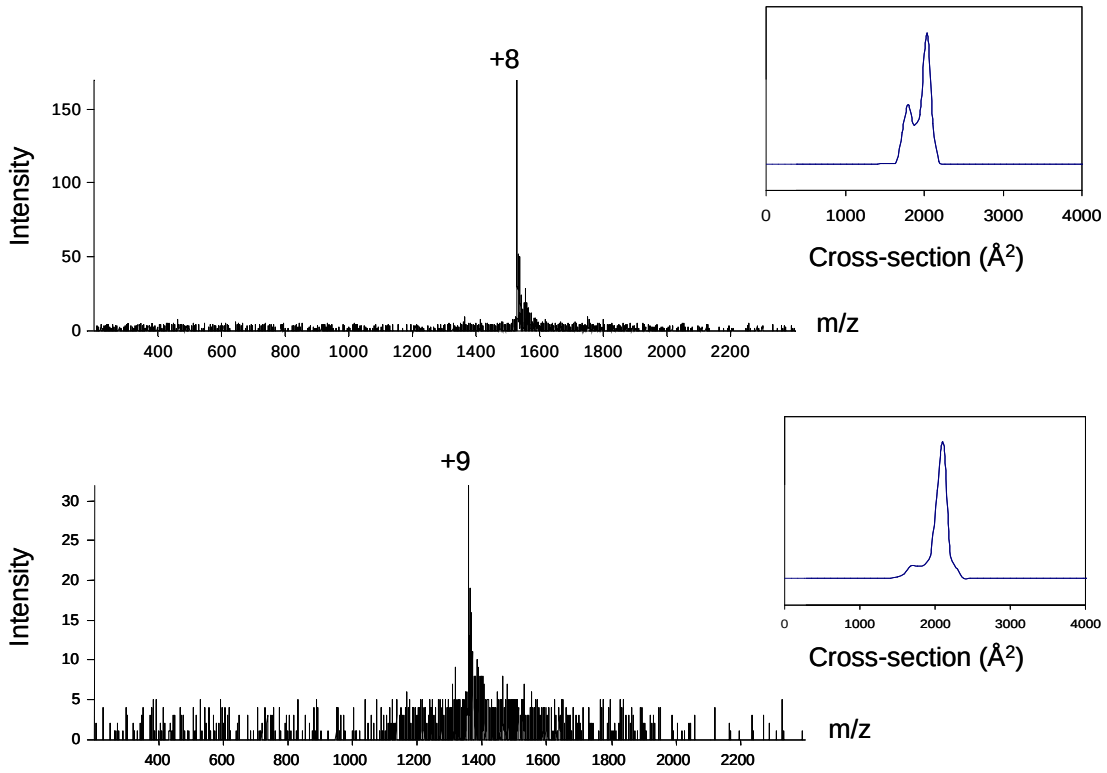

Figure 2. Mass and mobility spectra of +8 and +9 cytochrome *c* ions after isolation in the ion trap.

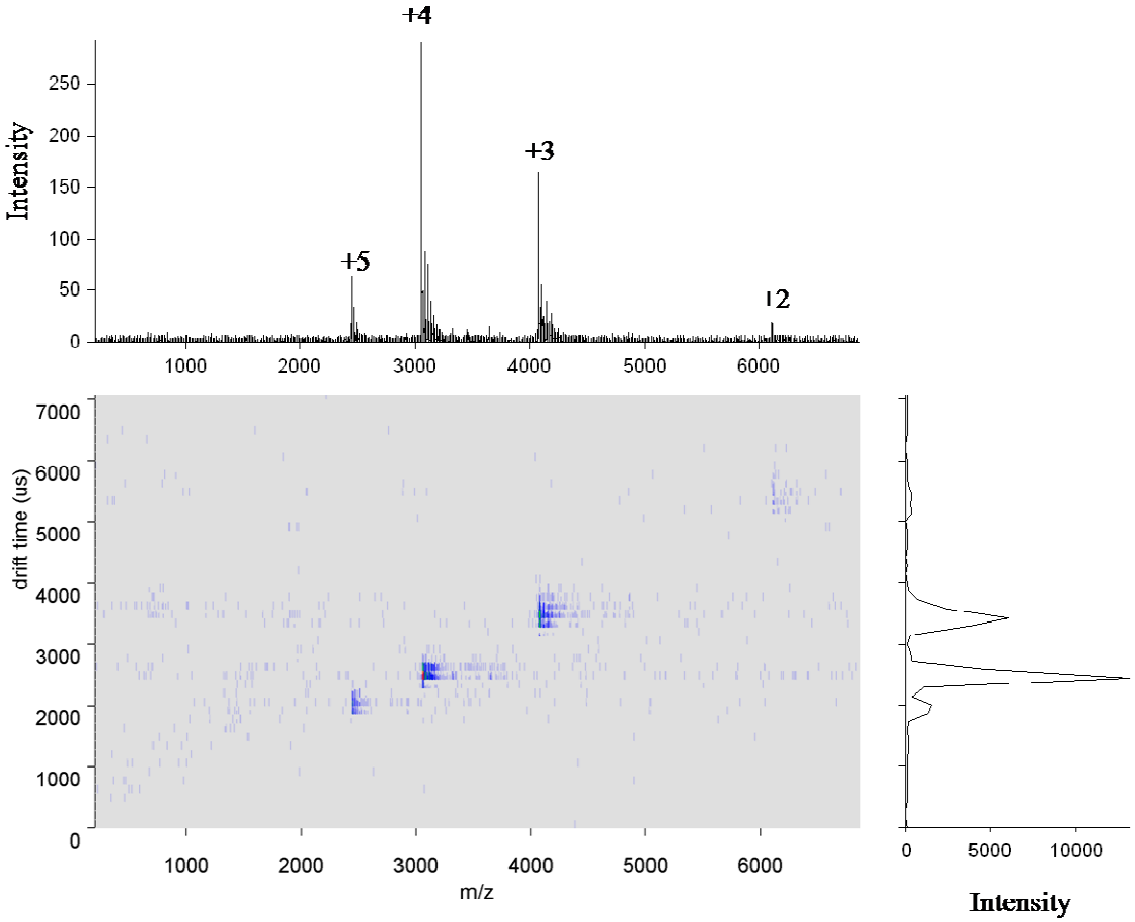

Figure 3. 3-D spectrum after isolated +8 cytochrome *c* ions react with PDCH anions in the ion trap for 100 ms.

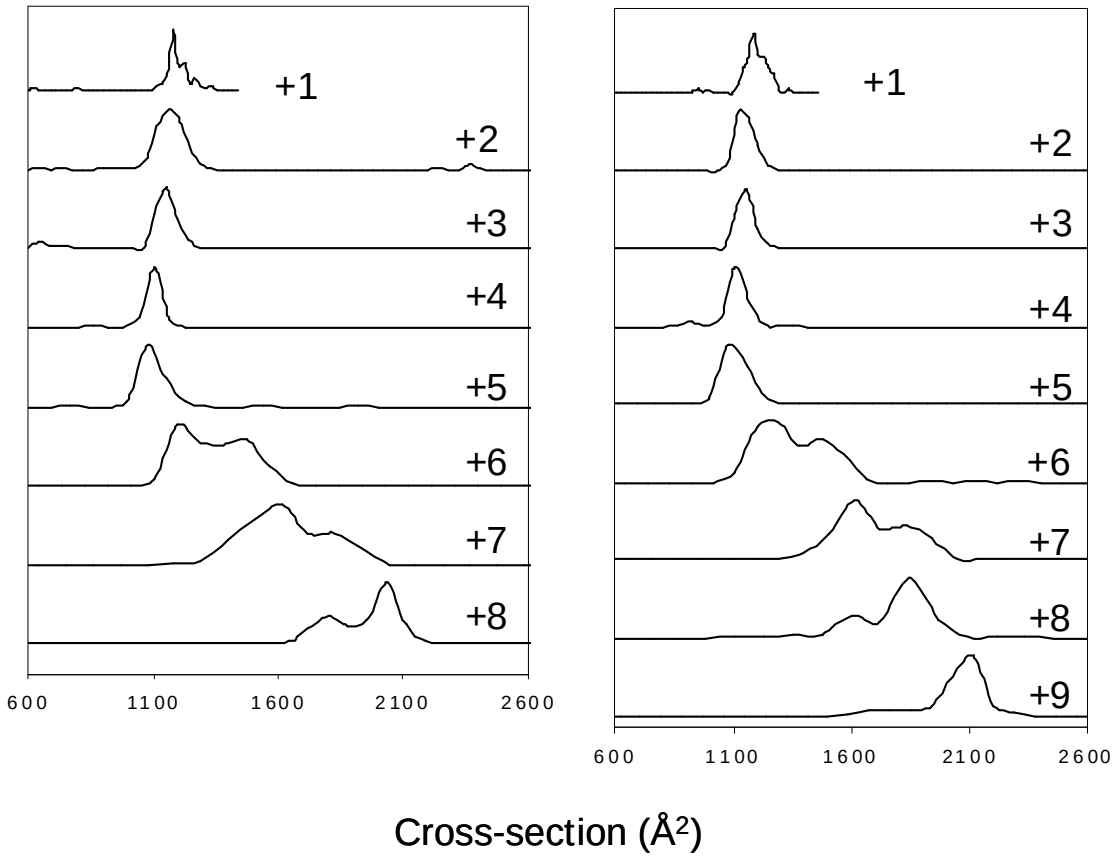

Figure 4. Distribution of cross sections for cytochrome *c* ions in each charge state. For the plots at the left, the cytochrome *c* ions were initially in the +8 state; ion/ion reaction time was 50 ms to go to +4 and 110 ms to go to +1. The right plots are for charge reduction of +9 cytochrome *c* ions for 40 ms to go to +4 and 80 ms to go to +1.

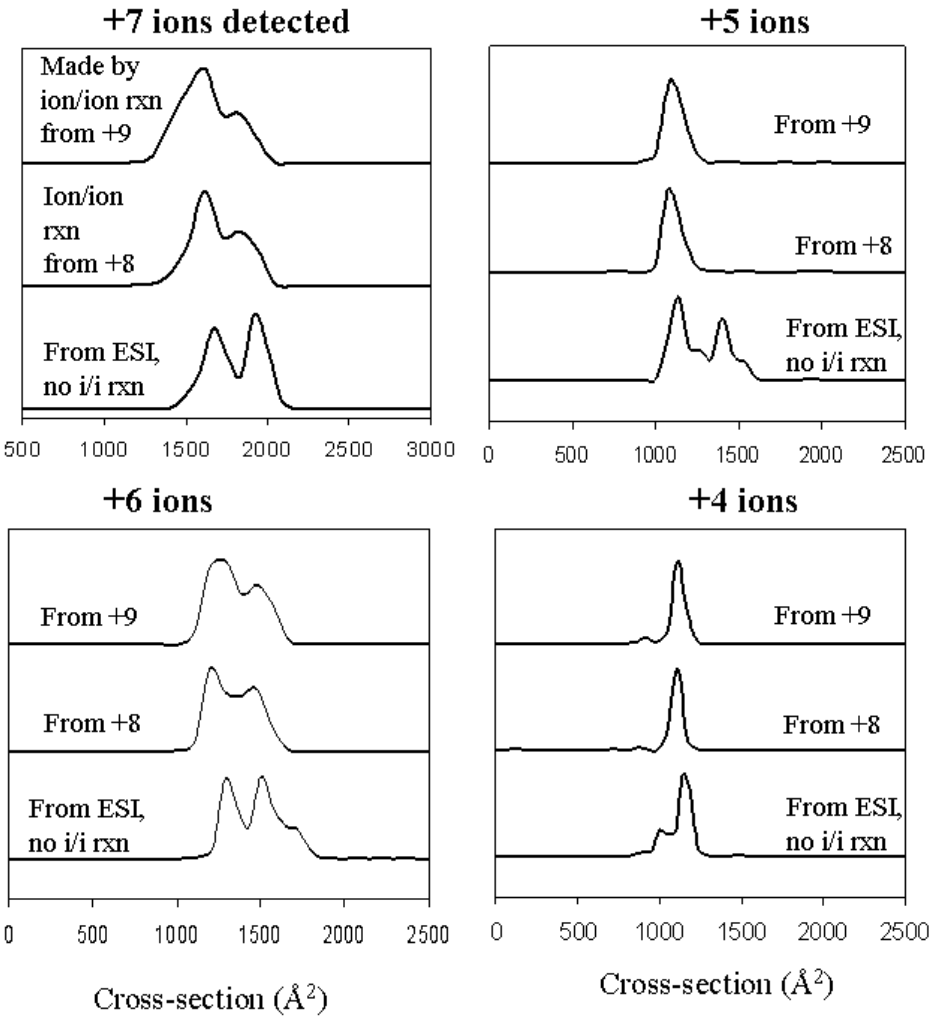

Figure 5. Distribution of cross sections for cytochrome *c* ions in each charge state. The charge state of the ions observed is noted outside each box. The top curve in each box is for ions made from +9 by ion/ion reaction (40 ms). The middle curves are for ions made from +8 (50 ms). The bottom curves are for the ions in the indicated charge state observed directly from ESI from water, without acetic acid.

CHAPTER 5

General Conclusions

This dissertation focused on the development of MS instrumentation for ion/ion reaction studies combined with IMS-TOF measurements. Chapter 2 described the construction and characterization of an LIT for ion/ion reactions made with primarily commercial components. The LIT's performance characteristics were examined, and its capability for both dual polarity trapping mode and transmission mode ion/ion reactions were demonstrated. Chapter 3 described the construction and performance of an IT-IMS-q-TOF. This instrument is the first MS to combine ion/ion reactions in an ion trap with IMS-TOF analysis. Top-down protein analysis of the intact protein ubiquitin was demonstrated using CID to fragment the protein followed by charge reducing the product ions via proton transfer ion/ion reactions. The ability of IMS to separate the product ions into charge state groups that fall on the same diagonal line on the drift plot gives this instrument an additional tool to identify fragment ions in protein MS/MS spectra.

Chapter 4 presented experiments investigating the effects of proton transfer ion/ion reactions on the conformation of cytochrome *c* ions. These results show that as protons are stripped off the protein ions during the ion/ion reactions, the cytochrome *c* ions fold to one resolvable conformation regardless of whether the initial population of ions had one or two resolvable conformations. Other results for cytochrome *c* showed differences in the gas-phase conformation of charge states created by ion/ion reaction and that of the same charge states created directly from ESI. Some charge states (+7 and +6) have similar conformations with different relative abundances, and one charge state (+5) has a conformation that could only be seen directly from ESI. No amount of heating, either in the ion trap or during

injection into the drift tube, could convert the more compact conformation of the +5 charge state into the more elongated conformation that is seen directly from ESI. Further experiments need to be conducted to determine the origin of this more elongated conformation of the +5 charge state of cytochrome *c*. One hypothesis is that the more elongated conformation is a result of different solution conditions. The +5 charge state generated directly from ESI is produced from a 100% water solution, and the +5 charge state produced via ion/ion reaction originated from a 1% aqueous acetic acid solution. Therefore, studies should be done to produce the +5 charge state via ion/ion reactions from a 100% water solution. For example, isolate the +7 charge state from a 100% water solution, charge reduce the isolated +7 via proton transfer ion/ion reactions to create the +5 charge state, and take an IMS-q-TOF spectrum to see what conformations this +5 charge state has. These experiments would provide a basis for comparison in which the solution conditions are equivalent between the ions formed directly from ESI and the ions formed via ion/ion reaction. Also, these experiments would give further insight into how the gas-phase conformation of cytochrome *c* ions compares to the solution-phase structure.

A major stumbling block in the pursuit of further experiments, like the ones described in the previous paragraph, is the sensitivity of the IT-IMS-q-TOF instrument. A significant source of ion loss is inside the drift tube, mainly due to radial diffusion. The ion losses in the drift tube were reduced with the incorporation of the ion funnel at the back end of the drift tube, as described in Chapter 3. However, a second significant source of ion loss is the 3d ion trap. The trapping efficiency of ions injected into a 3d ion trap is typically less than 10%. Meaning, 90% of the ions delivered to the ion trap are lost. Conversely, the trapping efficiency of the LIT discussed in Chapter 2 is ~ 83%. Therefore, replacing the 3d ion trap of

the IT-IMS-q-TOF with the LIT described in Chapter 2 would increase the sensitivity of the IMS-q-TOF measurements. While some technical issues will need to be worked out, such as how to efficiently inject the ions from the LIT into the drift tube, plans are being made to modify the instrumentation in our lab to create an LIT-IMS-q-TOF.

New chemical problems are always presenting themselves, especially in the field of protein identification and characterization. The solutions to these problems greatly depend on the quality and functionality of the analytical instruments. Therefore, instrumentation development will always be at the leading edge of analytical problem solving.

ACKNOWLEDGEMENTS

The funding for the research presented here was provided by Iowa State University College of Liberal Arts and Sciences, Office of Biotechnology, Plant Sciences Institute, Carver Trust, Waters Corp. via an ASMS Research Award, and the Iowa State University Vice Provost for research. I would like to thank the Velmer A. and Mary K. Fassel Fellowship (ISU 2006-2007), the Conoco-Phillips Fellowship (ISU 2006-2007), and the GAANN Fellowship (ISU 2008) for financial support in the form of tuition, fees, and stipend.

This work would not have been possible without the supervision of Dr. Ethan Badman as my major professor for the first three years of my graduate studies. He taught me a lot about ion traps, ion/ion reactions, and ion mobility. Approximately halfway through my graduate studies, Dr. Badman left ISU to pursue a career in the Pharmaceutical industry. At this unsettling time for our lab, Dr. R. S. Houk agreed to incorporate our lab with his own. Without Dr. Houk's supervision, I would never have been able finish my research and obtain my degree. I cannot express how grateful I am for Dr. Houk's guidance over the last two years. I would also like to thank the past and present Houk group members.

There are several other people in my life that also deserve recognition. Three professors from my undergraduate institution, Dr.'s Matt Johll, Jon Russel, and Kari Cunningham, each played key roles in my undergraduate education, and they encouraged me to pursue a graduate education. Our Oakwood Road Church family in Ames, IA has provided my family with spiritual support and opportunities for our faith to grow stronger. These connections will never be forgotten. My parents and sister have always provided me with

emotional support and encouragement, and I could not have completed my degree without them.

Finally, I would like to give very special recognition to the two most important people in my life, my wife April and daughter Emma. April was always very understanding of a graduate student's schedule and supportive of my research, and Emma always met me at the door when I got home with a great big smile. My hope is that April and Emma would be able to share in the accomplishment of completing my graduate degree.